Preface

This thesis is presented in order to obtain the Master of Science degree at the Delft University of Technology, sub-faculty of Civil Engineering.

The report deals with the run-up on rough, permeable slopes of a rubble mound breakwater. The experiments used in for this thesis are performed at the Laboratory of Fluid Mechanics of the sub-faculty of Civil Engineering of the Delft University of Technology and at the Jehad Water and Water management Research Company in Tehran, Iran.

I would like to thank the members of my thesis committee for their advise, support and critical comments:
Prof. ir. K. d'Angremond
Dr. ir. H.L. Fontijn
ir. T. van der Meulen
ir. W.H. Tutuarima

Furthermore I would like to thank Dr. J.H. Rakers for his efforts in the realisation of the journey to Iran. For their support in Iran, I would like to thank Dr. H. Eslami, Dr. M. Borghei and Dr. V. Chegini.

Finally, I would like to thank F.N. Jongerius and my parents for their unconditional support during this study.

Erwin Witteman
Delft, April 1999

Summary

This report is the result of the Master of Science thesis of the author, at the Delft University of Technology, sub-Faculty of Civil Engineering.

Although a lot is known nowadays about the run-up on smooth and impermeable slopes as well as the run-up on slopes covered with a rock armour layer, the physical properties of the armour layer of a rubble mound breakwater are not incorporated in the relations describing the run-up on a breakwater's slope. The roughness of a slope and its permeability, which can be described by a characteristic diameter of the armour unit and the porosity of the layer, are not used in the description of the run-up.

This report is an attempt to get insight into the influence that the roughness and the permeability of a slope have on the run-up on this slope. In order to achieve this goal, non-dimensional parameters are derived describing the roughness of a slope and its permeability.

Firstly, the framework of the design of a breakwater is given in order to place the run-up on a rough, permeable slope. The run-up itself is dealt with separately.

Experiments were performed in order to obtain data that can be used to quantify the influence of the roughness of the slope and its permeability. The experiments were performed leaving the permeability of the whole structure out of consideration. To achieve a difference in porosity of the armour layer, rock armour units were used as well as tetrapod armour units.

Two approaches of data analysis are applied on the data obtained from these experiments.

This first approach describes the run-up on a rough, permeable slope by a combination of a roughness parameter, a permeability parameter and the breaker parameter. The roughness parameter and the permeability parameter are derived by forming non-dimensional parameters that describe roughness and permeability. The run-up, usually made non-dimensional using the wave height (H) is made non-dimensional here using the nominal diameter. This gave better results in combination with the derived parameters describing the roughness and the permeability of a slope.

The second approach describes the run-up on a rough, permeable slope by using the relative run-up R_u/H and a newly derived non-dimensional parameter resembling the Iribarren parameter, but incorporating the influence of the permeability of the armour layer. When the relative run-up is put against the Iribarren parameter and is put against the newly derived non-dimensional parameter, the appearing scatter is less in the latter case.

In both approaches, two relations describing the run-up on a rough permeable slope are derived. One for breaking waves and one for non-breaking waves.

For the second approach, the found relations have a significant resemblance with the known formulae for run-up on a slope covered with rock armour units, derived by van der Meer and Stam.

When the relations derived following the both approaches are compared, the relations derived by the second approach are the relations that give the best feeling with the physical processes as they occur.

The relation for non-breaking waves, derived using the first approach, is applied on data obtained from physical model tests on a breakwater covered with tetrapod armour units. The calculated non-dimensional run-up is compared with the measured non-dimensional run-up. The results show that

the permeability of the whole structure can not be neglected, especially in the case of non-breaking waves.

Table of contents

Error! No table of contents entries found.

List of figures

figure 2-1, Statically stable and dynamically stable structures
figure 2-2, Governing parameters related to the cross-section
figure 2-3, Notional permeability factor P.
figure 2-4, Permeability versus grain size
figure 2-5, Different types of waves breaking on a slope
figure 2-6, Definition of wave transmission
figure 2-7, Wave transmission over and through low-crested structures
figure 2-8, Definition of wave overtopping
figure 2-9, Wave overtopping on slopes as a function of wave run-up
figure 3-1, Run-up definition
figure 3-2, Relative 2% run-up on rock slopes
figure 3-3, Run-up reduction due to berms for plunging waves (MUR, 1995)
figure 3-4, Run-up reduction due to berms for surging waves (MUR, 1995)
figure 3-5, Comparison of relative 2% run-up for smooth and rubble slopes
figure 3-6, Contributions of the different terms of the Forchheimer equation to the hydraulic gradient
figure 4-1, Dimensions of a tetrapod unit
figure 4.2, Dimensions of a rock unit
figure 4-3, Positions of wave height meters in wave flume
figure 4-6, Measuring run-up
figure 4-7, Dimensions of a tetrapod armour unit
figure 5-1, Hydraulic gradient
figure 5-2 Wall effect and surface definition
figure III-1, Drawings of case used in Delft
figure V-1, Cross-section of model used in Iran
figure VI-1, Plan view flume Iran
figure VIII-1, Influence of wave height on run-up
figure VIII-2, Influence of slope angles on the run-up, tetrapods
figure VIII-3, Influence of slope angles on run-up, rock
figure VIII-4, Influence of diameter on run-up, rock
figure VIII-5, Influence of diameter on run-up, tetrapods
figure VIII-6, Influence of porosity on the run-up
figure VIII-7, Influence of period on the run-up, rock
figure VIII-8, Influence of the period on the run-up, tetrapods
figure VIII-9, Influence of the period on run-up, rock
figure VIII-10, Influence of the period on the run-up, tetrapods
figure IX-1, Relative run-up (R_u/H) versus ξ
figure X-1, Relative run-up (R_u/H) versus $H/D_{n(50)}$
figure X-2, Relative run-up (R_u/H) versus roughness (H/D_{85}) and (H/Htet)
figure X-3, Run-up versus roughness (H/Htet), tetrapods
figure X-4, Run-up versus roughness (H/D_{85}), rock
figure X-5, Non-dimensional run-up ($R_u/D_{n(50)}$) versus non-dimensional roughness (H/D_{85}) and (H/Htet)
figure XI-1, Relative run-up (R_u/H) versus K, equation (5.11)
figure XI-2, Run-up versus K, equation (5.11)
figure XI-3, Non-dimensional run-up ($R_u/D_{n(50)}$) versus K, equation (5.11)
figure XI-4, Non-dimensional run-up ($R_u/D_{n(50)}$) versus K, equation (5.12)
figure XI-5, Non-dimensional run-up ($R_U/D_{n(50)}$) versus K, equation (5.15), and (5.16)
figure XIII-1, Le Méhauté's nomogram
figure XIV-1, Data obtained in Iran versus known run-up data
figure XV, Measured data versus calculated data, breaking waves

figure XVI-1, Measured data points versus calculated data points, non-breaking waves
figure XVII-2, Measured data points versus calculated data points, using data obtained in Iran and ξ_p
figure XVIII-1, Influence of tanα on run-up, tetrapods, D_n = 0.044 m
figure XVIII-1, Influence of tanα on run-up, tetrapods, D_n = 0.05 m
figure XVIII-1, Influence of tanα on run-up, rock, D_{n50} = 0.065 m
figure XVIII-1, Influence of tanα on run-up, rock, D_{n50} = 0.045 m
figure XVIII-1, Influence of tanα on run-up, rock, D_n = 0.027 m
figure XXII-2, Scatter for relative run-up versus Ω, non-breaking waves
figure XXII-3, Scatter for small units, non-breaking waves
figure XXIII-1, Relative run-up versus Ω, all data points
figure XXIII-2, Comparison of relative 2% run-up for smooth and rubble slopes
figure XXIV-1, Relative run-up versus Ω, all data points
figure XXIV-2, Relative run-up versus Ω, data fitting

List of tables

table 2-1, Values for a and b to be used in equation (2.25)
table 3-1, Coefficients in run-up equations (3.2)-(3.4)
table 4-1, Variation of parameters in the experiments performed in Delft
table 4-2, Variation of the properties of the tetrapods used in the Delft experiments
table 4-3, Variation of the properties of the rock used in the Delft experiments
table 4-4, Experimental program Iran
table 5-1, Matrix of fundamental dimensions
table I-1, Roughness reduction factors, γ_f
table VII-1 Data of experiments performed with $\lambda = 50$, prototype values
table VII-2 Data of experiments performed with $\lambda = 50$, model values
table VII-3 Data of experiments performed with $\lambda = 66$, prototype values
table VII-3 Data of experiments performed with $\lambda = 66$, prototype values

List of symbols

A_c	(m)	Armour crest freeboard, relative to still-water level
A_e	(m^2)	Erosion area under rock profile
B	(m)	Structure width, in horizontal direction normal to face
d	(m)	Armour crest level relative to the sea bed
D	(m)	Particle size, or typical dimension
D_{15}	(m)	Stone diameter where 15% of the total weight of the sample is lighter
D_{20}	(m)	Stone diameter where 20% of the total weight of the sample is lighter
D_{85}	(m)	Stone diameter where 85% of the total weight of the sample is lighter
D_{85}/D_{15}	(-)	Armour grading parameter
D_n	(m)	Nominal block diameter, $\sqrt[3]{\frac{M}{\rho_a}}$
$D_{n(50)}$	(m)	Diameter used to express that D_n for tetrapods and D_{n50} for rock are used in a formula
D_{n50}	(m)	Nominal diameter of stone, $\sqrt[3]{\frac{M_{50}}{\rho_r}}$
F_c	(m)	Difference of level between crown wall and armour crest = R_c-A_c
g	(m/s^2)	Gravitational acceleration
G_c	(m)	Width of armour berm at crest
H_{tet}	(m)	Height of the tetrapod unit
H	(m)	Wave height, from trough to crest
H_i	(m)	Incident wave height
H_{mo}	(m)	Significant wave height, calculated from the spectrum, $H_{mo}= 4\sqrt{m_o}$
H_r	(m)	Reflected wave height
H_s	(m)	Significant wave height
H_{si}	(m)	Incident significant wave height
h	(m)	Water depth
h_c	(m)	Armour crest level relative to seabed
h_t	(m)	Depth of toe below still-water level
i	(-)	Hydraulic gradient
K	(-)	Non-dimensional parameter describing the permeability of one layer
K_D	(-)	Stability coefficient in Hudson formula
K_t	(-)	Transmission coefficient
k	(-)	Permeability coefficient
k_D	(-)	Layer thickness coefficient
L	(m)	Wave length, in the direction of propagation
M	(kg)	Mass of an armour unit
M_{50}	(kg)	Stone mass exceeded by 50% of the total weight of the sample
N	(-)	Number of waves
N	(-)	Scale factor
N_a	(m^{-2})	Amount of armour units per square meter
n	(-)	Volumetric porosity
P	(-)	Notional permeability factor
Q	(m^3/s)	Discharge
q	(m^2/s)	Discharge per linear meter
R	(-)	Dimensionless freeboard parameter
R	(-)	Non-dimensional parameter describing the roughness of a slope
R_c	(m)	Crest freeboard, level of crest relative to still-water level
R_u	(m)	Run-up level, relative to still-water level

$R_{u2\%}$	(m)	Run-up level exceeded by only 2% of the incident waves
R_{us}	(m)	Run-up level of significant wave
S	(-)	Non-dimensional damage, used by van der Meer
s	(-)	Wave steepness
$s_{o,m}$	(-)	Wave steepness for mean period
$s_{o,p}$	(-)	Wave steepness for peak period
T	(s)	Wave period
T_m	(s)	Mean wave period
T_p	(s)	Peak wave period
t_a	(m)	Armour layer thickness
t_f	(m)	Filter layer thickness
u	(m/s)	Velocity
V	(m^3)	Volume
V_a	(m^3)	Volume of armour units
V_d	(m^3)	Volume of drained water
V_h	(m^3)	Volume of hollow spaces inside a layer
V_i	(m^3)	Volume of incoming amount of water
W_{85}	(kg)	Stone weight exceeded by 15% of the total weight of the sample
W_{15}	(kg)	Stone weight exceeded by 85% of the total weight of the sample

Greek symbols

α	(-)	Structure front face angle
β	(-)	Angle of wave attack
β	(-)	Coefficient, being the ratio D_{20}/D_{n50} (rock) and the ratio c/D_n (tetrapod)
Δ	(-)	Relative buoyant density of material considered
γ_b	(-)	Reduction factor for berm
γ_β	(-)	Reduction factor for oblique waves
γ_f	(-)	Reduction factor for slope roughness
γ_h	(-)	Reduction factor for shallow foreshore
λ	(-)	Scale factor
θ	(-)	Angle of incidence of the waves
ρ	(kg/m^3)	Mass density of rock
ρ_a	(kg/m^3)	Mass density of the armour
ρ_c	(kg/m^3)	Mass density of concrete
ρ_w	(kg/m^3)	Mass density of water
ξ	(-)	Surf similarity parameter or Iribarren number
ξ_m	(-)	Surf similarity parameter based on T_m
ξ_{mc}	(-)	Critical surf similarity parameter
ξ_p	(-)	Surf similarity parameter based on T_p
Ω	(-)	Non-dimensional parameter used to describe run-up on a rough permeable slope

Chapter 1 Introduction

When a harbour is built on a coast and no natural protection for ships against waves is present, the harbour has to be equipped with one or more breakwaters. The breakwaters are constructed to ensure that ships will be able to lower speed when entering the harbour. Functional requirements often do not demand total tranquillity in the designated area. Therefore breakwaters do not need to be constructed in order to absorb all wave action under severe weather conditions. The tranquillity in the designated area is dependent on two main mechanisms of energy transfer past the breakwater.

The first mechanism is overtopping due to wave action. The second is transmission of wave energy through the breakwater. Overtopping of a breakwater is dependent on the run-up capacity of the waves and the height of the breakwater. A low breakwater will have a lot of overtopping whereas a high breakwater will reduce overtopping. Since the volume of material involved in the construction, and thereby its costs, is proportional to the square of its height, it is worthwhile to consider the minimum crest level as carefully as the structural strength of the armour layer.

To be able to estimate the amount of overtopping, the level of run-up on a breakwater slope under severe weather conditions has to be known. The known formulae that describe run-up on a slope are a function of the wave height and the breaker parameter. The breaker parameter is a function of the slope angle and the wave steepness. Influences like porosity of the armour layer or diameter of the armour units are not included in the known formulae. In case of considering these influences, a constant has to be added to these formulae.

Above stated leads to the following definition of the problem:

Until now, the available relations describing run-up on a slope do not take the physical properties of the armour layer of a rubble mound breakwater into account. These physical properties consist of the diameter of the armour unit and the porosity of the armour layer.

Logical thinking leads to the assumption that a larger diameter of the armour units and a higher porosity of the armour layer lead to a lower run-up. One can think in terms of: a larger diameter gives more friction, or a larger diameter gives larger hollow spaces inside the armour layer. In the case of the porosity, a higher porosity will lead to more hollow spaces inside the armour layer. This roughness (diameter) and permeability (diameter and porosity) will affect the run-up capacity of a wave.

The goal of this thesis is:

To examine the influence of diameter of the armour unit and the porosity of the armour layer on the run-up on a rough, permeable slope.

Sub goals resulting from the main goal are:

- To derive parameters describing the roughness and the permeability of the slope, using the diameter of the armour unit and the porosity of the armour layer.
- To derive relations describing the run-up on a rough, permeable slope.

The research done in this thesis is restricted to the following:

- *Only slopes of a rubble mound breakwater are considered.*
- *The slopes are rough and permeable, but the structure supporting the slope is not necessarily permeable.*
- *The permeability of the whole structure is not taken into account.*

In order to achieve the goals, experiments were performed at the Laboratory of Fluid Mechanics at the sub-faculty of Civil Engineering of the Delft University of Technology. The experiments were performed with regular waves attacking an impermeable slope that was covered with a layer of armour units. These armour units were rock units or tetrapods; this implied two different values of the porosity of the armour layer. The other variables in the experiments were: diameter of the armour units, wave height, wave period and slope angle.

The data obtained from the Delft experiments are not the only data available to be used to get insight into the parameters that influence the run-up on a rough, permeable slope such as the slope of a rubble mound breakwater. During a stay in Iran, a rubble mound breakwater model was tested on run-up, reflection and overtopping due to irregular waves. These experiments were performed at the Jehad Water and Water management Research Company. The experiments were part of a design of a rubble mound breakwater covered with tetrapod armour units. The data on the run-up on this model are used to draw a comparison between the results of highly schematised model used in Delft and the data of the more realistic model tested in Iran.

This thesis is described chronologically now.
In the period September 1997 - December 1997, the experiments in Iran were performed. These experiments showed that run-up on a slope covered with an artificial armour unit like the tetrapod was lower than the run-up on a rock covered slope, see figure XIV-1. Birth was given to the hypothesis that porosity of the armour layer and the diameter of the armour units, resulting in the derivative roughness and permeability, have a significant influence on the run-up on a slope.
In the period following the Iran experiments, a literature study was performed in order to get insight into the present knowledge on run-up on a rough, permeable slope. During the literature survey, it became clear that on this specific topic not much data is available. The data obtained in Iran appeared to be insufficient in number and range to be able to find a relation between run-up on a slope and its roughness and permeability. Therefore, new experiments were performed in Delft in the period October 1998 – January 1999. The data of the Delft experiments were used to search for the relation describing run-up on a rough, permeable slope.

The outline of this report is as follows.
In Chapter 2, the general considerations concerning the design of breakwaters will be described. In Chapter 3, the run-up on a slope will be dealt with. Chapter 4 will describe the experiments that were performed to obtain the data used to derive the new formula. Further, the experiments performed in Iran are described. In Chapter 5, the data sets of the two experiments will be analysed and the most important parameters will be discussed. In Chapter 6, the derivation of the relations describing run-up on a rough, permeable slope based on the Delft experiment will be given. These relations will be used to describe the data from the Iran experiments. A comparison between the relations and the data from the Iran experiments is drawn. In Chapter 7, a discussion is given on the derived non-dimensional parameters and the derived relations from Chapter 5 and 6. From the discussion it followed that the data should be analysed once more. New non-dimensional parameters as well as new relations describing the run-up on a rough, permeable slope are derived. Finally in Chapter 8 the conclusions and recommendations as they can be originated from this study are given.

Chapter 2 A short review on the design of breakwaters

2.1 Introduction

In the following sections, the purpose of breakwaters is discussed followed by the functional requirements that come along with the purposes. Subsequently, the discussion on breakwaters will be restricted to one typical variation of breakwater: the rubble mound breakwater. For a rubble mound breakwater, the various parameters that are involved in its design will be dealt with. These parameters can be divided in structural and hydraulic parameters and are discussed separately. Furthermore, the phenomena of hydraulic response of a breakwater are explained.

Although the stability of a breakwater is of utmost importance in the designing process of a breakwater, stability will not be gone into here. No relation is present between the hydraulic response phenomena like wave run-up and stability of the breakwater. For a discussion on the stability of breakwaters the reader can address himself to for instance Van der Meer (1993).

2.2 Purpose of breakwaters

In the most general definition, the purpose of breakwaters is to change the coast. Changing the coast can have many faces. Not only the direct visible change of the coastal profile is covered by "changing the coast" but also the change of currents and wave activity can be defined so.

The most obvious purpose of a breakwater is to give protection against waves. This can imply the protection of an approach channel to a harbour as well as protection of the harbour itself. This kind of protection is needed to when ships want to navigate and moor. When a ship is moored and its cargo is handled, it is desirable that the motion of the ship is controllable. Wave action in the approach channel can increase the danger for the tugboats that guide the ship and its crew and will make the navigation more difficult. Furthermore, dredging in exposed areas is relatively expensive.

A breakwater can also serve to reduce the required amount of dredging needed to keep the approach channel at the right depth. Cutting of the littoral sediment supply to the approach channel is one way of going so. The other way is using the natural scouring action that occurs in an artificially narrowed channel.

When little natural protections are available for the construction of the harbour, the breakwater itself can serve as a quay facility. This dual usage will have special requirements to the design of the breakwater. From a harbour construction view this dual usage is very economical but from a breakwater construction view this might not be so.

Finally, the breakwater's purpose can be to guide currents in the approach channel or along the coast. When a strong cross current is present in the approach channel, a breakwater might be constructed in such a way that the gradient is reduced.

A breakwater can be constructed to serve more than one of these purposes. Each purpose might have its own requirements making the designing process a complicated one and different for each breakwater.

In the next section four different types of breakwaters are discussed. All of them are capable of providing one of the four main purposes as mentioned above.

2.3 Different types of breakwaters

Breakwater structures can be distinguished into two types: statically stable and dynamically stable structures.

Statically stable are structures where no or minor damage is allowed under design conditions. Damage is defined as displacement of armour units. The mass of individual units must be large enough to withstand the wave forces during design conditions. Caisson and traditionally designed, or conventional, breakwaters belong to the group of statically stable structures.

Dynamically stable structures are structures where profile development is concerned. Units like stone gravel or sand are displaced by wave action until a profile is reached where the transport capacity along the profile is reduced to a very low level.

In figure 2-1, four different types of breakwaters are shown.

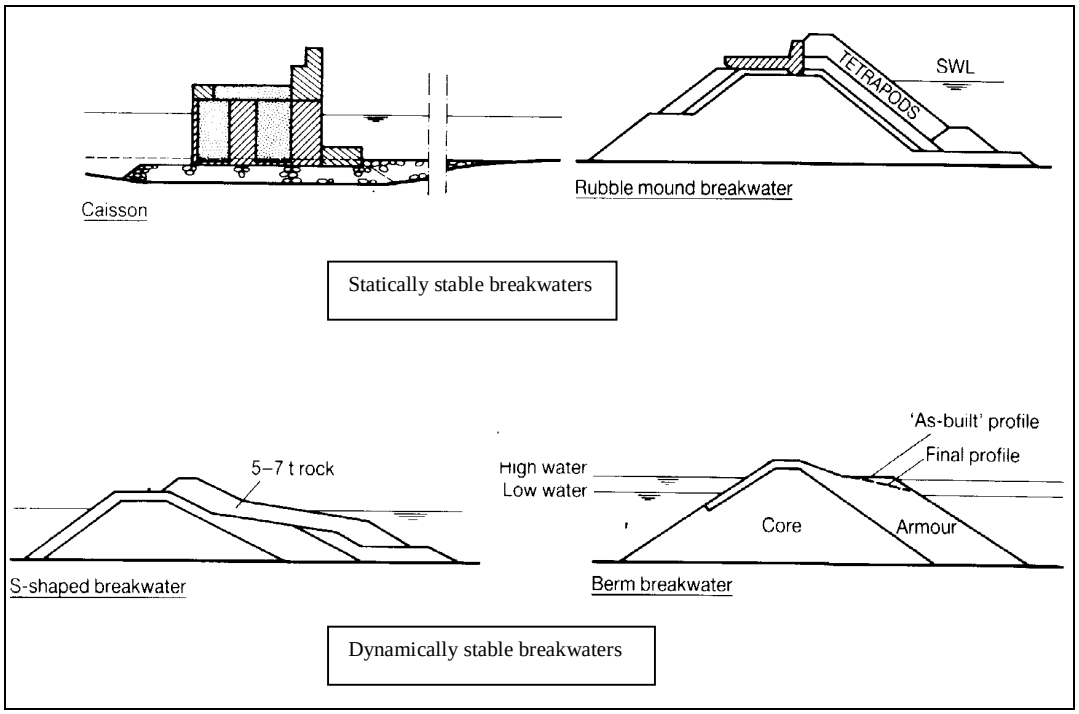

figure 2-1, Statically stable and dynamically stable structures

In the remainder of this thesis, rubble mound breakwaters will be focussed on. Their structural parameters will be discussed in the next section.

2.4 Structural parameters related to the cross-section of a rubble mound breakwater

A rubble mound breakwater can considered to be an orderly piled amount of densely packed material such as stone or concrete elements. Many parameters characterise this “pile”, below the parameters that describe the cross-section are given.

- crest freeboard, relative to still water level (SWL) R_c (m)
- armour crest level relative to the sea bed d (m)

–	structure width	B	(m)
–	thickness of armour, filter layer	t_a, t_f	(m)
–	area porosity	n_a	(-)
–	angle of structure slope	α	(-)
–	depth of toe below SWL	h_t	(m)

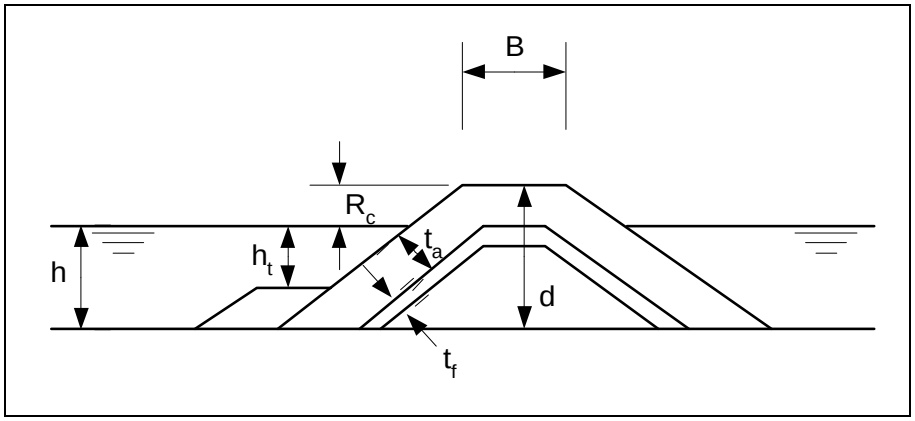

figure 2-2, Governing parameters related to the cross-section

2.4.1 Diameter of material

The diameter that is used to describe the characteristic size related to the mass of rock is the nominal diameter, D_{n50}. This is the size of the cube with equivalent volume to the block with median mass and is given by:

$$D_{n50} = \sqrt[3]{\left(M_{50} / \rho_r \right)} \tag{2.1}$$

For concrete units, like tetrapod or Dolosse, the nominal diameter is given by:

$$D_n = \sqrt[3]{\left(M / \rho_c \right)} \tag{2.2}$$

In these formulae are:

M_{50}	=	median mass of unit given by 50% on the mass distribution curve
M	=	mass of concrete armour unit
ρ_r	=	mass density of rock
ρ_c	=	mass density of concrete

2.4.2 Porosity

The porosity of a layer constructed of (armour) units is the volume of hollow space given as a percentage of the volume of the units and the hollow spaces.

$$n = \frac{V_h}{V_h + V_a} \cdot 100\% \qquad (2.3)$$

where V_h = Volume of hollow spaces
V_a = Volume of armour units

2.4.3 Permeability

Permeability can be divided into permeability of the structure as a whole and permeability of each layer of the structure. The permeability of the structure is described first.

When comparing different structures it is often very hard to compare the permeability of these structures. Mostly only the indication “permeable” or “impermeable” is given. Van der Meer (1988) proposed the following values for the notional permeability factor *P* for various structures:

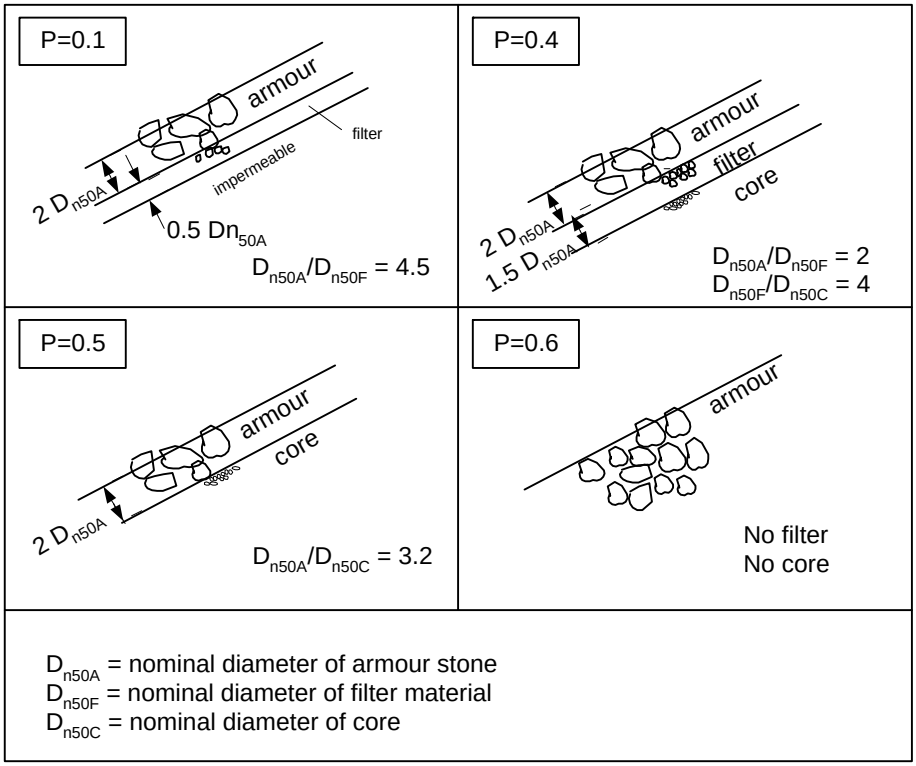

figure 2-3, Notional permeability factor P.

This factor is derived from stability tests performed by Van der Meer. It is a factor that he uses to include permeability in the formulae for stability of armour units on a slope. This factor has no physical meaning; it is only a mathematical way of taking into account the permeability of a structure.

The permeability of each layer can be described for a turbulent regime and large diameters by the Forchheimer equation (see also section 3.5) and by a practical formula given by the Manual on the use of rock (1995).
When permeability is taken according to Forchheimer, it is given by:

$$k \sim n^a D g \qquad (2.4)$$

where n = the porosity of the layer
D = a characteristic diameter
g = gravitational acceleration
a = a constant

Permeability defined by the Manual on the use of Rock (1995) gives:

$$k = 2 \cdot \sqrt{\frac{n^5 gD}{|i|}} \tag{2.5}$$

where n = the porosity of the layer
D = a characteristic diameter
g = gravitational acceleration coefficient
i = hydraulic gradient

In figure 2-4, the relation between diameter and permeability for turbulent flow and laminar flow is given.

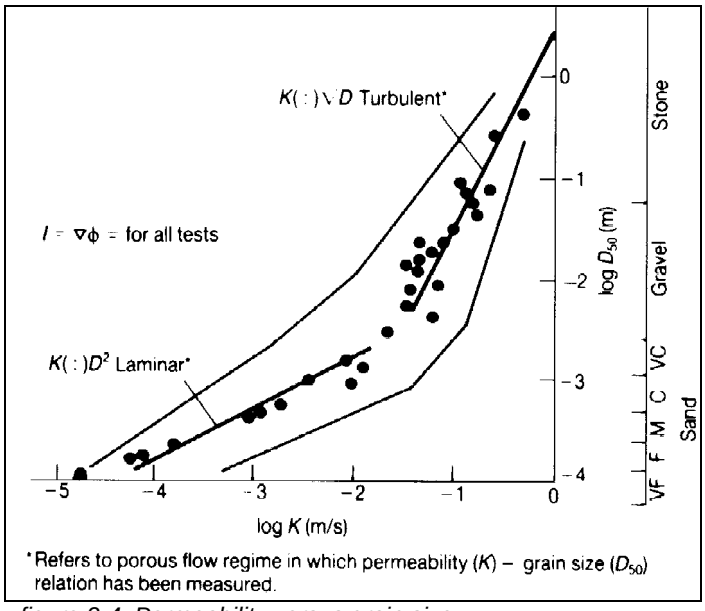

figure 2-4, Permeability versus grain size

.

2.5 *Hydraulic parameters related to the design of rubble mound breakwaters*

The hydraulic parameters, which are important for the design of breakwaters, are given by:

- H_s or H_{m0} incident wave height at the toe of the structure, given by the significant wave height (the average value of the highest 1/3 part of the waves) or based on the energy density wave spectrum ($4\sqrt{m_0}$)
- T_p peak period based on spectral analysis
- β the angle of wave attack
- h the water depth at the toe of the structure

2.5.1 Wave height

The wave height distribution at deep water can be described by the Rayleigh distribution and in that case one characteristic value, for instance the significant wave height, describes the whole distribution. In shallow and depth limited water, the highest waves break and in most cases the wave height distributions cannot longer be described by the Rayleigh distribution. This phenomenon can have considerable influence on the wave run-up since in most case the $R_{u2\%}$ is considered. With the highest waves breaking, also the highest value of run-up will be diminished. Other characteristic values that are often used are $H_{2\%}$ or $H_{1/10}$. $H_{2\%}$ is the value where only 2% of all waves are higher. $H_{1/10}$ is the average of the highest 10% of all waves.

2.5.2 Wave period

The influence of the wave period is often described using the deep-water wave length related to the wave height at the toe of the structure. Since most breakwaters are constructed in shallow water, the wave length at the structure will differ from the wave length at deep water. When the wave length at deep water is chosen to represent the wave field in front of the structure and for the value of the wave height, the value in front of the structure is taken, the result is called the fictitious wave steepness:

$$s = \frac{2\pi H_s}{gT^2} \tag{2.8}$$

When substituting the peak period, T_p, in this formula, the wave steepness will be denoted as s_{op}, when the mean period, T_m is substituted, s_{om} is used.

2.5.3 Surf similarity parameter

The surf similarity parameter can be seen as a combination of the properties of the waves and the properties of a smooth, impermeable slope. According to Battjes (1974), the combination of a slope angle and a wave steepness leads to the surf similarity parameter, or the Iribarren number:

$$\xi = \frac{\tan\alpha}{\sqrt{s}} \tag{2.9}$$

Usually, the subscripts *p* and *m* are used, denoting the Iribarren number using respectively the peak period and the mean period of the wave spectrum in deep water.
The Iribarren number is used often to be able to distinguish different types of breaking waves. In the figure below, the breaking types are related to a ξ for a smooth beach. Van der Meer (1992) stated that non-breaking waves on a rough permeable slope occur for ξ_p>2 and breaking waves occur for ξ_p<2. When ξ_m is used, breaking waves occur for ξ_m < 1.5 and non-breaking waves occur for ξ_m > 1.5. When regular waves are considered, breaking waves are present when ξ < 2.5 and non-breaking waves are present when ξ > 2.5. The boundary for plunging and surging waves differs for different structures, especially for the composition of the structure.

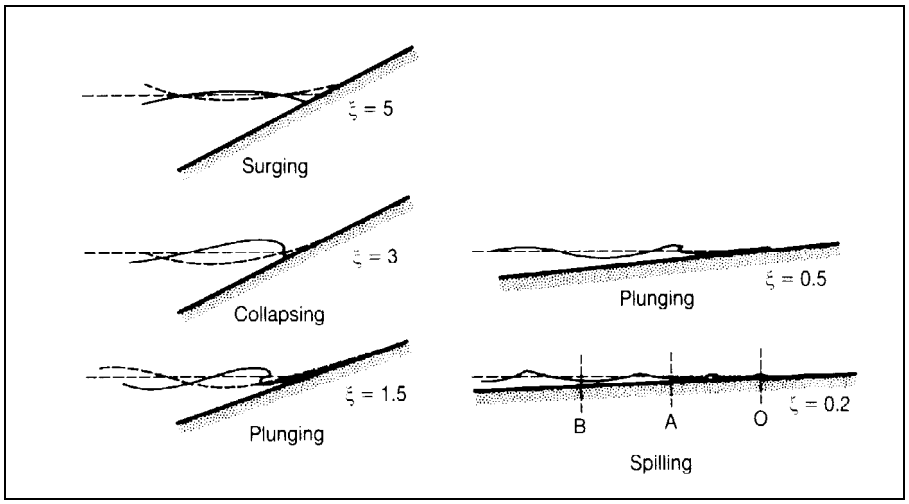

figure 2-5, Different types of waves breaking on a slope

2.6 Hydraulic response

The interaction between the breakwater and the waves is called the hydraulic response of the breakwater. Hydraulic response of a breakwater consists of the phenomena: wave transmission, wave overtopping, wave run-up and wave reflection. The following sections give a concise description of the phenomena wave transmission and wave overtopping. Reflection is not discussed here since it mainly plays a role at the outer slope of the breakwater. The run-up phenomenon is discussed in chapter 3 since it is the main subject of this thesis.

2.6.1 Wave transmission

Wave transmission is the phenomenon that wave energy will overtop and pass through the breakwater, see figure 2-10.

Transmission is expressed by the ratio of transmitted wave height (H_t) to incident wave height (H_i):

$$K_t = \frac{H_t}{H_i} \tag{2.34}$$

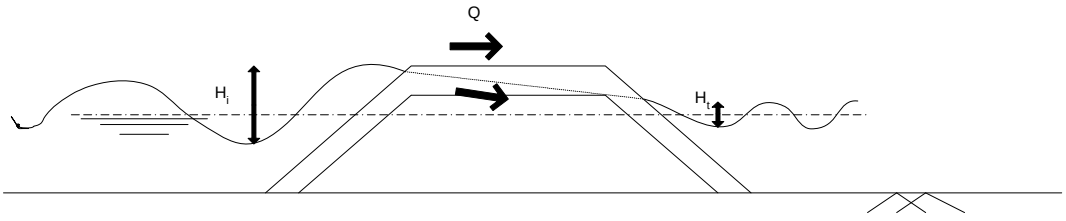

figure 2-6, Definition of wave transmission

The governing parameters related to transmission are: structural geometry, permeability, the crest freeboard, crest width, surface roughness, water depth, wave height and wave period.

Most formula express K_t dependent on a dimensionless crest freeboard. Van der Meer (1990b) gives K_t dependent on the ratio crest freeboard divided by the wave height (R_c/H_i), see figure 2-11.
His formulae for wave transmission are:

$$K_t = 0.8 \qquad \text{when} \quad -2.00 < \frac{R_c}{H_s} < -1.13 \tag{2.35}$$

$$K_t = 0.46 - 0.3\frac{R_c}{H_s} \qquad \text{when} \quad -1.13 < \frac{R_c}{H_s} < 1.2 \tag{2.36}$$

$$K_t = 0.10 \qquad \text{when} \quad 1.2 < \frac{R_c}{H_s} < 2.0 \tag{2.37}$$

where R_c is the crest freeboard, the distance between still water level and the crest of the structure.

Disadvantages of this expression are that all influence of the wave height is lost when R_c becomes zero, resulting in large scatter and that not much information on breakwater properties are taken into account, which also leads to considerable scatter around the proposed line.

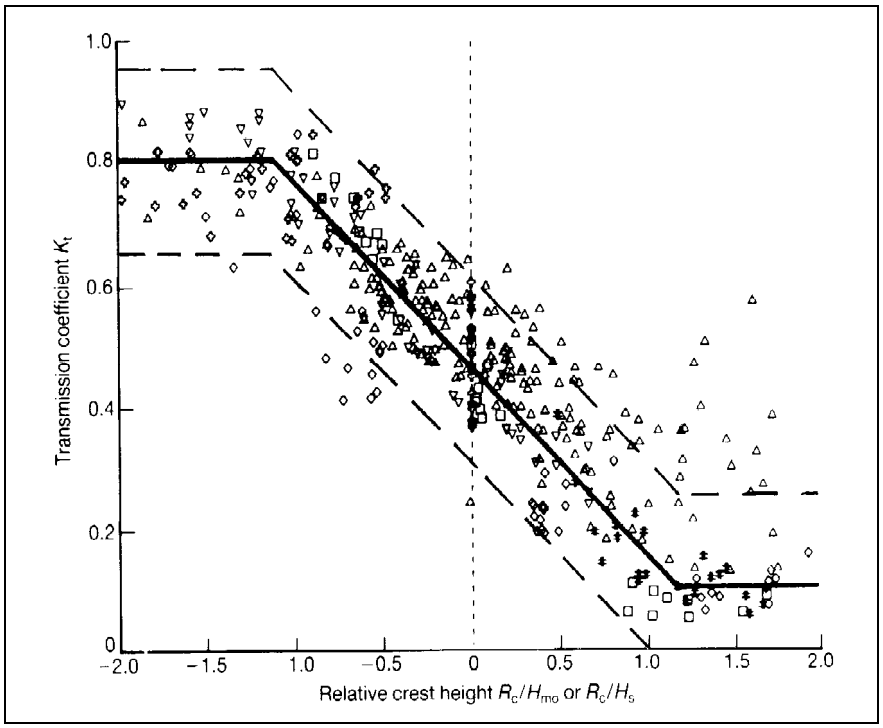

figure 2-7, Wave transmission over and through low-crested structures

Daemen (1991) used another parameter to create a dimensionless crest freeboard, namely D_{n50}. He found the following formula for wave transmission:

$$K_t = a\frac{R_c}{D_{n50}} + b \tag{2.38}$$

where:

$$a = 0.031\frac{H_i}{D_{n50}} - 0.24 \tag{2.39}$$

$$b = -5.42 \cdot s_{op} + 0.0323 \frac{H_i}{D_{n50}} - 0.0017 \left(\frac{B}{D_{n50}} \right)^{1.84} + 0.51 \qquad (2.40)$$

where H_i = the incident wave height at the toe of the structure
D_{n50} = the nominal diameter
s_{op} = fictitious wave steepness, using T_p
B = the crest width

This formula is valid when:

$$1 < \frac{H_s}{D_{n50}} < 6 \text{ and } 0.01 < s_{op} < 0.05$$

De Jong (1996) collected data from several investigations on wave transmission and formulated a new relation describing wave transmission:

$$K_t = -0.4 \frac{R_c}{H_{si}} + \left(\frac{B}{H_{si}} \right)^{-0.31} * \left(1 - e^{-0.5 \cdot \xi} \right) * 0.64 \qquad (2.41)$$

here $0.075 < K_t < 0.8$

The formula is valid within the following limits:

$$1.57 < \xi < 6.63$$
$$0.75 < \frac{B}{H_{si}} < 8.33$$

2.6.2 Wave overtopping

If extreme run-up levels exceed the crest level, the structure will be overtopped. This overtopping occurs for relatively few waves under the design event. It is therefore not possible to avoid overtopping, only some limits to overtopping have to be investigated.
The definition of overtopping that is used in this study is:

Overtopping deals with the total amount of water passing the line where the slope of the breakwater changes into the crest of the breakwater.

Since run-up and overtopping are closely related this definition is of use when describing run-up as well. Run-up is measured at the exterior of the armour layer since overtopping according to the definition is measured at the exterior of the armour layer. In figure 2-8, wave overtopping is depicted.

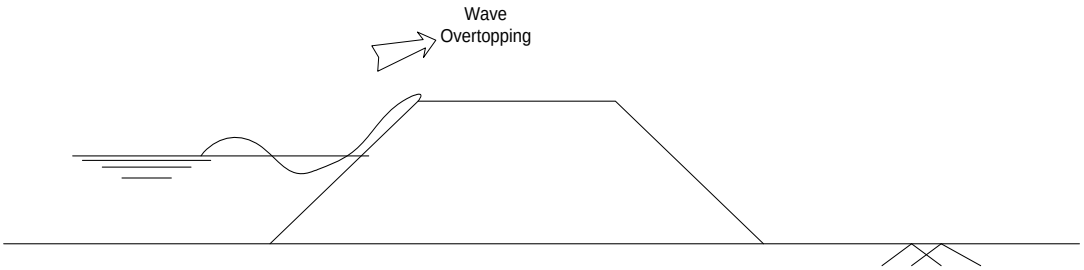

figure 2-8, Definition of wave overtopping

Owen (1980) relates a dimensionless discharge parameter, *Q*, to a dimensionless freeboard parameter, *R*, by an exponential equation of the form:

$$Q = ae^{-bR/\gamma} \tag{2.25}$$

The definitions of *Q* and *R*, as given by Owen are:

$$Q = \frac{q}{\sqrt{gH_s^3}}\sqrt{\frac{s_{om}}{2\pi}} \tag{2.26}$$

$$R = \frac{R_c}{H_s}\sqrt{\frac{s_{om}}{2\pi}} \tag{2.27}$$

The values of a and b were derived from the test results and given in the next table:

Slope	a	b
1:1	0.00794	20.12
1:1.5	0.0102	20.12
1:2	0.0125	22.06
1:3	0.0163	31.9
1:4	0.0192	46.96
1:5	0.025	65.2

table 2-1, Values for a and b to be used in equation (2.25)

De Waal and Van der Meer (1992) used the Owens data besides their own measurements. They came to two approaches to describe overtopping, one by relating the overtopping to wave run-up and the other by treating overtopping on its own.

When relating the overtopping to wave run-up De Waal and Van der Meer defined a relative crest freeboard as a "shortage of run-up height" divided by the significant wave height: $(R_{u2\%}-R_c)/H_s$. In figure 2-9, on the X-axis, the zero value is equal to the 2% run-up height.

The formula that describes more or less the average of the data in the figure is given by an exponential function, as proposed by Owen (1980):

$$Q = 8\cdot 10^{-5} e^{3.1\frac{(R_{u2\%}-R_c)}{H_s}} \tag{2.28}$$

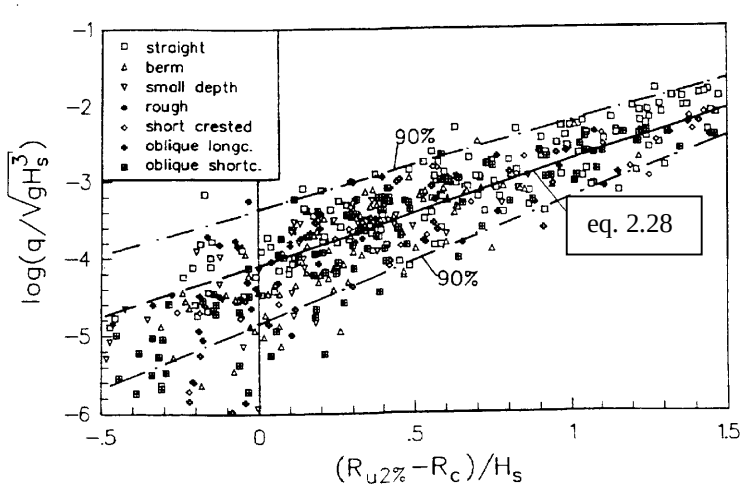

figure 2-9, Wave overtopping on slopes as a function of wave run-up

Analysing wave overtopping as a separate phenomenon, De Waal and Van der Meer found that the wave overtopping should be divided into situations with breaking and non-breaking waves. The definitions for dimensionless overtopping discharge and dimensionless crest height are:

$$Q_b = \frac{q}{\sqrt{gH_s^3}} \sqrt{\frac{s_{op}}{\tan\alpha}} \tag{2.29}$$

$$R_b = \frac{R_c}{H_s} \frac{\sqrt{s_{op}}}{\tan\alpha} \frac{1}{\gamma} \tag{2.30}$$

$$Q_n = \frac{q}{\sqrt{gH_s^3}} \tag{2.31}$$

$$R_n = \frac{R_c}{H_s} \frac{1}{\gamma} \tag{2.32}$$

Here γ is a reduction factor taking the influences of slope roughness, oblique wave attack, a berm and a shallow foreshore into account. The reduction factor γ is described by De Waal and Van der Meer (1992), and is dealt with in detail in section 3.2.

Chapter 3 Wave run-up

3.1 Introduction

In this chapter the wave run-up on a rough, permeable slope is described. When a rubble mound breakwater is considered, the outer slope can be defined as rough and permeable. First the phenomenon wave run-up itself is discussed. After that, the parameters that play a role in the run-up on a rough, permeable slope will be dealt with. The aim of this review of the parameters that play a role in the run-up on a rough permeable slope is to get insight in the mechanisms that cause the run-up on a rock armoured breakwater to be different from the run-up on a breakwater covered with a concrete armour unit like the tetrapod.

3.2 Wave run-up phenomenon

When waves encounter the slope of a breakwater, these waves will move up the slope. This so-called wave run-up can be defined as:

Wave run-up is the extreme level of water oscillation that is reached in each wave caused by wave action.

Run-up is defined relative to the static water level. The run-up level is used to determine the level of the structure crest, the upper limit of protection or other structural elements, or as an indicator of possible overtopping.
Wave run-up is often indicated by $R_{u2\%}$, this is the run-up level that is exceeded by two percent of the incoming waves.

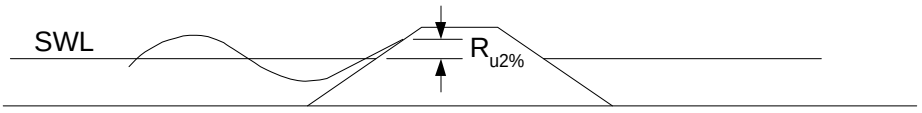

figure 3-1, Run-up definition

The analysis and especially the description of wave run-up can be done in two different ways. One way is using the Iribarren parameter as it is defined by Battjes (1974), see section 2.5.3.
For a gentle smooth impermeable slope, Battjes (1974) defined run-up as:

$$\frac{R_{u2\%}}{H_s} = C\xi_p \qquad (3.1)$$

in which ξ_p = the surf similarity parameter, using T_p instead of T_m, with C between 1.3 and 1.7.

Van der Meer (1993) concluded that the existing formulae for run-up on impermeable smooth slopes could not be adapted for run-up on permeable rough slopes. Relationships of the run-up relative to the Iribarren number proposed by Van der Meer and Stam (1992) for a rock slope with an impermeable core ($P = 0.1$) are given by:

$$\frac{R_{ux}}{H_s} = a\xi_m \qquad \text{for } \xi_m < 1.5 \qquad (3.2)$$

$$\frac{R_{ux}}{H_s} = b\xi_m^c \qquad \text{for } \xi_m \geq 1.5 \tag{3.3}$$

The maximum run-up for permeable structures (*P > 0.4*) is limited to the maximum:

$$\frac{R_{ux}}{H_s} = d \tag{3.4}$$

The notional permeability parameter *P* is described in section 2.4.3.

The coefficients *a, b, c* and *d* are given in table 3.1. They are dependent on the exceedance level *x*. Mostly the 2% or significant run-up is used.

Run-up level	**a**	**b**	**c**	**d**
0.1%	1.12	1.34	0.55	2.58
1%	1.12	1.24	0.48	2.15
2%	0.96	1.17	0.46	1.97
5%	0.86	1.05	0.44	1.68
10%	0.77	0.94	0.42	1.45
significant	0.72	0.88	0.41	1.35
mean	0.47	0.60	0.34	0.82

table 3-1, Coefficients in run-up equations (3.2)-(3.4)

In figure 3-2, the equations (3.1)-(3.4) are shown.

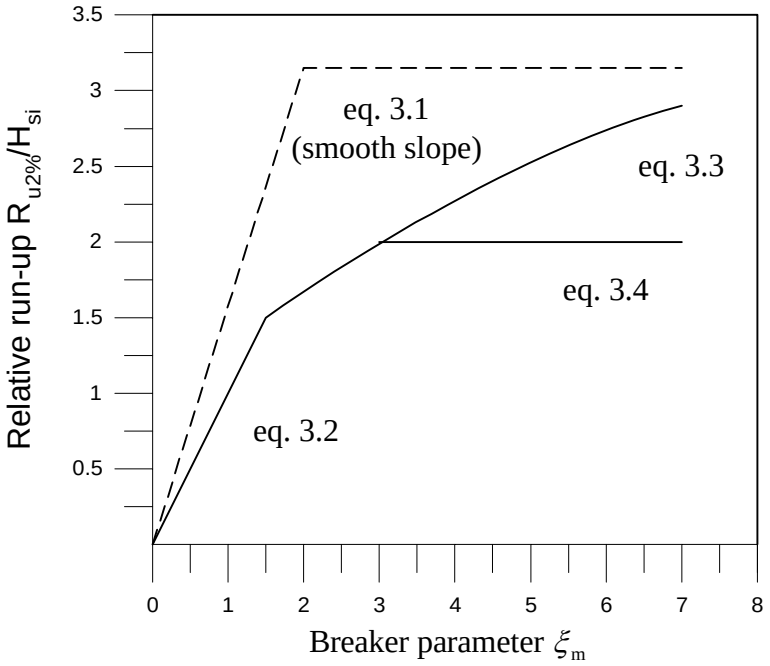

figure 3-2, Relative 2% run-up on rock slopes

The other method of describing the wave run-up is by using a Weibull distribution.

This Weibull distribution can be written as:

$$R_{up} = b\left(-\ln p\right)^{\frac{1}{f}} \tag{3.5}$$

where p = probability of exceedance (between 0 and 1); R_{up} = run-up level exceeded by p*100 per cent of the run-up levels; b = scale parameter; f = shape parameter.

The shape parameter f defines the shape of the curve. For $f = 2$, a Rayleigh distribution is found.

Analysis by van der Meer showed that the scale parameter b could not be described by ξ_m. A graph of b/H_s versus ξ_m showed different curves for different slope angles. Therefore, the slope $cot\alpha$ and the wave steepness s_m were treated independently. The scale parameter can be described as following:

$$\frac{e}{H_s} = 0.4 s_m^{-0.25} \cot\alpha^{-0.2} \tag{3.6}$$

The shape parameter is described by:

$$f = 3.0\xi_m^{-0.75} \qquad \text{for plunging waves} \tag{3.7}$$

and

$$f = 0.52 P^{-0.3} \xi_m^{p} \sqrt{\cot\alpha} \qquad \text{for surging waves} \tag{3.8}$$

Here P is the notional permeability parameter as described in section 2.4.3.

The transition between the two shape parameters is described by a critical value for the surf similarity parameter, ξ_{mc}:

$$\xi_{mc} = \left(5.77 P^{0.3} \sqrt{\tan\alpha}\right)^{1/(P+0.75)} \tag{3.9}$$

For $\xi_m < \xi_{mc}$, the first formula should be used and for $\xi_m > \xi_{mc}$, the second formula is appropriate. The wave run-up distribution formulas are only applicable for slopes with $cot\alpha \geq 2$. For steeper slopes, the run-up distribution on a 1:2 slope may give a first estimation.

For dikes and revetments Van der Meer and Janssen (1994) gave a prediction formula based on the surf similarity parameter. Reduction factors were used to take slope roughness (γ_f), oblique wave attack (γ_β), a berm (γ_b) and a shallow foreshore (γ_h) into account. This formula is given by:

$$\frac{R_{u2\%}}{H_s} = 1.6 \cdot \gamma_f \gamma_\beta \gamma_h \xi_{eq} \tag{3.10}$$

with a maximum of 3.2 $\gamma_f \gamma_\beta \gamma_h$

in which $\xi_{eq} = \gamma_b \xi_{op}$

The slope roughness reduction factor (γ_f) is only applicable for ξ_p < 3 to 4. The range of values covered by these values is: 1.0 for smooth, impermeable slopes to 0.5 for rock/riprap slopes. The exact values are given in appendix I.

The reduction factor that is found empirically for run-up of oblique waves (γ_β) can be described by the following formulae (Manual on the use of Rock, 1995):

- short-crested waves: $\gamma_\beta = 1 - \left(\frac{\beta}{500}\right)$
- long-crested waves: $\gamma_\beta = 1$ for $0° < \beta < 10°$

  $\gamma_\beta = 1 - \cos(\beta - 10°)$; $\min(\gamma_\beta) = 0.6$ for $\beta \geq 60°$

When a berm is considered, the reduction factor (γ_b) is derived for plunging and surging waves:

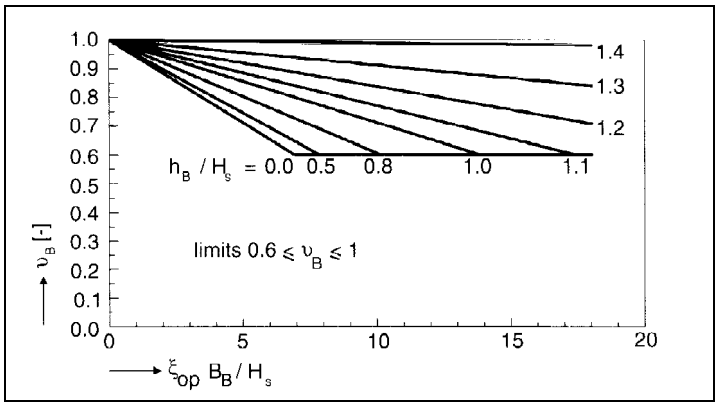

figure 3-3, Run-up reduction due to berms for plunging waves (MUR, 1995)

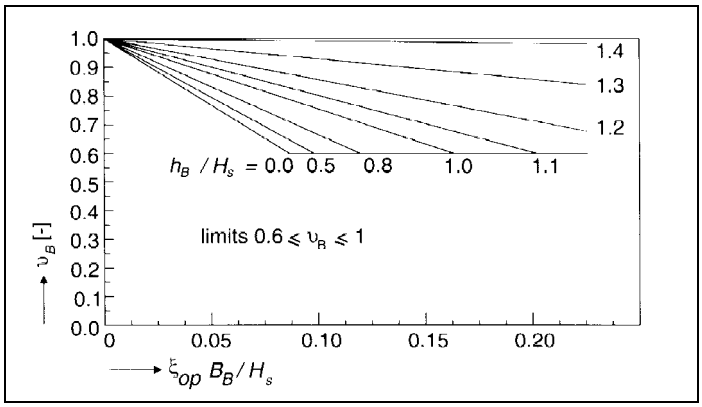

figure 3-4, Run-up reduction due to berms for surging waves (MUR, 1995)

The reduction factor for a shallow foreshore can be calculated using the following formula (van der Meer and Janssen, 1994):

$$\gamma_h = \frac{H_{2\%} / H_s}{1.4}$$

where $H_{2\%}$ = the wave height exceeded by 2% of the waves

3.3 Parameters involved in the run-up

3.3.1 Introduction

Run-up, the maximum water elevation due to wave action on a slope has been discussed in the previous section. In the following sections, the various parameters influencing the run-up on a slope will be dealt with. The various parameters are:

1. Hydraulic parameters (characteristics of the waves)
   - Wave height
   - Wave period and connected with this, the wave steepness
2. Structural parameters (characteristics of the structure)
   - Slope angle
   - Slope roughness
   - Permeability of the structure
   - Permeability of the armour layer

3.3.2 Wave height

The run-up on a slope is directly related to the height of the waves that attack the slope. The higher the waves, the higher the run-up will be.
The wave height can not be separated from the wave period and the water depth; altogether they make up the wave steepness. Researchers like Battjes (1974) and Van der Meer (1988) have given a relationship between the run-up and the wave height looking like:

$$\frac{R_{ux}}{H_s} = a\xi_{op}^b \tag{3.11}$$

The subscript x indicates whether the 2%, significant (s) or mean (m) run-up is meant. The parameter ξ_{op} is the Iribarren parameter calculated with the peak period and the deep water wave height. The two parameter a and b are constants. The wave height is used to obtain a dimensionless parameter in combination with the run-up.

3.3.3 Wave period

The influence of the wave period is taken into account by using the fictitious wave steepness. The fictitious wave steepness is a measure for the kind of wave that attacks the structure. It is given by:

$$s_{op} = \frac{2\pi H_s}{gT_p^2} \tag{3.12}$$

When a wave encounters a slope it can break or it can not break. The two different kinds of wave breaking, as it is called, result in two different kinds of energy dissipation. The transition between breaking and non-breaking of the waves on a slope is not only dependent on the wave steepness, but also on the slope angle. The combination of slope angle and wave steepness is given by the Iribarren number or breaker parameter, which is given by (see also section 2.3.3):

$$\xi = \frac{\tan\alpha}{\sqrt{s}} \tag{3.13}$$

Roughly it can be said that breaking waves occur when $\xi < 2.5$ and surging or non-breaking waves occur when $\xi > 2.5$. For the two different kind of breaking waves two different kind of formula to describe the run-up on a slope are derived by Van der Meer (see also section 2.5.1).

3.3.4 Slope angle

The influence of the slope angle on the run-up is partly described by the Iribarren number. There it is used to describe the kind of waves breaking on the slope. This is not the only influence, when the angle of the slope is smaller, the slope is milder and the run-up will reduce. This is due to the fact that a mild slope will increase the distance that the waves have to travel in order to reach the crest. So here the influence of the slope angle has to be seen in combination with roughness of the slope.

3.3.5 Slope roughness

The roughness of the armour layer surface will influence the run-up on a given slope. The rougher the slope, the more turbulence will be induced to the waves that attack the slope. More turbulence gives more energy dissipation and therefore the run-up will be lower. In figure 3-1, this can be seen. There is a great difference in relative run-up between rough and smooth slopes, when $\xi_p < 6$. For $\xi_p < 2.5$ the largest difference is visible. So especially in the region of breaking waves, the roughness seems to have influence on the run-up on a slope.

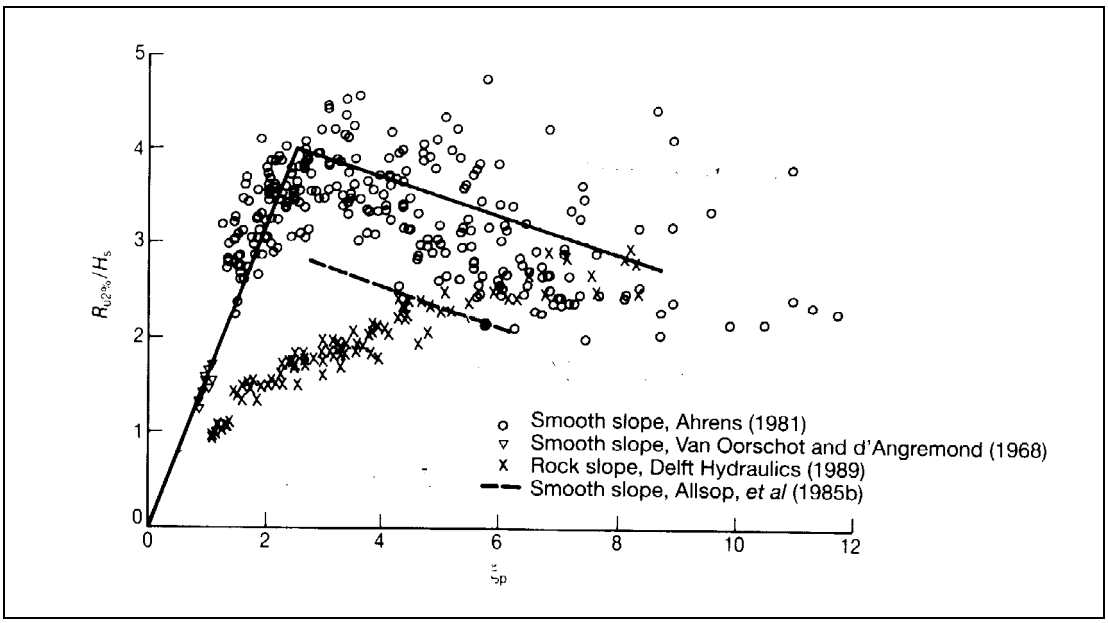

figure 3-5, Comparison of relative 2% run-up for smooth and rubble slopes

Up until now, the roughness of a slope is accounted for by a reduction factor, which is used in the run-up formulae. Klein Breteler and Pilarczyk (1996) introduced a run-up reduction factor that is based on the ratio of run-up on a rough slope and run-up on a smooth slope. The factor is given by:

$$f = \frac{\left[R_{u2\%}\right]_{rough}}{\left[R_{u2\%}\right]_{smooth}} \tag{3.14}$$

with: $[R_{u2\%}]_{rough}$ = wave run-up on a slope with roughness elements
$[R_{u2\%}]_{smooth}$ = wave run-up on a smooth slope without roughness elements

The maximum run-up reduction was found for a slope where 4% of the area was covered with roughness elements. The reduction factor is derived for a smooth slope like a dike, where the run-up can be lowered by placing artificial roughness elements.

The formulae of Van der Meer for the run-up on a rock slope, equations (3.2) and (3.3) incorporate the influence of the roughness of the slope but they do not use a physical defined roughness to describe the wave run-up.

3.3.6 *Permeability of the structure*

The influence of the permeability of the structure is usually given by a notion that the structure is permeable or impermeable. Van der Meer (1988) defined a notional permeability factor (*P*) to take the permeability of a structure into account when he derived the formula for stability of a breakwater. It is a mathematical way of implementing the permeability of the structure into his formulae. The notional permeability factor is associated with the ratio of the diameters of the different layers.
When the permeability of a breakwater is considered, one has to keep in mind that most breakwaters consist of multiple layer, which all have different hydraulic properties. When permeability is considered in soil mechanic science, the permeability of one layer is considered in combination with the permeability of the other layers. The smallest permeability has the largest effect on the permeability of the structure as a whole.

The flow of water in a porous medium that is permeable is described by the equation of Forchheimer:

$$I = a \cdot u + b \cdot u \cdot |u| + c \cdot \frac{\partial u}{\partial t} \tag{3.5}$$

here:

$$a = \alpha \frac{(1-n)^2}{n^3} \frac{\nu}{gD^2} \tag{3.6}$$

$$b = \beta \frac{1-n}{n^3} \frac{1}{gD} \tag{3.7}$$

$$c = \frac{1+\gamma \frac{1-n}{n}}{ng} \tag{3.8}$$

with

α,β and γ	=	dimensionless coefficients
n	=	the porosity of the layer
ν	=	the kinematic viscosity

D	=	a characteristic diameter
g	=	the gravitational acceleration

Equation (3.6) gives the laminar term of the Forchheimer equation, (3.7) is the turbulent term and (3.8) is the inertial term.

Van Gent (1995) performed experiments to find out what the contribution of the three above-mentioned terms of the Forchheimer equation to the pressure gradient. He found that the turbulent term was the first and the inertial term was second in influence. The results are given in figure 3-2.

Inertia can be linked to the permeability of the structure. A structure that is permeable according to definition of Van der Meer (fig 2-3), will have an influence on the run-up. Water is present inside the structure and when waves attack the structure, the inertia of the water inside the structure will reduce the run-up capacity of the waves. It is likely that this will happen in case of non-breaking waves. This type of waves usually has large periods and therefore, the water inside the structure is able to 'follow' the waves. Breaking waves usually move faster and it is likely that the energy dissipation of those waves will mainly not take place by inertia of the water inside the structure; these waves will loose energy by breaking and dissipating their energy inside the armour layer. According to Battjes (1988), the formation of a large-scale vortex takes place so quickly that viscosity can have no significant effects except at microscales. Vortex formation as such therefore causes no immediate decrease of the total kinetic energy of the large-scale motion, although it does imply a loss of energy that can be ascribed to the wave. A rapid decay of wave height can take place that is not accompanied by an induced mean horizontal pressure gradient.

Due to the quick motion of swash and back swash, the phreatic surface inside the slope will not be able to keep up. The water will infiltrate into the unsaturated zone and dissipate energy due to turbulent friction. So, breaking waves dissipate energy due the breaking phenomenon itself and due to turbulent friction on and in the slope.

Permeability of the structure therefore will have the biggest influence on the run-up when surging waves are considered. Its influence on breaking waves probably can be neglected.

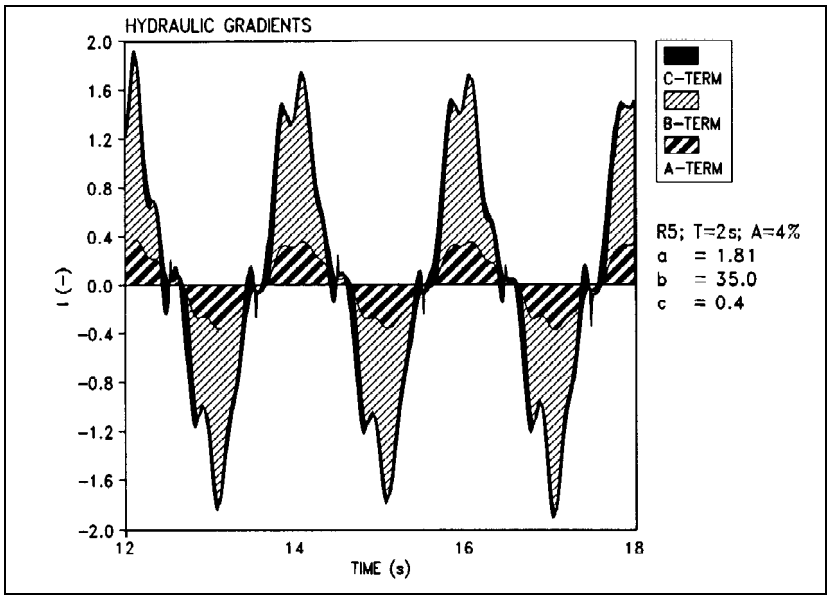

figure 3-6, Contributions of the different terms of the Forchheimer equation to the hydraulic gradient

3.3.7 Permeability of the armour layer

The permeability of the armour layer is the main driving force when waves break on the structure's slope. As can be seen in figure 3-6, the turbulence that arises inside the armour layer is the main contribution to the energy dissipation inside a porous layer. In order to describe the permeability of the layer, many investigators have used different equations. Although the equations all differ, they have one thing in common: the permeability is a function of the porosity of the layer and the diameter of the armour units.

When turbulence is taken as the main term of the Forchheimer equation, the permeability that can be derived from it looks like:

$$k \sim \left(n^3 - n^2\right)Dg \text{ or } k \sim n^a Dg \tag{3.9}$$

where *a* is a constant.

According to the Manual on the use of Rock (1995),

$$k \sim \sqrt{\left(n^5 Dg\right)} \tag{3.10}$$

The fact that run-up is affected by the permeability of the layer, which consists of the porosity of the layer combined with the diameter of the armour units can be explained. To have pores, or said differently, to have air inside the layer, the layer has to be porous. The size of pores inside the layer is dependent on the size of the units. When the size of the pores is big, water waves will be enabled to lose energy inside the pores. More space is available for the waves to dissipate energy through turbulence. This permeability has to be seen relative to the size of the waves that attack the structure. Huge waves attacking a layer of relatively small permeability will dissipate energy, but the effect on the total run-up will be small.

One other thing has to be said about permeability in relation to porosity. The layer has to consist of loose material in order to be permeable. One can compare this with Swiss cheese, no permeability but the layer is porous.

Chapter 4 Experiments

4.1 Introduction

In this chapter experiments that are performed both in Delft, the Netherlands and in Iran, will be described and discussed. The goal of the experiments performed in Delft is to give insight in the parameters that play a role in the run-up of waves on a rubble mound breakwater. This goal was inspired by the question why run-up on a rock-armoured breakwater is lower than run-up on a tetrapod-armoured breakwater, which was found due to the experiments performed in Iran, see also figure XIV-1.

The experiments as performed in Delft at the Laboratory of Fluid Mechanics of the Delft University of Technology were designed to give insight in the physic parameters that play a role. The experiments in Delft were performed to be able to give an answer to the question:

"How can the influence of roughness of the slope and resistance of the armour layer to water movement on the run-up of waves on a permeable rough slope be quantified?"

The experiments performed at the Delft University of Technology are a schematisation of reality with no permeability of the layer beneath the armour layer, whereas the experiments performed in Iran used a model that is more close to reality. Since the experiments in Iran were performed with a cross-section of a breakwater, the permeability of the whole structure plays a role in the run-up levels reached by waves. The experiments as performed in Iran are used to draw a comparison between the results of these two model situations.

In order to be able to give an answer to the above posed question, the experiments performed at the Delft University of Technology had to be carried out changing all the properties of the armour layer independently. The behaviour of waves on the slope is changed for each composition of the armour layer.

4.2 Experiments performed at the Delft University of Technology

4.2.1 Introduction

The experiments took place in the Laboratory of Fluid Mechanics of the subfaculty of Civil Engineering of the Technical University of Delft. Here a flume of 36.5 meters was available, in which a wave paddle was placed that was able to generate regular waves. A specially designed case was placed at the end of the flume on which the run-up could be measured for different angles and different armour units. In the next sections the experimental set-up will be described and after that, the measurements are discussed.

The main goal of the experiments in Delft is to distinguish a relation between run-up on a slope and the roughness of this slope and the resistance of the slope to water movement inside the slope respectively.

In order to achieve the goal, some constraints have to be defined:

- The waves used to attack the slope are regular waves, this is defined by the available wave flume
- The structure beneath the layer of armour units will be impermeable
- Wave trains are used in order to prevent re-reflected waves from the wave paddle to disturb the observations of the run-up on the slope
- The water depth is kept constant.

4.2.2 Experimental program

The run-up on the rough and porous slope will be measured at different compositions of the slope. The parameters that can be altered to achieve different compositions of the slope are:

- Diameter ($D_{n(50)}$) of the armour unit
- Porosity of the slope

Using different kinds of armour units can alter the porosity of the slope. The porosity of a layer of rock units will be around 38 %, the porosity of a layer consisting of tetrapods is around 50 %. By using these two armour units the porosity of the slope will be changed.

Changing the porosity of a layer consisting of one armour unit is difficult since the wave action will make the layer as compact as possible. A porosity of 50% that is laid on a layer of rock by placing the units more apart of each other will reduce under wave attack to a value that will be close to the earlier mentioned value of 38 %. The actual porosity is hard to determine and the composition of the slope has altered during the experiments, which make the result of the experiments less reliable.

The diameters of the armour layer that were to be used were dependent on the available model size tetrapods. These tetrapods were borrowed from Delft Hydraulic, location "De Voorst". Three clearly different diameters in right amount were available at Delft Hydraulics. The diameters of the rock that was used were chosen around the values of the diameters of the tetrapods.

The grading of the rock material was chosen narrow, this is in line with coastal engineering practice where narrow rock gradings are used for the construction of breakwaters. A narrow grading means that:

$$\frac{D_{85}}{D_{15}} = 1.2 \text{ to } 1.5$$

Where D_{85} is the value of the gradation for which 85% of the gradation is smaller.
D_{15} is the value of the gradation for which 15% of the gradation is smaller

The value of D_{85} is a measure for the largest stones in a rock gradation whereas the value of D_{15} is a measure for the smallest stones in the gradation.

In the case of tetrapods, the values of D_{85} and D_{15} have no meaning since all tetrapod units have equal size. The values of D_{85} and D_{15} will be equal to the height of the unit.

Each composition of the slope will be attacked by waves with different behaviour on the slope. This will be achieved by changing the value of the breaker parameter, ξ. The value of ξ can be altered by changing the variables H, T and α (wave height, wave period and slope angle respectively).

The slope angle is varied three times. Although the slope angle for a tetrapod breakwater is hardly even different from 1:1.5 due to economic reasons, slope angles of 1:3 and 1:4 are applied as well. this because the slope angles of a breakwater covered with rock armour units are constructed in the range of 1:3 and 1:4. When a comparison has to be made between run-up on a rock slope (porosity of ≈ 38%) and tetrapods slope (porosity ≈ 50%) these slopes have to be tested with equal slope angles.

The influence of the wave period had to be inquired to get a full picture of the influences of different behaviour of the waves on the slope. To keep the amount of experiments in check, the period is varied only two times. The wave flume determined the values of the wave period.

The wave height is varied five times for each composition of the slope, each slope angle and each wave period. The maximum value of the wave height was determined by the stability of the stones on the steepest slope. No movement of stones was to appear in the experiments since movement of stones would alter the composition of the slope. Each experiment is carried out twice in order to obtain a consistent experiment.

So in total, the following parameters are varied:

Variable	Notation	Variation	Range
Diameter rock	D_{n50}	3 times	0.027 m, 0.045 m, 0.065 m
Diameter tetrapods	D_n	3 times	0.036 m, 0.044 m, 0.050 m
Porosity	n	2 times	38%, 50%
Wave height	H	5 times	0.03 m – 0.14 m
Wave period	T	2 times	1.12 s, 1.54 s
Slope angle	α	3 times	1:1.46, 1:3, 1:3.87

table 4-1, Variation of parameters in the experiments performed in Delft

The water depth was kept constant at a value of 0.3 meter. This value represents shallow water at the toe of the structure and is a result of a balancing procedure to obtain the maximum wave height attacking the slope in combination with the maximum permissible run-up along the slope where this run-up will not reach the end of the slope.

4.2.3 Material

As mentioned before, rock and tetrapods were used to construct the slope. The tetrapods were obtained from Delft Hydraulics and the typical dimensions of the tetrapods are:

Height (m)	Nominal diameter, D_n (m)	Weight (kg)	mass density, ρ (kg/m^3)	material
0.055	0.036	0.102	2324	epoxy
0.068	0.044	0.202	2303	mortar
0.079	0.050	0.313	2435	epoxy+

table 4-2, Variation of the properties of the tetrapods used in the Delft experiments

In figure 4-1, the dimensions of a tetrapod are given. Here the height of the tetrapod unit is given by H.

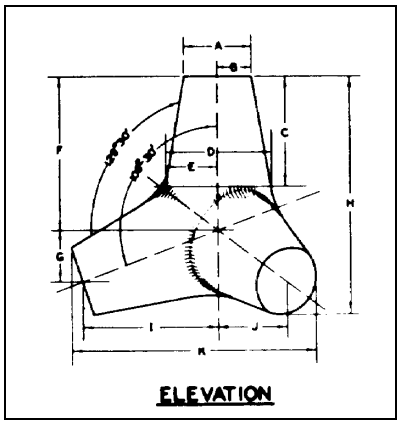

figure 4-1, Dimensions of a tetrapod unit

The rock units that were used had to be sorted from a big pile of rock. By weighing the rock the gradation was formed. The available sieves at the Laboratory of Fluid Mechanics were not big enough to sieve the stones that were needed for these experiments. The gradation had to be narrow, so for the weight of the stones, the following restriction was given:

$$\frac{W_{85}}{W_{15}} = 1.7 \text{ to } 3.4$$

Using this criterion, the stones were selected. After selecting them by weight, the stones were measured in three directions:

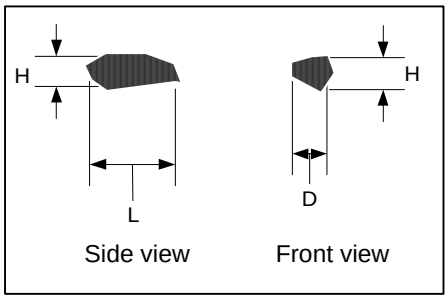

figure 4.2, Dimensions of a rock unit

The largest value of H and D is used as representative for the dimension of a sieve.

This results in the following characteristics of the stones used in the experiments:

M_{50} (kg)	ρ_s (kg/m^3)	D_{n50} (m)	D_{85} (m)	D_{15} (m)
0.84	3005	0.065	0.074	0.048
0.25	2680	0.045	0.048	0.030
0.05	2600	0.027	0.03	0.021

table 4-3, Variation of the properties of the rock used in the Delft experiments

4.2.4 *Wave flume*

As mentioned before, the wave paddle in the flume was only capable of making regular waves. As a result, the experiments were carried out with wave trains. Wave trains can be described as a short

burst of waves released from the wave paddle. This is done since the waves reflect on the slope and the reflected waves return to the wave paddle where they reflect once again. The interaction between reflected waves from the slope and waves generated by the paddle results in waves that no longer can be described by a combination of the parameters *H* and *T*. So before the re-reflected waves reach the slope, all measurements have to be done and the experiment can be stopped. For this, the wave trains are used. An experiment with wave trains only lasts for about 20-30 seconds.

In the flume two wave height meters are placed in order to be able to measure the period of the waves and the wave height. One wave height meter was placed on the toe of the structure in order to measure the wave height there. The second was placed near the wave paddle. The wave height meter that was placed near de wave paddle was placed with some distance from the paddle in order to let the waves develop themselves after being generated by the paddle. Figure 4-3 gives a sketch of the wave flume with the positions of the wave height meters in it.

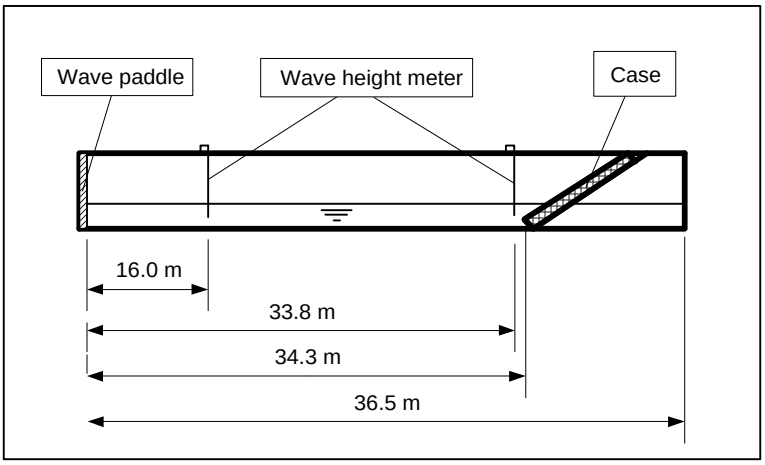

figure 4-3, Positions of wave height meters in wave flume

4.2.5 Model

The model that was used to perform the experiments consists of a wooden board that is supported by a steel frame. The steel frame was fixed to the board to keep the board inflexible under wave attack. On top of the wooden board a steel girder was fixed, attached to the steel girder was a steel fence work. The task of the fence work is to form a basket or case that can hold the rock or tetrapod units. The case that is formed with the wooden board as base and the fence work as sides is open at the top side and the permeable at the sides. On the wooden board gravel was glued to give the armour units some grip. The gravel is assumed to have no influence on the hydraulic behaviour of the layer that is constructed with the armour units.

By fixing two bars with screw thread to the steel framework at one side of the model, this side could be lifted of the bottom of the flume. Each desired slope angle could be obtained by fixing the bars with screw thread with a nut. Figure III-1 in appendix III, shows the case that is used to perform the experiments.
In figure 4-4 a close look is taken at the case when it is placed inside the wave flume.

4.2.6 Measuring run-up

The run-up of waves on the slope was recorded by a digital video camera that was placed above the slope. The video camera recorded the movements of the waves on the slope and the signal of the wave height meter that was placed at the toe of the structure. This signal was displayed on a

computer screen that was placed on a table next to the wave flume, see the sketch in figure 4-5. In this way the run-up was recorded simultaneously with the signal of the wave gauge. A direct relation between the run-up on the slope and the measured waves was established.

To be able to measure the run-up along the slope, a ruler was fixed on top of the armour layer during each experiment. So when the videotape with the movements of the waves on the slope was analysed, the Still Water Level (SWL) could be read from the ruler and the run-up level could be read as well. The run-up on the slope was measured here at the outer side of the slope. Deducting the Still Water Level from the run-up level gives the run-up height along the slope. By multiplying this run-up height along the slope by $\sin\alpha$, the run-up height was determined. See also figure 4-6 for an illustration.

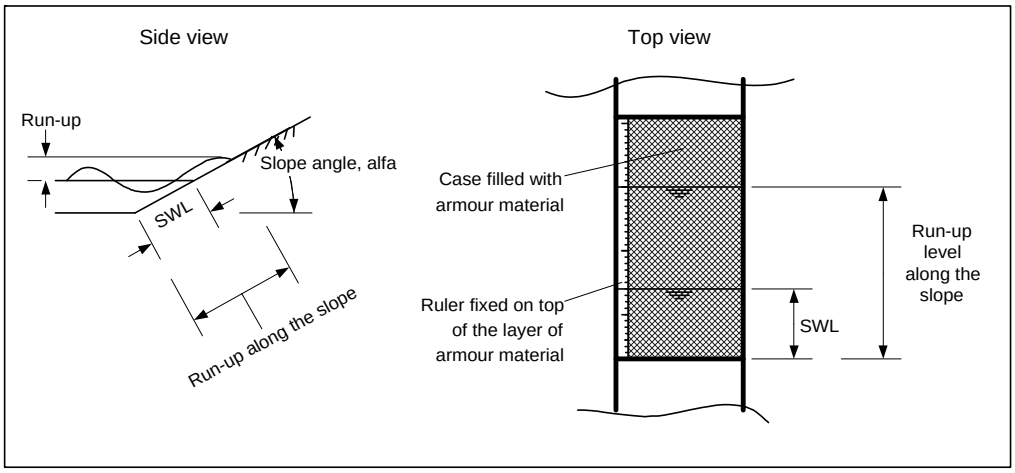

figure 4-6, Measuring run-up

The recordings made with the digital video camera were analysed on a television screen. By using a small ruler to fix the water level that was seen on the television screen, the Still Water Level and run-up height along the slope could be determined for each experiment with an accuracy of 1 centimetre.

In appendix IV, the results of the analysis of the video recordings are given.

4.3 Experiments performed in Iran

4.3.1 Introduction

During a stay in Tehran, Iran, as a guest of the Sharif University of Technology, experiments were performed at the Jehad Water and Water management Research Corporation (JWRC) in Tehran. These experiments were performed in the designing process of a breakwater that was to be constructed of tetrapods. As a part of the design, the hydraulic responses of breakwater covered with a tetrapod armour layer were investigated. The hydraulic responses of a breakwater consist of run-up, run down, overtopping, reflection and transmission waves that attack the breakwater. From these responses all but the transmission were investigated through experiments. The goal of the experiments was to obtain data of the hydraulic responses on a breakwater covered with tetrapod armour units that could be compared to data of hydraulic responses on a breakwater covered with rock armour units. The experiments on the run-up of waves attacking a tetrapod breakwater are used in this thesis. They will be discussed here.

4.3.2 Experimental set-up

The original preliminary design of the breakwater was based on the program BREAKWAT. In this design a limited amount of overtopping of the breakwater was allowed. Since the measurements of run-up on a slope require the slope to be of infinite length, the design had to be altered a little and the scale of the experiment was doubled. In this way also the maximum run-up could be measured. Although run-up is usually represented as the 2% run-up, this is the run-up level that is exceeded by 2% of the waves, all run-up, including the maximum run-up, has to be measured to be able to calculate the 2% figure. When measuring the entire range of run-up levels during an experiment, including the maximum run-up level, no water will pass the crest and therefor no overtopping will take place.

When performing experiments on run-up, the stability has to be absolute. No armour units are allowed to displace. During the experiments it was found that at the beginning of the experiment one or two units moved, but after a small period of settlement, all units remained at their place.

4.3.3 Scale

The available model tetrapods were designed for a geometrically undistorted scale of $N = 53$. Geometrically undistorted means that the horizontal length scale is equal to the vertical length scale. So the model was geometrically equal to the prototype situation.

This scale was calculated using the weather conditions at the prototype site. Recalculations showed that with a scale of $N = 50$, the tetrapods were not to move as well.

The experiments were performed with two different model scales. The first scale of $N = 50$, was used to measure overtopping and reflection. In the case no overtopping occurred, the maximum wave run-up could be measured and these data have been used here too. The second scale of $N = 66$, was used to measure only wave run-up and reflection. In this case all the waves could reach their maximum run-up level and therefore all data on wave run-up collected in these experiments are used here.
An experiment were a scale is applied to model reality has to meet two mean scaling laws:

Froude law: $$\left(\frac{V}{gL}\right)_p = \left(\frac{V}{gL}\right)_m \tag{4.1}$$

where V = velocity
g = gravitational acceleration
L = length
The subscripts m and p stand for model and prototype respectively.

Expressing in terms of scale ratios and rearranging gives:

$$\frac{N_V}{\sqrt{N_g N_L}} = 1 \tag{2.2}$$

where N = scale factor

Reynolds law: $$\left(\frac{\rho LV}{\mu}\right)_p = \left(\frac{\rho LV}{\mu}\right)_m \tag{4.3}$$

where: ρ = fluid density

L = length
V = velocity
μ = dynamic viscosity

In terms of scale ratios, the Reynold model criterion is:

$$\frac{N_V N_L N_\rho}{N_\mu} = 1 \qquad (4.4)$$

When for both Froude and Reynolds law the similitude time scale is derived one gets:

Froude: $$N_t = \sqrt{\frac{N_L}{N_g}} \qquad (2.5)$$

Reynolds: $$N_t = \frac{\left(N_L\right)^2 N_\rho}{N_\mu} \qquad (2.6)$$

From equations (2.5) and (2.6) it is clear that in one model the both scale laws can not be applied. It is impossible to scale the time to the square root of the length and at the same time scale time to the square of the length.

Since it is not possible to meet both scaling laws, the Froude law is applied and a lower boundary for the Reynolds number of a model is given. This because gravity forces predominate in free-surface flows; and consequently, most models is designed using the Froude law.
If the Reynolds number of the model to be tested is higher than the boundary, one can say that water movement on and in both model and prototype is turbulent.

The Reynolds number (Re) was calculated using the shallow water wave velocity: $\sqrt{(gH)}$. This because the velocity of the wave on the slope is the driving force of the turbulence on and in the slope.

Using the formula:

$$\mathrm{Re} = \frac{\sqrt{gH}D_n}{\upsilon} \qquad (2.7)$$

with: g = gravitational acceleration
H = wave height (smallest applied in the experiments)
D_n = nominal diameter of the armour unit
ν = coefficient of kinematic viscosity, taken $1*10^{-6}$ for water

the Reynolds numbers of the models as tested are:

N = 50: $Re = 2.4*10^4$
N = 66: $Re = 2.3*10^4$

Different investigators give different lower boundaries for the Reynolds number, the range of these boundaries is: $6*10^3 - 4*10^5$. Van der Meer suggested a value of $4*10^4$. According to these values, no definite judgement can be given about viscous scale effects in the results of these experiments.

4.3.4 Material

Use is made of one size model tetrapod, so two sizes prototype tetrapods were used since two scales were applied. The dimensions of the model tetrapods are:

H_{tet} = 5.2 cm
D_n = 3.8 cm

where H_{tet} is the height of the tetrapod

This results in the following prototype dimensions:
N = 50 H_{tet} = 2.60 m
D_n = 1.69 m

N = 66 H_{tet} = 3.43 m
D_n = 2.23 m

Figure 4-7 shows the dimensions of a tetrapod

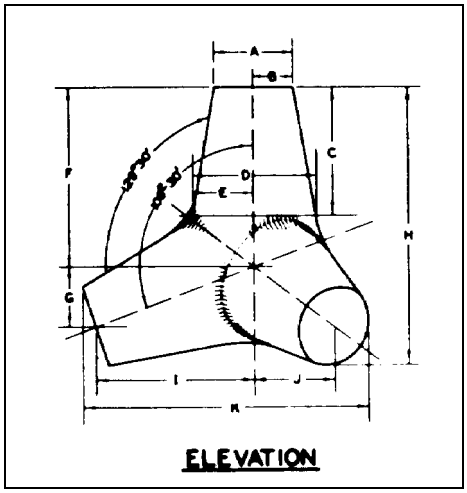

figure 4-7, Dimensions of a tetrapod armour unit

4.3.5 Hydraulic parameters

The wave generator was able to generate irregular waves. The program Wave Syntesizer, written by the Danish Hydraulic Institute operated the wave paddle. The wave spectrum that was used was the JONSWAP spectrum. This spectrum is a good representation of the wave conditions as they can be found in the Persian Gulf. The wave height and wave period were taken according to conditions to be found at the proposed site of the breakwater. These conditions are:

Significant wave height: H_s = 5 meter
Peak period: T_p = 14 seconds
Water depth: d = 13.5 meters

The conditions found at the proposed site are taken as upper boundary values for the experimental program. The prototype values of the experimental program are given below:

H_s (m)	2.5	3.5	4.5	5	5.5
T_p (s)	6	8	10	12	14

table 4-4, Experimental program Iran

In Appendix V, the cross-section of the model breakwater as it was tested in Iran can be found. Appendix VI gives the plan of the wave flume.

The program Wave Synthesizer was able to compute the reflection of waves from the structure. In order to measure the reflection, three wave gauges were placed in the middle of the flume between the wave paddle and the structure. The distance between the gauges can be calculated according to Goda:

$$0.05 < \frac{\Delta l}{L} < 0.45 \qquad (4.1)$$

where: Δl = the distance between two gauges
L = the wave length

Here the distance between two gauges was set to 35 cm, this is the distance between the two gauges that are most close to the structure. The distance between the second and the third gauge was set to half Δl.

After the program Wave Syntesizer determined the reflection coefficient, the incoming wave height could be calculated using:

$$H_{si} = \frac{H_{si+r}}{\sqrt{1+K_r^2}} \qquad (4.2)$$

4.3.6 Measuring devices

The run-up on the slope was measured by placing two wave gauges parallel to the slope. These gauges were fixed at an angle of 33.7 degrees (slope 1:1.5) and the distance between the slope and the gauge was about zero. The gauges were placed between the tetrapods, but care was taken that the gauge never touched a tetrapod. The water movement that was recorded in this way is discrete; at any moment in time, the location of the waterfront is known. Both wave gauges produced a signal that was acquired by the program Wave Syntesizer with a frequency of 40 Hz. From both signals the maximum value in each wave motion is extracted and from those value, the average is taken as representative for the run-up levels along the slope.

When a wave gauge is placed in water to measure the water movement, a layer of 4 cm water have to be present underneath the end of the gauge. Not in all experiments that were performed, the run-down of the waves staid above the end to gauges. The results of these experiments are not used in the analysis of wave run-up since the accuracy can not be guaranteed.

In total the data of 43 experiments could be used for the analysis of wave run-up on a breakwater covered with tetrapod armour units. In Appendix VII, the data of all different tests are given. They are given as prototype values since the program Wave Synthesizer gave the results as such.

The run-up on the slope was calculated by running a computer program that calculated the run-up for each wave. This was done by comparing the water level at one time step, measured by the two wave height meters, with the water level at the next time step. This resulted in an amount of run-up level for one test series. This amount corresponded with the amount of waves that was send from the wave paddle. From this amount of run-up levels, the 2% value was calculated.

The results of the experiments are discussed in chapter 5 and 6.

Chapter 5 Analysis of data

5.1 Introduction

In this chapter, two data sets are analysed. The data obtained from the experiments in the regular wave flume in Delft as described in section 4.2 will be analysed here first. The influences of the parameters H, $\cot\alpha$, D, n and T, on the run-up on a porous slope will be dealt with. Also the combination of the above-mentioned parameters like breaker parameter (ξ, roughness and permeability (a combination of D and n) will be discussed. Expressions that describe roughness and permeability of the armour layer are derived.

Secondly, the data obtained from the experiments in Iran as described in section 4.3 will be dealt with. These data will be compared to the results of experiments performed by other researchers.

5.2 Experiments performed in Delft

5.2.1 Introduction

In this section the data of the Delft experiments as given in appendix IV, are analysed and used to derive non-dimensional parameters describing roughness and permeability of a rubble mound breakwaters slope. These non-dimensional parameters have to be representative for the physical processes taking place when waves run-up a rough, permeable slope.

5.2.2 Results

In this section the rough data are used to obtain insight into the influence of each single parameter on the run-up on a slope. When analysing one parameter, all others are taken constant. The influence of each parameter is described qualitatively. Arrows are used to give an indication of positive or negative influence.

In appendix VIII, the figures of the run-up versus wave height for different parameters are given. The conclusions that can be drawn from these figures are discussed below.

From figure VIII-1 it can be noted:

$H \uparrow,\ R_u \uparrow$

If waves get higher, the run-up will be higher. Waves are the main driving force for run-up so there has to be a direct relation between run-up and wave height. This is also a result of the definition of run-up; the extreme level of water elevation reached at every wave action.

From figures VIII-2 and VIII-3 it can be noted:

$Cot\ \alpha \uparrow, R_u \downarrow$

If the slope gets milder, the run-up will be less. This can be explained by the fact that when the waves pass over a longer slope, the roughness of this slope will have a longer route to interact with the waves. More energy can be dissipated on the slope and less energy is available for run-up.

From figures VIII-4 and VIII-5 it can be concluded:

$D_{n(50)} \uparrow, R_u \downarrow$

If the diameter of the armour unit (rock or artificial) gets bigger, the run-up will be less. The reason for this phenomenon could be found in two factors. The first is the influence of the roughness of a slope. If the diameter gets bigger, the roughness or the amount of resistance a wave encounters will be bigger. More resistance results in less run-up due to energy loss. The second influence is the permeability of the armour layer. The combination of porosity and diameter of the armour unit gives a permeability. The diameter of the armour unit is proportional to the size of the pores. When the size of the pores is larger, more space for the waves to dissipate energy is available. This will again reduce the run-up due to energy loss.

From figure VIII-6 it can be seen:

$n \uparrow, R_u \downarrow$

If the porosity of an armour layer increases, the run-up will decrease. The reason for this can be found in the energy dissipation of the waves running up the slope. If the porosity is higher, there will be more hollow spaces inside the slope. The waves are able to lose energy inside the slope better then.

From figures VIII-7 through VIII-10 it can be deducted:

$T \downarrow, \ R_u \downarrow$

The decrease of the wave period causes steeper waves. Steeper waves are more likely to break on a slope dissipating energy and therefore not reaching as high as levels as flat waves. In the last figures it was visible that no direct relationship as posited here could be distinguished. In these cases the transition between breaking and non-breaking waves can be the reason for this. These two types of wave behaving on a slope have totally different characteristics and have to be dealt with separately.

The conclusions that can be drawn from the exercise performed above are:

- $R = f(\Omega)*H$ (5.6)
- $\Omega :: T$ (5.7)
- $\Omega :: 1/\cot\alpha$, so $\Omega :: \tan\alpha$ (5.8)
- $\Omega :: 1/D$ (5.9)
- $\Omega :: 1/n$ (5.10)

where :: means, is a function of..
D is a characteristic diameter

5.2.3 Non-dimensional parameters

The run-up on a slope is usually presented as a relative run-up, the run-up is divided by the wave height. This non-dimensional parameter is presented versus the breaker parameter, ξ. As a start, this way of presenting data will be used here too.

Since the relative run-up is a non-dimensional parameter, a relation that describes the non-dimensional run-up has to consist of parameters that are non-dimensional as well. A non-dimensional parameter consists of one or more parameters with a positive influence of the run-up relative to one or more with a negative influence on the run-up. Furthermore, the non-dimensional parameters used to describe the run-up on a rough, permeable slope will be a combination of parameters describing the slope and parameters describing the waves.

In the previous section the different parameters and their influence on the run-up represent the data. From that examination non-dimensional parameters can be formed.

The different non-dimensional parameters that could be formed are:

- $$\xi = \frac{\tan\alpha}{\sqrt{\frac{2\pi H}{gT^2}}} \qquad (5.1)$$

Which is a parameter that describes the behaviour of waves on a slope. This parameter is derived for smooth, impermeable slopes (Battjes, 1974)

- A parameter that contains *H/D* as description of the roughness
- A parameter that contains a combination of *H* and ($D^a n^b g$) to describe the permeability of the structure

with *H* = wave height
D = characteristic diameter
n = porosity
g = gravitational acceleration
a, *b* = constants

As mentioned before, run-up is usually made non-dimensional by dividing it by the wave height. The data obtained from the experiments are put in figure A5.2-1 where on the y-axis the relative run-up (R_u/H) is placed and on the x-axis the breaker parameter (ξ). As can be seen, a lot of scatter occurs. In this figure, the influences of permeability and roughness are not filtered out of the data.

5.2.4 Roughness

To obtain a non-dimensional parameter describing the roughness of a slope (*R*), a combination of a property of the wave and a property the slope has to be found. For roughness, the wave is characterised by the wave height. The slope is characterised by a characteristic diameter. This leads to:

$$R = \frac{H}{D}$$

When roughness (*H/D)* is depicted versus the relative run-up (R_u/H), for *D* many different characteristic diameters could be used. The first diameter that is used is the nominal diameter. This parameter is easy to determine so if a relationship can be found in this way, it will make using a formula more simple.

In figure X-1 the data are presented as a function of the relative run-up versus the non-dimensional roughness using the nominal diameter. In this figure a lot of scatter is present so a better way of describing the relation between relative run-up and non-dimensional roughness has to be found.

When looking at the physics of a rough slope, a good parameter to describe the resistance of the slope could be the D_{85}, a measure for the largest stones in a quarry run. Since a comparison with tetrapods has to be made, for tetrapods the height of the unit is taken as a characteristic diameter for roughness, see also figure 4-1, page 28. In figure X-2 the data are presented as a function of relative run-up (R_u/H) versus relative diameter, with the D_{85} for stone and the H_{tet} for tetrapods as the

characteristic diameter. Still a lot of scatter remains, but the data seems to be more concentrated around one line. Therefore, the D_{85} for stone and the *Htet* will used to describe roughness. Roughness (R) will be described as:

$$R = \frac{H}{D_{85}} \qquad \text{for rock} \qquad (5.4)$$

and

$$R = \frac{H}{height\_unit} \qquad \text{for tetrapods} \qquad (5.5)$$

Since there is still a lot of scatter in the data, the data are presented as a function of the run-up versus the non-dimensional roughness in order to get insight in the mechanisms that play a role here. In figure X-3 the data of the experiments performed with tetrapods are presented as a function of the run-up and the non-dimensional roughness. A linear relationship between run-up and the non-dimensional roughness can be distinguished. In figure X-4 the data of the experiments performed with stone are presented as a function of run-up and the non-dimensional roughness. Here more scatter appears than in previous figure.

The scatter is due to different diameters of the material. In this fact may lie a solution for the scatter of the relative run-up versus non-dimensional roughness. When run-up is made non-dimensional by the diameter of the material, for instance the nominal diameter, the scatter in figures X-3 and X-4 might disappear and even a more clear relationship between relative run-up and non-dimensional roughness could be found. Figure X-5 shows the data presented as a function of the relative run-up made non-dimensional by the nominal diameter ($R_u/D_{n(50)}$) and the non-dimensional roughness. A significantly linear relationship is present. Since a significant relationship is present here, it might be better to use the nominal diameter to make the run-up non-dimensional. This will be examined for all different non-dimensional parameters.

5.2.5 *Permeability*

The non-dimensional parameter describing the permeability of the slope will again have to be a combination of a wave characteristic and a slope characteristic. First the wave characteristic will be discussed here, followed by the slope characteristic.

Since permeability is a measure for the amount of water that can pass a cross-section of material in a period of time, the characteristic of the wave is taken as the amount of water presented by the wave in a period of time.

The amount of water presented by the wave can be calculated by using:

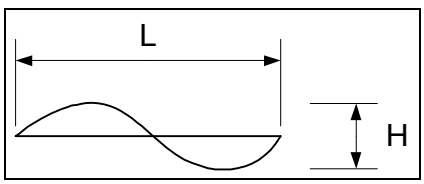

$$V = \alpha LH$$

Where V is the volume of water, α is a shape factor, L is the deep-water wave length and H is wave height.

This volume is taken per linear meter to reduce calculations. Per period of time, here the wave period, the volume of water presented by the wave per linear meter becomes:

$$V_i = \frac{\alpha g T H}{2\pi} \quad (\text{m}^2/\text{s}) \tag{5.6}$$

where V_i is the incoming amount of water.

The slope will have to drain this amount of water. Its capability of doing so is dependent on the permeability of the slope and the thickness of the slope.
Permeability can be presented in many ways. The most neutral way of presenting it might be:

$$k \sim n^a D_x^b g \tag{5.7}$$

with k = the permeability of a layer
n = the porosity of the layer
D_x = a characteristic diameter
g = gravitational acceleration
a = a constant
b = a constant

As a start the practical formula provided by the Manual on the use of Rock (1993) will be used:

$$k = 2\sqrt{\frac{n^5 g D}{|i|}} \quad (\text{m/s}) \tag{5.8}$$

with i = hydraulic gradient (-)

The hydraulic gradient is defined as:

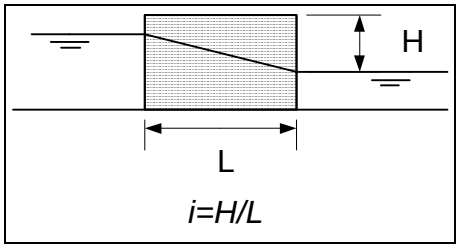

figure 5-1, Hydraulic gradient

When the permeability is described using equation (5.7), the hydraulic gradient in combination with the gravitational acceleration can be seen as the driving force that makes the water flow. When the slope of a breakwater is considered, the hydraulic gradient can not be marked as the driving force. The hydraulic gradient is even hard to describe in that case. Waves move up and down the slope, so the gradient will change in time. This time dependency makes the hydraulic gradient a non-usable parameter describing the wave-induced flow in the armour layer. It will therefore not be considered here. All other variables that appear in equation (5.7) are usable and the dimension of the combination of these variables is (m/s) which is the dimension of permeability.

The volume of water that can be drained by the layer per linear meter and per period of time can be written as:

$$V_d = kd \tag{5.9}$$

where V_d = volume of drained water
k = permeability of the layer
d = thickness of the layer

The permeability parameter can be constructed as:

$$K = \frac{V_i}{V_d} \tag{5.10}$$

When the non-dimensional parameter is put together, all constants are left out of it. The non-dimensional parameter describing the permeability becomes after re-arranging:

$$K = \frac{gTH}{D_{n(50)}\sqrt{\left(n^5 gD\right)}} \tag{5.11}$$

with: D = characteristic diameter

First of all the data will be presented as a function of the relative run-up, made non-dimensional with the wave height (R_u/H), and the non-dimensional permeability parameter. The permeability is taken as a combination of porosity and the D_{20}, a measure for the smallest pieces of rock in a quarry run. It is likely that the smallest pieces in the armour layer will have the biggest influence on the hollow spaces inside the layer. The small pieces are an indication for the size of the hollow spaces. In order to be able to compare rock and tetrapods with each other, for tetrapods the size of one leg of the tetrapod is taken as the characteristic diameter. The size of one leg is written as c, see also figure 4.1, page 28. In appendix XI, figure XI-1, R_u/H is presented versus equation (5.11).

Like with in the case of the non-dimensional roughness, also a lot of scatter is present. When the data points calculated with equation (5.11) are put against the run-up (R_u), the scatter has become less, see figure XI-2. The scatter is even more reduced when the run-up is made non-dimensional with the nominal diameter, see figure XI-3. But the influence of the porosity seems to be overrated. Porosity is now put into equation (5.11) to unity:

$$K = \frac{gTH}{D_{n(50)}\sqrt{\left(ngD\right)}} \tag{5.12}$$

When equation (5.12) is used to compute the non-dimensional permeability the scatter in the figure depicting the non-dimensional run-up ($R_u/D_{n(50)}$) versus K is less, see figure XI-4.

Now a closer look is taken on the porosity. When a breakwater is build, the armour layer will have a thickness that can vary between 1 and 3 times the nominal diameter of the armour units. Since this is a very thin layer when the porosity has to be determined, it will be likely that accuracy of the porosity will be low. Furthermore, the effect of the walls on the porosity has to be taken into account as well. A simple drawing can explain this effect:

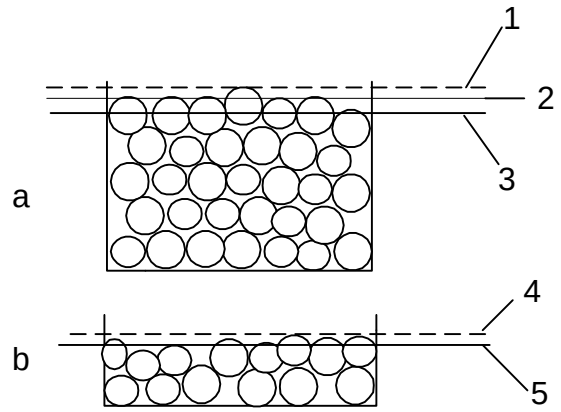

figure 5-2 Wall effect and surface definition

In the drawing 5-2 a, the porosity will be lower than in the case of drawing 5-2 b, although the same material is used. The walls make the hollow spaces bigger. Not only the walls themselves give a problem, also the surface of the layer is hard to define. In all cases the question can be posed, what is the surface of the layer, 1, 2 or 3 and 4 or 5. This problem has a big influence as well on the definition of porosity. Bregman (1998) found that accuracy of porosity is mainly determined by the reduction factor for the wall effect. He found that the porosity has to be corrected up to a 30% due to the wall effect. Since an armour layer of a breakwater has more resemblance with the case in drawing 5-2 b and the surface of the filter layer of a breakwater can be taken as a wall, the question arises whether the porosity is a good parameter to describe the amount of hollow spaces available in the layer.

This problem might be avoided when using the amount of armour units placed on a certain area, N_a. In this way the wall effect is taken into account and the layer is better described since less mistakes can be made in measuring the layer thickness and determining the porosity. In this number, the layer thickness is incorporated. When the layer is thicker, more armour units are present on one defined area. The value of N_a can be calculated using the following formula (SPM, 1984):

$$N_a = k_D n(1-n_v) D_n^{-2} \tag{5.13}$$

here, k_D is the layer thickness coefficient, n is the number of stones in a layer, see Shore Protection Manual and n_v is the porosity of the material. So the porosity of the material can be written as:

$$n_v \sim N_a D_{n(50)}^2 \tag{5.14}$$

This is used in the expression for the permeability parameter.

In total the expression for the permeability parameter becomes after some re-writing:

$$K = \frac{TH\sqrt{g}}{D_n^2\sqrt{(N_a c)}} \quad \text{for tetrapods} \tag{5.15}$$

$$K = \frac{TH\sqrt{g}}{D_{n50}^2\sqrt{(N_a D_{20})}} \quad \text{for rock} \tag{5.16}$$

In figure XI-5, equations (5.15) and (5.16) are used to calculate K and these data points are put against the non-dimensional run-up, $R_u/D_{n(50)}$.

If the run-up is made non-dimensional by using the nominal diameter, a relation that contains this non-dimensional run-up is only applicable for rubble mound breakwaters. Such a relation cannot be used to describe run-up on a rough impermeable slope or a dike.

5.3 Experiments performed in Iran

The experiments performed in Iran are model experiments unlike the experiments performed in Delft, which were axiomatic experiments. Axiomatic experiments are not performed in order to make model of a prototype situation, but they are meant to examine one specific phenomenon. In order to be able to compare the data of the Delft experiments with the data of the Iran experiments, the experiments have to be of the same scale. Although all data from the Iran experiments are acquired as prototype values, it might be better to scale them back to model values and use these values to make a comparison with the data from the Delft experiments. By doing so, both data sets are model values and this gives a better ground for comparison.

When the data of the Iran experiments are scaled back to model values, not much variation in variables is left. Only the wave height, $H_{s,}$ and the wave period, T_p or T_m are variables. Variation in roughness and permeability is not available. In order to take a first glance at the data, the data can be shown as a function of the relative run-up, $R_{u2\%}/H_s$ and the breaker parameter, ξ_m. This is an often used way displaying relative run-up versus breaker parameter. In appendix XII, figure XII-1 the prototype values of the two data sets acquired from the Iran experiments are depicted as function of the wave height based relative run-up and the breaker parameter based on the mean period.

According to figure XII-1, the relative run-up ($R_{u2\%}/H_s$) in the 1200-series is less than the relative run-up in the 1100-series. Since the two test series were performed with different scales, the characteristics of the prototype armour layers were different. The diameter of the tetrapods in the 1200-series is 1.5 times the diameter of the tetrapods in the 1100-series. The difference in relative run-up can be due to three factors:

1. difference of roughness of the two different armour layers
2. difference of permeability of the two different armour layers
3. difference of structural permeability

Since these influences can not be scaled in a proper way up to now, the influences of the three mentioned factors on the run-up are took along when scaling from prototype values to model values.

The prototype values of the Iran experiments might have a scale effect in them. When designing the experiments scaling the filter and core material according to Le Méhauté was not taken into account. More about scaling according Le Méhauté is given in appendix XIII.

In appendix XIV, the data obtained in Iran are compared to the present equations for run-up on a permeable slope, equation (3.2)-(3.4). From figure XIV-1 it can be noted that the run-up on a rubble mound breakwater covered with tetrapod armour units is lower than the run-up on a rock covered slope. Equation (3.2) and (3.3) represent the run-up on a rock armour covered slope, when the slope itself is impermeable. One is referred here to section 2.4.3. Equation (3.2) and (3.3) are derived for notional permeability factor $P = 0.1$. Equation (3.4) represents a fully permeable slope covered with rock armour units. Here the notional permeability factor is $P > 0.4$.

The run-up on the model tested in Iran is lower than the run-up that is described by the equation (3.2)-(3.4). The difference might be a result of the difference in roughness and permeability of the slope and a difference in permeability of the whole structure. In chapter 6, the relation that is derived by fitting the data obtained in Delft is applied to the data obtained in Iran. Doing so might give an indication about the legitimacy of the hypothesis posed above.

Chapter 6 Derivation of the relations describing run-up on a rough, permeable slope

6.1 Introduction

In this chapter two relations for the run-up on a rough, permeable slope will be derived. Two relations will be derived since in the previous chapters it became clear that run-up on a slope is different for breaking and non-breaking waves. First the relation for breaking waves will be derived followed by the relation for non-breaking waves. Then a back coupling is made with the data that are obtained in Iran. These data are filled in into the relations obtained from the experiments performed at the Delft University of Technology and a comparison is made between measured and computed data in order to see if the relations that are found can be justified to some extend. Finally a discussion is given about the influence of the results of this thesis on the design of rubble mound breakwaters.

6.2 Relation for breaking waves

The transition between breaking and non-breaking waves in the case of regular waves lies around $\xi = 2.5$ to $\xi = 3$. This value is found from figure IX-1 where a transition can be seen around the value of $\xi = 3$. The breaking waves occur when $\xi < 3$ and non-breaking waves occur when $\xi \geq 3$.

In chapter five it was found that a linear relationship exists between non-dimensional run-up ($R_u/D_{n(50)}$) on one hand and non-dimensional roughness (R) and non-dimensional permeability (K) on the other hand. When looking at the definitions of non-dimensional roughness and permeability, it seems likely that there is correlation between the two non-dimensional parameters. Both parameters are derived using the wave height and a characteristic diameter of the armour unit. When roughness is zero, permeability has to be zero as well. This hypothesis about the correlation between roughness and permeability is checked by using the statistical program *SPSS* and was found right. When the data obtained from the experiments performed in Delft are considered, a strong correlation is found between R and K. This means that R and K have to appear in the same factor when a the non-dimensional run-up is described.

From figure X-5 in appendix X, it is clear that a linear relation is present between $R_u/D_{n(50)}$ and R. So the following relation can be given for the non-dimensional run-up versus the roughness parameter:

$$\frac{R_u}{D_{n(50)}} = aR \tag{6.1}$$

where a is a constant

From figure XI-5 in appendix XI, one can conclude that also a linear relation is present between $R_u/D_{n(50)}$ and K. The following relation might represent the non-dimensional run-up versus the permeability parameter:

$$\frac{R_u}{D_{n(50)}} = bK \tag{6.2}$$

where b is a constant

Furthermore a correlation between roughness and Iribarren parameter and a correlation between permeability and Iribarren parameter is supposed.

From a physical point of view this can be explained as follows. A change in the behaviour of the waves on the slope (ξ) will change the interaction between the waves and the slope. The interaction can be divided into interaction at the outer side of the slope (roughness) and inside the slope (permeability).

From a more statistical point of view this can be explained by the fact that the wave height is used in the Iribarren parameter, the roughness parameter and the permeability parameter.

The possibility of correlation was checked also using the statistical program *SPSS*. The correlation was not as strong as appeared between roughness and permeability but it is present. So roughness parameter and Iribarren parameter have to appear in one factor describing the non-dimensional run-up. The same accounts for the permeability parameter and the Iribarren parameter.

The run-up is dependent on the all three factors described above, KR, ξK and ξR. All these factors add their part to the run-up on a rough, permeable slope. So combined with the above stated this leads to the assumption that the non-dimensional run-up should look like:

$$\frac{R_u}{D_{n(50)}} = lKR + m\xi K + n\xi R \tag{6.3}$$

with l, m, n are constants

K = non-dimensional permeability, defined as:

$$K = \frac{TH\sqrt{g}}{D_n^2\sqrt{(N_a c)}} \quad \text{for tetrapods} \tag{6.4}$$

$$K = \frac{TH\sqrt{g}}{D_{n50}^2\sqrt{(N_a D_{20})}} \quad \text{for rock} \tag{6.5}$$

R = non-dimensional roughness, defined as:

$$R = \frac{H}{D_{85}} \quad \text{for rock} \tag{6.6}$$

$$R = \frac{H}{height\_unit} \quad \text{for tetrapods} \tag{6.7}$$

ξ = Iribarren parameter, defined as:

$$\xi = \frac{\tan\alpha}{\sqrt{\frac{2\pi H}{gT^2}}} \tag{6.8}$$

For the derivation of the non-dimensional parameters for roughness and permeability, one is referred to chapter five.

The assumed relation describing the run-up on a rough permeable slope is used to fit the data from the Delft experiments. The statistical program *SPSS* is used to find values for the constants *a*, *b* and *c*. A non-linear regression is applied to the data, using the Levenberg-Marquard method. The result of the non-linear regression is:

$$\frac{R_u}{D_{n(50)}} = 7.93\cdot 10^{-3} KR - 2.13\cdot 10^{-4}\xi K + 0.37\xi R \tag{6.9}$$

This relation is only valid for the rough and porous slope of a rubble mound breakwater.

The fact that the values of the constants *l* and *m* are very small is a result of the definition of the permeability parameter. The values of *K* that are used to derive the relation (6.9) are large while the values of $R_u/D_{n(50)}$ are much smaller.

Not all of the factors, *KR*, ξK and ξR, given in equation (6.9) may have equal influence on the non-dimensional run-up. Their contribution to the calculation of the non-dimensional run-up is calculated and it is found that the influences are as follows:

factor	contribution to $R_u/D_{n(50)}$
$7.93*10^{-3}KR$	≈ 34%
$-2.13*10^{-4}\xi K$	≈ 1%
$0.37\xi R$	≈ 65%

Regarding the contributions, the relation can be reduced to:

$$\frac{R_u}{D_{n(50)}} = 0.37R\left(0.021K + \xi\right) \tag{6.10}$$

This relation is valid within the following boundaries:

$11.7 < K < 104.3$
$0.43 < R < 3.00$
$1.07 < \xi < 2.99$

In appendix XV, the measured values of $R_u/D_{n(50)}$ are presented together with the calculated values from equation (6.9) and equation (6.10). The formulae seem to give a significantly good description of the data points for the experiments as performed in Delft.

6.3 Non-breaking waves

In this section a formula for run-up on a rough permeable slope is derived when $\xi \geq 3$. This value of the breaker parameter denoting the transition between breaking and non-breaking waves is only valid for regular waves.

Again, the correlation between *K* and *R* is calculated using *SPSS*. Just like in the case of breaking waves, the correlation is significant. Also, the correlation between ξ and *K* and between ξ and *R* is calculated. Correlation is present again, but weaker than the correlation between *K* and *R*. Just like with breaking waves, the formula is assumed to be of the following form:

$$\frac{R_u}{D_{n(50)}} = lKR + m\xi K + n\xi R \tag{6.11}$$

The definitions for *R*, *K* and ξ are given by equations (6.4)-(6.8).
When applying non-linear regression on the data of non-breaking waves, the formula for run-up on a rough permeable slope has the form:

$$\frac{R_u}{D_{n(50)}} = 4.57 \cdot 10^{-3} KR - 4.1 \cdot 10^{-4} \xi K + 0.27 \xi R \tag{6.12}$$

factor	contribution to $R_u/D_{n(50)}$
$4.57*10^{-3}KR$	≈ 17%
$-4.1*10^{-4}\xi K$	≈ 5%
$0.27\xi R$	≈ 78%

Due to the low contribution of the term containing ξK, this term is left out of equation (6.12). The equation therefore reduces to:

$$\frac{R_u}{D_{n(50)}} = 0.27R(0.017K + \xi) \tag{6.13}$$

This relation is only valid within the following range:

$13.6 < K < 156.0$
$0.41 < R < 3.46$
$3.01 < \xi < 7.61$

Appendix XVI shows the measured data points versus the calculated data points, using equation (6.13). Equation (6.13) is a reasonably well fit for the data, but some scatter is present. Mainly data points lying beneath the line of unity may be the cause of the scatter. The origin of the data is not known, but these data might be the result of measuring errors.

Compared with the relation for breaking waves (6.10), the total influence of *R* on the run-up has decreased, the same accounts for *K*. The decrease of the contribution of the roughness to the run-up can be explained. Since the waves do not break, these waves apparently do not “feel” the bottom when running up the slope. The roughness of this bottom therefore does not hinder the propagation of the waves and the influence of this roughness is small compared to other influences.

Another parameter that causes the influence of the roughness of the slope to reduce is the slope angle. The combination of the slope angle and the wave steepness, the breaker parameter, is a good measure for breaking and non-breaking waves. The non-breaking waves appear mostly when the slope is steep. The area where the waves are in contact with the slope is smaller in the case of non-breaking waves then in the case of breaking waves. The waves simply will encounter less resistance due to roughness.

A change in permeability has less effect on the run-up in the case of non-breaking waves than in the case of breaking waves. This can be explained like this. The breaking waves need the permeability of the slope to dissipate energy, energy that is used otherwise to run-up the slope. Non-breaking waves do not dissipate much of their energy inside the slope and therefore the permeability of the slope is of less importance. A change of permeability will have less effect on the run-up in the case of non-breaking waves than in the case of breaking waves.

The total influence of ξ on the run-up has increased for non-breaking waves compared to breaking waves. The reason for this is clear; breaking waves occur when $\xi < 3$ and non-breaking waves occur when $\xi \geq 3$. So the value of ξ is higher in the case of non-breaking waves than in the case of breaking waves.

6.4 Application of the derived relations on the Iran data

The data obtained in Iran can be used as a kind of justification of the relations that are derived above. Stress has to be put on "kind of" since the relations are derived for regular waves and the applied layer underneath the armour layer was impermeable. During the experiments performed in Iran, irregular waves were used and the whole structure was permeable.

The data set collected in Iran consist of data where the waves are all non-breaking waves when the definition for breaking waves as given by Van der Meer is used. He states that when $\xi_m > 1.5$, the waves do not break. All data obtained in Iran lie in this area. The relation for breaking waves can not be justified using this data set.

The results of the calculation of the relative run-up using equation (6.13) and the data obtained in Iran are shown in appendix XVII. The results are giving a good match. This might just be the case for the selected run-up and ξ. In figure XVII-1, use is made of the $R_{u2\%}$ and the ξ_m. In figure XVII-2, instead of ξ_m, ξ_p is used.

In general it can be said that the relation for non-breaking waves is a significantly good description for the data obtained in Iran. Especially the data points of the experiments performed with the scale of $N = 66$ are perfectly fit by the relation, when ξ_m is used. This probably is more a coincidence then reality. From both figures in appendix XVII it can be seen that the measured data points for the scale of $N = 66$ compared to the calculated data points are lower than the measured data points for the scale of $N = 50$ compared to the calculated data points. The reason for this might be that the permeability of the whole structure is higher in the case of $N = 66$ than in the case of $N = 50$. The waves here are non-breaking and as posed in section 3.3.6, the influence of the permeability of the structure will have influence on the run-up in the case of non-breaking waves. Since the influence of the structure's permeability is not incorporated into equation (6.13), this might cause the difference in run-up between the two experimental series performed in Iran.

Chapter 7 Discussion

7.1 Relations derived in chapter 6

When a closer look is taken at the relation derived for the description of run-up on a rough, permeable slope, the following conclusions can be drawn:

For tetrapod armour units, the relation describing the run-up of breaking waves can be re-written as:

$$\frac{R_u}{D_n} = 0.37 \frac{H}{H_{tet}} \left[0.021 \left(\frac{TH\sqrt{g}}{D_n^2 \sqrt{(N_a c)}} \right) + \frac{\tan\alpha}{\sqrt{\left(\frac{2\pi H}{gT^2} \right)}} \right] \tag{7.1}$$

valid for: $0.41 \le \frac{H}{H_{tet}} \le 2.22$

$$14.27 \le \frac{TH\sqrt{g}}{D_n^2 \sqrt{N_a c}} \le 104.32$$

$$1.07 \le \frac{\tan\alpha}{\sqrt{\frac{2\pi H}{gT^2}}} \le 2.99$$

From this relation it can be seen that run-up reduction can only be achieved by varying the diameter of the units. By increasing the diameter of the tetrapods, the run-up will be reduced. All other variables are fixed by the environmental circumstances at the proposed prototype site (*H*, *T*) or fixed by economic considerations ($tan\alpha$).

For rock the relation describing the run-up of breaking waves can be written as:

$$\frac{R_u}{D_{n50}} = 0.37 \frac{H}{D_{85}} \left[0.021 \left(\frac{TH\sqrt{g}}{D_{n50}^2 \sqrt{(N_a D_{20})}} \right) + \frac{\tan\alpha}{\sqrt{\left(\frac{2\pi H}{gT^2} \right)}} \right] \tag{7.2}$$

valid for: $0.53 \le \frac{H}{D_{85}} \le 3.46$

$$13.6 \le \frac{TH\sqrt{g}}{D_{n50}^2\sqrt{N_a D_{20}}} \le 156.0$$

$$1.07 \le \frac{\tan\alpha}{\sqrt{\frac{2\pi H}{gT^2}}} \le 2.99$$

In the case of rock units, the diameter of the rock units itself is not the only variable that could lead to a change of the run-up height on a rough, permeable slope. When a rock mass is considered, the grading of the mass can be altered. A wide grading leads to a higher value for D_{85} and a lower value for D_{20} than a narrow grading when the same D_{n50} is considered. So here some advantage could be achieved in the reduction of the run-up capacity of the waves by altering the grading.

The influence of the grading can be divided into two: the influence on the roughness parameter and the influence on the permeability parameter.

Firstly, the roughness parameter. The reduction of the run-up capacity is largest when the D_{85} is large relative to D_{n50}. This means that a wide grading would lead to a maximum reduction of the run-up capacity.

The permeability parameter is dependent on the D_{n50}, which is supposed constant here, and is dependent on D_{20} and the number of units per square meter. When D_{20} is large, the maximum reduction of the run-up capacity is achieved. This means that the grading should be as narrow as possible.

The demands towards the width of the grading is opposite for the roughness and the permeability, when maximum reduction of run-up capacity is concerned. Therefore the influences of the two phenomena on the run-up reduction are compared here.

An increase of the width of the grading will increase the reduction due to the roughness. An increase of the width of the grading causes a decrease of the reduction due permeability. Only the decrease of the permeability is by the square root of the increase of the width. So the decrease due to the permeability will be eliminated by the increase due to the roughness. This is the case for the factor $K*R$.

When the factor $R*\xi$ is concerned, the increase of the reduction of the run-up capacity is linear with the increase of the width of the grading.

So totally, the reduction of the run-up capacity will be maximal when the width of the grading is maximal.

When a close look is taken at equations (7.1) and (7.2), these equations are quite complicated. One can pose the question whether these equations are easier to use than the common formulae describing run-up as:

$$\frac{R_u}{H} = a\xi^b \qquad (7.3)$$

Not only are equations (7.1) and (7.2) very complicated, they also do not accord with the main relation found in section 5.2.2: $R_u = \Omega*(H)$. When equations (7.1) and (7.2) are put as R_u = X, the

result looks like: $R_u = \Lambda H^2$. Also the non-dimensional parameter $R_u/D_{n(50)}$ is a parameter that gives little feeling with the physical processes that take place when waves attack a slope. So in total, describing the run-up on a rough, permeable slope, using the Iribarren parameter, a roughness parameter and a permeability parameter does seem to result in a complicated relation which does not reproduce the physical processes properly. Therefore, the analysis of the data obtained from the Delft experiments will be performed once more. This time a more fundamental approach will be used.

7.2 Re-analysis of the data from the Delft experiments

7.2.1 non-dimensional parameters

The basis for the derivation of the non-dimensional parameters is the set of relations derived in chapter five:

- $R = \Omega^*(H)$ (7.4)
- $\Omega :: T$ (7.5)
- $\Omega :: 1/\cot\alpha$, so $\Omega :: \tan\alpha$ (7.6)
- $\Omega :: 1/D$ (7.7)
- $\Omega :: 1/n$ (7.8)

where :: means, is a function of..
D is a characteristic diameter

These relations are used to perform a dimensional analysis. A set of non-dimensional parameters is derived using the variables: R_u, *H*, *T*, $\tan\alpha$, *D* and *n*. The gravitational acceleration is not varied in the experiments, but it is used in the derivation of the non-dimensional parameters since it is an important variable when waves are concerned.

In order to derive non-dimensional parameters, a dimensional analysis is made. Use is made of the Buckingham Pi theorem:

In a dimensionally homogeneous equation involving "n" variables, the number of dimensionless products that can be formed from "n" variables is "n-r" where "r" is the number of fundamental dimensions encompassed by the variables.

This theorem is called Buckingham Pi because Buckingham used the symbol Π to represent the non-dimensional products.

Setting up a matrix of variables and their fundamental dimensions eases determining the number of fundamental dimensions in a set of variables. Table 5-1 shows the matrix of variables in the case of run-up on a rough, permeable slope. Note that the porosity, *n*, and $\tan\alpha$ are not included here, since these variables are already dimensionless. The three fundamental dimensions are length (L), time (T) and mass (M).

	R_u	*H*	*T*	*D*	*g*
L	1	1	0	1	1
T	0	0	1	0	-2
M	0	0	0	0	0

table 5-1, Matrix of fundamental dimensions

Because the unit of mass is not included in any of the variables, the number of fundamental dimensions is $r = 2$ and the number of non-dimensional products that can be formed from the variables is 5-2 = 3.

Each of the non-dimensional products will have the form given by the following expression:

$$\Pi = R_u^{k_1} H^{k_2} T^{k_3} D^{k_4} g^{k_5} \tag{7.9}$$

where Π is the notation for a non-dimensional product and the k_n's are exponents to be determined.

When the fundamental units for each of the variables in the above equation are substituted, the equation for Π is given by:

$$\Pi[=][L]^{k_1}[L]^{k_2}[T]^{k_3}[D]^{k_4}\left[LT^{-2}\right]^{k_5} \tag{7.10}$$

which can be rearranged to give:

$$\Pi[=][L]^{k_1+k_2+k_4+k_5}[T]^{k_3-2k_5} \tag{7.11}$$

In order for the product, Π, to be non-dimensional, it is necessary for the exponents of [L] and [T] to be zero, which produces the independent set of two equations:

$$(k_1+k_2+k_4+k_5) = 0 \tag{7.12}$$
$$(k_3-2k_5) = 0 \tag{7.13}$$

Any solution of the above set of equations will give values for the exponents, which can be substituted into the Π-equation to give a viable non-dimensional product. Because the above set of equations consists of 2 equations of 5 unknowns, the set is indeterminate and an infinite number of solutions exist. So for this case, it is necessary to specify three of the exponents, then solve for the remaining two values.

Since an infinite number of solutions exist, it is necessary to use the knowledge of the physical reality when the non-dimensional products are derived. Therefor, the relations between run-up and the different variables as given by equations (7.4)-(7.8) are used.

Furthermore the dependent variable, here the run-up, has to appear in only one non-dimensional product. The non-dimensional products will represent the physical phenomena best when every variable occurs only once in the non-dimensional products.

From equations (7.4)-(7.8) it can be seen that run-up (R_u) is linear to the wave height. Since the relative run-up (R_u/H) is widely used when run-up is described, the exponents will be chosen in such a way that the relative run-up is the result:

$k_1 = 1$, $k_2 = -1$, $k_3 = 0$, this leads to: $k_5 = 0$ and $k_4 = 0$

$$\text{so, } \Pi_1 = \frac{R_u}{H} \tag{7.14}$$

The second non-dimensional product should not contain R_u and H and should contain T. This gives: $k_1 = 0$, $k_2 = 0$, $k_3 = 1$, this leads to: $k_5 = ½$ and $k_4 = -½$.

$$\text{so, } \Pi_2 = \frac{T\sqrt{g}}{\sqrt{D}} \tag{7.15}$$

One more non-dimensional product could be derived, but all dimensional variables have been used to derive non-dimensional products and the relations derived in section 5.2.2 are met. So in total, the expression describing the run-up on a rough, permeable slope should be of the form:

$$\frac{R_u}{H} = f\left(\frac{T\sqrt{g}}{\sqrt{D}}, \tan\alpha, n\right) \tag{7.16}$$

The relation (7.16) still has two variables (*tan* α and *n*) that are not incorporated into one of the two non-dimensional products, Π_1 and Π_2. Since Ω:: *tan*α, as was found in section 5.2.2, the run-up is put against Π_2. While doing so, *n* is kept constant and *tan*α is varied. In appendix XVIII, these figures are given. From these figures it can be seen that *tan*α has a linear influence on the run-up, so it can be incorporated easily into a parameter that describes the run-up. The parameter describing the run-up on a rough, permeable slope now looks like:

$$\Pi_2 * \tan\alpha = \frac{\tan\alpha T\sqrt{g}}{\sqrt{D}} \tag{7.17}$$

In the figures of appendix XVIII it can be seen that when *tan*α = 0.33 and 0.68, two lines describe the run-up. These lines are the result of run-up due to breaking waves and run-up due to non-breaking waves.

So equation (7.16) can be rewritten as:

$$\frac{R_u}{H} = f\left(\frac{\tan\alpha T\sqrt{g}}{\sqrt{D}}, n\right) \tag{7.18}$$

Still the porosity is not taken into account when the non-dimensional parameters are concerned. In section 5.2.5 it was found that when porosity is concerned, this could be best incorporated in into equation (7.18) as follows:

$$\frac{R_u}{H} = f\left(\frac{\tan\alpha T\sqrt{g}}{D_n\sqrt{(N_a c)}}\right) \quad \text{for tetrapods} \tag{7.19}$$

$$\frac{R_u}{H} = f\left(\frac{\tan\alpha T\sqrt{g}}{D_{n50}\sqrt{(N_a D_{20})}}\right) \quad \text{for rock} \tag{7.20}$$

For the choices made in section 5.2.5, dealing with porosity, again reasoning is given now. Permeability can be described according to the Manual on the Use of Rock (1995) like:

$$k = 2\sqrt{\frac{n^5 gD}{|i|}} \tag{7.21}$$

So porosity should be incorporated to the power of 5. Since no relation like this was found in section 5.2.2, it seems that this overrates the influence of n. In Appendix XIX, the porosity is put into equation (7.18) to the power 5 and to unity. The scatter reduces significantly when *n* to unity is used. So therefore *n* is used in equation (7.18) to unity. Furthermore, in section 5.2.5, the choice of using $N_a D^2_{n(50)}$ instead of using *n* is discussed. In Appendix XX, the figures are given where in one occasion *n* is used and in the other, $N_a D^2_{n(50)}$. From these figures it can be concluded that the usage of $N_a D^2_{n(50)}$ results in less scatter.

When the characteristic diameter is regarded, for rock, the D_{20} and for tetrapods *c* is used. In both cases, these values have a relationship with respectively D_{n50} and D_n. Since a small grading was used in all experiments performed with rock units, the ratio $D_{n50}/D_{20} \approx 1.3$. For tetrapods, the ratio $D_n/c = 1.36$. This since the D_n is derived from the height of the unit and the size of one leg of a tetrapod always has a fixed relation with the height. So the values of D_{20} and *c* can be rewritten as $\beta^* D_{n50}$ and $\beta^* D_n$. This results in the following relations for the relative run-up:

$$\frac{R_u}{H} = f\left(\frac{\tan\alpha T\sqrt{g}}{D_n\sqrt{(\beta N_a D_n)}}\right) \qquad \text{for tetrapods} \qquad (7.22)$$

$$\frac{R_u}{H} = f\left(\frac{\tan\alpha T\sqrt{g}}{D_{n50}\sqrt{(\beta N_a D_{n50})}}\right) \qquad \text{for rock} \qquad (7.23)$$

where β is fixed at 0.735 for tetrapods
depends on W_{85}/W_{15} for rock and is 0.77 for these experiments

So one can conclude that the unknown factor Ω in equation (7.4) can be written as:

$$\Omega = \frac{\tan\alpha T\sqrt{g}}{D_n\sqrt{(\beta N_a D_n)}} \qquad \text{for tetrapods} \qquad (7.24)$$

$$\Omega = \frac{\tan\alpha T\sqrt{g}}{D_{n50}\sqrt{(\beta N_a D_{n50})}} \qquad \text{for rock} \qquad (7.25)$$

The parameter Ω has some resemblance with the parameter ξ, which is used widely to describe run-up on a slope. The two parameters are compared below:

$$\xi = \frac{\tan\alpha T\sqrt{g}}{\sqrt{2\pi H}} \qquad (7.26)$$

$$\Omega = \frac{\tan\alpha T\sqrt{g}}{D_{n(50)}\sqrt{(\beta N_a D_{n(50)})}} \qquad (7.27)$$

The two parameters do have a resemblance, only in the case of Ω, a term describing the permeability of the armour layer is incorporated and H is omitted. When the data available from the Delft experiments are displayed as $R_u = H^*\xi$ and as $R_u = H^*\Omega$, in appendix XXI, it can be concluded that the data are described better with Ω than when ξ is used.

7.2.2 Discussion on reliability of measurements

All the data discussed above are represented as $R_u = \Omega^*(H)$. This is done since some scatter is present in the data. This scatter is the result accuracy of the measurements of the run-up. Since the run-up is measured in cm and the wave height is measured in mm, in a non-dimensional product, R_u/H inaccuracy is introduced.

This can be best illustrated by figures XXII-1 and XXII-2 in appendix XXII. For one unique combination of slope angle, wave period, diameter and porosity, one unique value of R_u/H should be measured, but this is not the case. Important in this figure is whether no unique value of R_u/H is present due to scatter or due to a trend that is not incorporated into the parameter Ω. After a research on these data points, no trend was found in the divergent data points. So these data points are likely to be scatter. The data points that were checked, are encircled in figures XXII-1 and XXII-2.

The scatter is mainly caused by the method of measuring run-up. In these experiments, the run-up is estimated from video images, the accuracy of these estimations is 1 cm. The inaccuracy of this method is around 15%.

Secondly in figure XXII-3 in appendix XXII, it can be noted that the smallest units, rock with a diameter of D_{n50} = 0.027 m and tetrapods with a diameter of D_n = 0.036 m, the relative run-up decreases with increasing Ω. This accounts for non-breaking waves. While D_{20}, D_{n50} and the porosity for the rock units are constant, only the change of slope angle and wave period influences the value of the relative run-up.

The reason for this may lay in the fact that the small stones might react more like an impermeable slope than like a permeable layer that can drain water. The influence of the impermeable underlayer, the wooden board is large. A comparison can be made with figure XXIII-2 in appendix XXIII. The data of Ahrens (1981) for smooth slopes show the same trend as the smallest rock units. So for the small units, in the case of non-breaking waves another phenomenon than described by equation (7.20) plays a role. So in the case of non-breaking waves, the results of the experiments for the small rock units should not be used to derive a relation describing the run-up.

7.2.3 Derivation of the relations describing run-up

In this section relations are derived describing the run-up on a rough, permeable slope, for breaking and non-breaking waves. The data set from the Delft experiments is reduced by omitting the data points that were found to be scatter in section 7.2.2. Since these points are due to measurement faults, they will influence the derivation of the relations in a negative way.

Relation for breaking waves

The transition between breaking and non-breaking waves in the case of regular waves lies around ξ = *2.5* to ξ = 3. This value is found from figure IX-1 where a transition can be seen around the value of ξ = 3. The breaking waves occur when $\xi < 3$ and non-breaking waves occur when $\xi \geq 3$.

In section 7.2.1 it was found that the following relation exists:

$$\frac{R_u}{H} = f(\Omega), \text{ where:} \tag{7.28}$$

$$\Omega = \frac{\tan\alpha T\sqrt{g}}{D_{n(50)}\sqrt{(\beta N_a D_{n(50)})}}$$

with β is 0.735 for tetrapods and 0.77 for rock

For breaking waves, R_u/H is plotted against Ω and given in figure XXIV-1, appendix XXIV. Although the scatter as discussed in section 7.3 is present, a trend can be found. A line that has the form
$y = ax^b$ can be drawn through the data points.

When a non-linear regression is performed on the data, reduced with the scatter (see figure XXIV-2), assuming the above given relation, the result is:

$$\frac{R_u}{H} = 0.89(\Omega)^{0.22} \tag{7.29}$$

which is valid within the following boundaries:

$19.49 \leq \Theta \leq 36.80$
$0.26 \leq tan\alpha \leq 0.68$
with:

$$\Theta_{tet} = \frac{T\sqrt{g}}{D_n\sqrt{\beta N_a D_n}} \quad \text{for tetrapods}$$

$$\Theta_r = \frac{T\sqrt{g}}{D_{n50}\sqrt{\beta N_a D_{n50}}} \quad \text{for rock}$$

Relation for non-breaking waves

In this section a formula for run-up on a rough permeable slope is derived when $\xi \geq 3$. This value of the breaker parameter denoting the transition between breaking and non-breaking waves is only valid for regular waves.

Again the starting point is the relation:

$$\frac{R_u}{H} = f(\Omega) \tag{7.30}$$

When this relation is plotted, the result (figure XXIV-1, appendix XXIV) shows that two lines might represent the data for non-breaking waves: $y = c$ and $y = bx$.

When a linear regression is performed on these data, assuming relation (7.30) being of the form $y = c$ and of the form $y = bx$, the best representation of the data, reduced with the scatter, was found to be:

$$\frac{R_u}{H} = 1.043 \qquad (7.31)$$

Equation (7.31) is valid within the boundaries:

$19.42 \leq \Theta \leq 36.80$
$0.33 \leq tan\alpha \leq 0.68$
$0.036 \text{ m} \leq D_{n(50)} \leq 0.065 \text{ m}$

$$\Theta_{tet} = \frac{T\sqrt{g}}{D_n\sqrt{\beta N_a D_n}} \qquad \text{for tetrapods}$$

$$\Theta_r = \frac{T\sqrt{g}}{D_{n50}\sqrt{\beta N_a D_{n50}}} \qquad \text{for rock}$$

The above derived relations (7.29) and (7.31) show a significant resemblance with the relations derived by van der Meer and Stam (1992), see figure 3-2. The difference between the relations derived by van der Meer and Stam and equations (7.29) and (7.31) is the non-dimensional parameter that is used to describe R_u/H. Equations (7.29) and (7.31) make use of a non-dimensional parameter that incorporates the permeability of the armour layer of a slope, whereas the relations derived by van der Meer and Stam make use of the breaker parameter, ξ.

The relations (7.29) and (7.31) also seem to give a better description of the physical processes as they occur when waves attack a rough, permeable slope, than the relations derived in chapter 6, equations (6.10) and (6.13).

Chapter 8 Conclusions and recommendations

In this chapter the conclusions and recommendations, which can be drawn from this study on the run-up on a rough, permeable slope, are given.

8.1 Conclusions

- During the investigation of the data of the experiments performed in Delft, it became clear that run-up can be described by the following parameters:

  - Wave height H
  - Wave period T
  - Slope angle $\cot\alpha$
  - Nominal diameter of the armour unit $D_{n(50)}$
  - porosity of the armour layer n

- In order to be able to compare various structures, non-dimensional parameters have to be formed. Two different approaches are followed to analyse the data obtained from the Delft experiments. The first makes use of the generally know non-dimensional parameter ξ and of two parameter describing roughness and permeability. The non-dimensional parameters are a combination of typical properties of the slope and typical properties of the waves. When this approach is followed, for roughness and permeability, the following parameters are found:

  – $R = \dfrac{H}{H_{tet}}$, for tetrapods and $R = \dfrac{H}{D_{85}}$, for rock

  – $K = \dfrac{TH\sqrt{g}}{D_n^2\sqrt{(N_a c)}}$, for tetrapods and $K = \dfrac{TH\sqrt{g}}{D_{n50}^2\sqrt{(N_a D_{20})}}$, for rock

- The usual way of presenting the run-up, as a non-dimensional parameter, (R_u/H) is for above followed approach not the best way of presenting the influence of the roughness and the permeability. Instead of the wave height, the nominal diameter of the armour units is used to make the run-up non-dimensional. The non-dimensional run-up ($R_u/D_{n(50)}$) gives a better insight into the influence of roughness and permeability on this run-up. So $R_u/D_{n(50)} = f(R, K, \xi)$.

- The newly found relations for run-up on a rough permeable slope are divided into a relation for breaking waves and a relation for non-breaking waves.

$$\frac{R_u}{D_{n(50)}} = 0.37R(0.021K + \xi) \qquad \text{breaking waves} \qquad (6.10)$$

The range for which this relation is valid is:
$11.7 < K < 104.3$; $0.43 < R < 3.00$; $1.07 < \xi < 2.99$, regular waves

for non-breaking waves, the run-up can be expressed as:

$$\frac{R_u}{D_{n(50)}} = 0.27R(0.017K + \xi) \qquad \text{non-breaking waves} \qquad (6.13)$$

This relation is only valid within the following boundaries:
$13.6 < K < 156.0$; $0.41 < R < 3.46$; $3.01 < \xi < 7.61$, regular waves

- The non-dimensional parameters and the relations that are found by examining the data using the Iribarren parameter and parameters describing roughness and permeability are complicated and do not represent the physical processes in a satisfactory way. Therefore in the second approach, ξ is not used and non-dimensional parameters are derived by a dimensional analysis, combined with knowledge on the physical processes that take place when waves attack a rough, permeable slope. Using the non-dimensional parameters, relations are derived describing the run-up of breaking and non-breaking waves on a rough, permeable slope.

- The non-dimensional parameters describing run-up on a rough permeable slope are:

  – $\frac{R_u}{H}$

  – $\Omega = \frac{\tan\alpha T\sqrt{g}}{D_{n(50)}\sqrt{\left(\beta N_a D_{n(50)}\right)}}$,

  with β is fixed at 0.735 for tetrapods and is dependent on W_{85}/W_{15} for rock and is 0.77 for these experiments

- The relations describing the run-up on a rough permeable slope using R_u/H and Ω:

  – $\frac{R_u}{H} = 0.89(\Omega)^{0.22}$ for breaking waves, with the following boundaries:

  $19.49 \le \Theta \le 36.80$
  $0.26 \le tan\alpha \le 0.68$

  where: $\Theta_{tet} = \frac{T\sqrt{g}}{D_n\sqrt{\beta N_a D_n}}$ for tetrapods

  $\Theta_r = \frac{T\sqrt{g}}{D_{n50}\sqrt{\beta N_a D_{n50}}}$ for rock

  – $\frac{R_u}{H} = 1.043$ for non-breaking waves, valid within the following boundaries:

  $19.42 \le \Theta \le 36.80$
  $0.33 \le tan\alpha \le 0.68$
  $0.036 \text{ m} \le D_{n(50)} \le 0.065 \text{ m}$
  with Θ defined as above

- The porosity was not used to take the amount of hollow spaces into account. Instead of the porosity, the total number of armour units in the area considered, N_a, is used. By using this parameter, the uncertainties on wall-effects and the definition of the surface of the armour layer are avoided.

- The relations found for run-up are found by examining the data of experiments using a non-permeable structure. Still the relation for breaking waves is likely to give a good prediction for the run-up on a permeable structure with rough surface since the permeability of a structure has little influence on the run-up of breaking waves.

- The fact that the structure is impermeable seems to have influence on the run-up of non-breaking waves on a layer with small armour units. The layer behaves more like an impermeable smooth slope than as a rough, permeable slope. From this it can be deducted that the thickness of the layer might also have an influence on the run-up. This was not tested in these experiments.

- The relations found in this thesis are derived for a rough and permeable slope. Due to the usage of D_n and D_{n50} to form non-dimensional parameters, these relations cannot be used to describe run-up on a rough impermeable slope. Also structures with an armour layer consisting of rock units penetrated with asphalt lie not in the range of the derived relations.

- The data obtained from the Delft experiments show a large amount of scatter. This is due to the method of measuring the wave run-up. Visual estimation of the run-up results in an inaccuracy of around 15%.

- Data obtained from model experiments on a breakwater covered with tetrapods in Iran were applied to the relation for non-breaking waves (6.13). The measured data showed correlation with the calculated data but the calculated data were higher than the measured data. Reason for this can be threefold:

  – The structure used in Iran was permeable whereas the structure used in Delft was not.
  – The structure used in Iran was not designed taking viscous scale effect inside the core into account
  – The waves applied in Delft were regular whilst the waves applied in Iran were irregular. This gives cause for uncertainty to the wave height and run-up level to be used.

8.2 Recommendations

- The relations describing the run-up on a rough, permeable slope are derived for very specific circumstances. Especially the fact that the structure as a whole was impermeable introduces laboratory effects that should be avoided if experiments in this field are to be performed again.

- The permeability of the structure will have influence on the run-up of non-breaking waves. Especially the permeability of the core will play a role in this since the permeability of the core is the smallest of the structure. A good definition for the permeability of the structure has to be developed and using this permeability, tests can be performed that describe the influence of this permeability on the run-up on a structure.

- The method of measuring the run-up on a slope needs to be optimised. Visual estimation does not seem to be the best way of measuring run-up. The method used in Iran, placing wave height meters along the slope seems to be a better method. Still, a lot of attention should be paid to the accuracy of the measurements and the side effects that are introduced by placing wave height meters along a slope.

- The influence of the layer thickness could be subject of further investigation. In the Delft experiments the layer thickness, as function of the diameter of the armour units, is not varied. Since the run-up on a rough permeable slope is reduced by the energy dissipation inside the armour layer, the thickness might have a significant influence on the run-up.

References

Battjes, J.A. (1974). Computation of set-up, longshore currents, run-up and overtopping due to wind-generated waves. PhD-thesis at the Delft University of Technology.

Battjes, J.A. (1988). Surf-zone dynamics. Annual Review of fluid mechanics 1988, pp 257-293.

Battjes, J.A. and Roos, A. (1975). Characteristics of flow in run-up of periodic waves. Communications on Hydraulics. Department of Civil Engineering. Delft University of Technology. Report number 75-3.

CUR/RWS (1995). Manual on the Use of Rock in Hydraulic Engineering. Center for Civil Engineering Research and Codes. CUR Report 169.

Goda, Y. and Suzuki, Y. (1976). Estimation of incident and reflected waves in random wave experiments. 15th conference on coastal engineering, chapter 48, pp. 828-845.

Hughes, S.A. (1993). Physical Models and Laboratory Techniques in Coastal Engineering. Advances series on Ocean Engineering-Volume 7. World Scientific Publishing Co. Pte. Ltd.

Jong, R.J. de (1996). Wave transmission at low-crested structures. Stability of tetrapods at front, crest and rear of a low-crested breakwater. MSc-thesis at the Delft University of Technology.

Klein Breteler, M. and Pilarczyk, K.W. (1996). Stability of roughness elements and run-up reduction. Proc. 25th ICCE, ASCE, Orlanda, USA, 1996, pp. 1556-1568.

SPM (1984). Shore Protection Manual. Coastal Engineering Research Center. U.S. Army Corps of Engineers.

Van der Meer, J.W. (1988). Rock slopes and gravel beaches under wave attack. Delft Hydraulics publication number 396.

Van der Meer, J.W. (1993). Conceptual design of rubble mound breakwaters. Delft Hydraulics publication no. 483.

Van der Meer, J.W. and Janssen, J.P.F.M. (1994). Wave run-up and wave overtopping at dikes and revetments. Delft Hydraulics publication no. 485.

Van der Meer, J.W. and Stam, C.-J. (1992). Wave run-up on smooth and rock slopes of coastal structures. Journal of Waterway, Port, Coastal and Ocean Engineering, vol. 118, no.5 Sept/Oct 1992.

Van Gent, M.R.A. (1992). Numerical model for wave action on and in coastal structures. Communications on Hydraulic and Geotechnical Engineering. Report number 92-6.

Van Gent, M.R.A. (1995). Wave interaction with permeable coastal structures. PhD-thesis at the Delft University of Technology.

Appendices

Appendix I Reduction factor γ_f

Structure	γ_f
Smooth, impermeable (including asphalt, smooth closely pitched concrete blocks)	1.0
Stone blocks, pitched or mortared and open-stone asphalt	0.95
Grass (length 0.03 m)	0.9-1.0
Concrete blocks	0.9
Stone blocks, granite sets	0.85-0.9
Turf	0.85-0.9
Rough concrete	0.85
One layer of stone rubble on an impermeable basis (loading conditions: H_s/D = 1.5 to 3)	0.55-0.60
Stones set in cement	0.7-0.8
Gravel, gabion mattresses	0.7
Dumped round stones	0.6-0.65
Rock/riprap (total layer thickness, $t_a > 2D_{n50}$ and loading conditions: H_s/D = 1.5 to 3)	0.5-0.55

table I-1, Roughness reduction factors, γ_f

Appendix II Variation of the material used in Delft

Large Stone, experiments 400-series

ρ = 3000 kg/m^3
total weight: 146.4 kg

total amount: 178 pieces
amount/m^2: 153.4

D_{n50} = 0.065 m
D_{85} = 0.074 m
D_{20} = 0.05 m
D_{15} = 0.048 m

L/D average = 2.15

Middle stone, experiments 500-serie

ρ = 2680 kg/m^3

total weight: 97.4 kg

total amount: 389 pieces
amount/m^2: 335.3

D_{n50} = 0.045 m
D_{85} = 0.048 m
D_{20} = 0.035 m
D_{15} = 0.030 m

L/D average = 2.12

Small stone, experiments 600-series

ρ = 2600 kg/m^3

total amount: 1242 pieces
amount/m^2: 1070.7

total weight: 65.5 kg

D_{n50} = 0.027 m
D_{85} = 0.03 m
D_{20} = 0.022 m
D_{15} = 0.021 m

L/D average = 2.13

Large tetrapods, experiments 200-series

h = 0.079 m
D_n = 0.05 m

c = (0.477*h) = 0.038 m

amount: 341
amount/m^2: 294

Middle tetrapods, experiments 100-series

h = 0.068 m
D_n = 0.044 m
c = (0.477*h) = 0.032 m

amount: 429
amount/m^2: 369.8

Small tetrapods, experiments 300-series

h = 0.055 m
D_n = 0.036 m
c = (0.477*h) = 0.026 m

amount: 597
surface: 0.77*1.24= 0.955 m2
amount/m^2: 625.1

Appendix III Drawing of case used in Delft

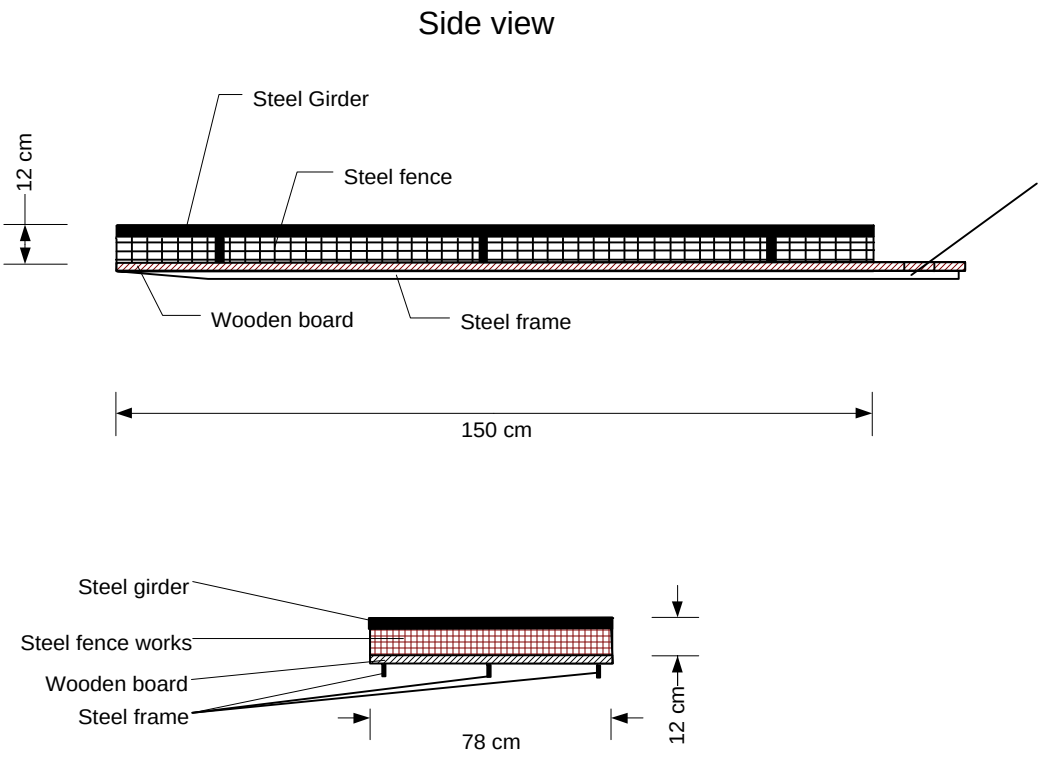

figure III-1, Drawings of case used in Delft

Appendix IV Data sets of the Delft experiments

Experiments performed with tetrapods, 100-series through 300-series

100-series

Experiment #	*H* (m)	*T* (s)	D_n (m)	$cot\alpha$	Run-up (m)
100	0.05	1.54	0.044	1.5	0.049923
101	0.07	1.54	0.044	1.5	0.074885
102	0.101	1.54	0.044	1.5	0.099846
103	0.131	1.54	0.044	1.5	0.127581
104	0.16	1.54	0.044	1.5	0.160863
105	0.047	1.54	0.044	1.5	0.049923
106	0.067	1.54	0.044	1.5	0.072111
107	0.099	1.54	0.044	1.5	0.099846
108	0.129	1.54	0.044	1.5	0.122034
109	0.162	1.54	0.044	1.5	0.160863
110	0.036	1.12	0.044	1.5	0.038829
111	0.051	1.12	0.044	1.5	0.05547
112	0.065	1.12	0.044	1.5	0.072111
113	0.08	1.12	0.044	1.5	0.077658
114	0.093	1.12	0.044	1.5	0.094299
115	0.103	1.12	0.044	1.5	0.11094
116	0.033	1.12	0.044	1.5	0.033282
117	0.051	1.12	0.044	1.5	0.05547
118	0.081	1.12	0.044	1.5	0.072111
119	0.069	1.12	0.044	1.5	0.066564
120	0.093	1.12	0.044	1.5	0.094299
121	0.103	1.12	0.044	1.5	0.116487
150	0.032	1.54	0.044	3	0.025298
151	0.053	1.54	0.044	3	0.04111
152	0.078	1.54	0.044	3	0.063246
153	0.126	1.54	0.044	3	0.117004
154	0.103	1.54	0.044	3	0.094868
155	0.031	1.54	0.044	3	0.018974
156	0.055	1.54	0.044	3	0.047434
157	0.079	1.54	0.044	3	0.066408
158	0.102	1.54	0.044	3	0.094868
159	0.129	1.54	0.044	3	0.113842
166	0.039	1.12	0.044	3	0.031623
167	0.054	1.12	0.044	3	0.04111
168	0.069	1.12	0.044	3	0.053759
169	0.091	1.12	0.044	3	0.066408
170	0.098	1.12	0.044	3	0.082219
171	0.11	1.12	0.044	3	0.091706
172	0.041	1.12	0.044	3	0.037947
173	0.055	1.12	0.044	3	0.044272
174	0.07	1.12	0.044	3	0.056921
175	0.084	1.12	0.044	3	0.06957
176	0.099	1.12	0.044	3	0.082219
177	0.109	1.12	0.044	3	0.094868

Experiment #	H (m)	T (s)	D_n (m)	$cot\alpha$	Run-up (m)
180	0.082	1.12	0.044	4	0.050932
181	0.097	1.12	0.044	4	0.058209
182	0.108	1.12	0.044	4	0.065485
183	0.083	1.12	0.044	4	0.053358
184	0.096	1.12	0.044	4	0.063059

200-series

Experiment #	H (m)	T (s)	D_n (m)	$cot\alpha$	Run-up (m)
200	0.04	1.54	0.05	1.5	0.022188
201	0.063	1.54	0.05	1.5	0.05547
202	0.093	1.54	0.05	1.5	0.077658
203	0.123	1.54	0.05	1.5	0.11094
204	0.147	1.54	0.05	1.5	0.149769
205	0.04	1.54	0.05	1.5	0.033282
206	0.063	1.54	0.05	1.5	0.05547
207	0.094	1.54	0.05	1.5	0.138675
208	0.123	1.54	0.05	1.5	0.116487
216	0.072	1.12	0.05	1.5	0.016641
217	0.04	1.12	0.05	1.5	0.033282
218	0.057	1.12	0.05	1.5	0.05547
219	0.091	1.12	0.05	1.5	0.094299
220	0.108	1.12	0.05	1.5	0.105393
221	0.121	1.12	0.05	1.5	0.116487
222	0.037	1.12	0.05	1.5	0.044376
223	0.055	1.12	0.05	1.5	0.044376
224	0.073	1.12	0.05	1.5	0.061017
225	0.088	1.12	0.05	1.5	0.088752
226	0.106	1.12	0.05	1.5	0.094299
227	0.121	1.12	0.05	1.5	0.105393
250	0.032	1.54	0.05	3	0.037947
251	0.056	1.54	0.05	3	0.050596
252	0.077	1.54	0.05	3	0.063246
253	0.102	1.54	0.05	3	0.094868
254	0.033	1.54	0.05	3	0.018974
255	0.055	1.54	0.05	3	0.047434
256	0.081	1.54	0.05	3	0.063246
257	0.102	1.54	0.05	3	0.072732
266	0.069	1.12	0.05	3	0.053759
267	0.055	1.12	0.05	3	0.047434
268	0.054	1.12	0.05	3	0.047434
269	0.034	1.12	0.05	3	0.02846
270	0.084	1.12	0.05	3	0.066408
271	0.097	1.12	0.05	3	0.075895
272	0.109	1.12	0.05	3	0.091706
273	0.039	1.12	0.05	3	0.034785
274	0.066	1.12	0.05	3	0.050596
275	0.088	1.12	0.05	3	0.06957
276	0.099	1.12	0.05	3	0.075895

Experiment #	H (m)	T (s)	D_n (m)	$cot\alpha$	Run-up (m)
277	0.108	1.12	0.05	3	0.091706
278	0.081	1.12	0.05	4	0.03153
279	0.079	1.12	0.05	4	0.041231
281	0.095	1.12	0.05	4	0.082462
282	0.107	1.12	0.05	4	0.089738
283	0.107	1.12	0.05	4	0.097014

300-series

Experiment #	H (m)	T (s)	D_n (m)	$cot\alpha$	Run-up (m)
300	0.042	1.54	0.036	1.5	0.044
301	0.076	1.54	0.036	1.5	0.078
302	0.102	1.54	0.036	1.5	0.100
303	0.13	1.54	0.036	1.5	0.133
304	0.165	1.54	0.036	1.5	0.178
306	0.045	1.54	0.036	1.5	0.039
307	0.072	1.54	0.036	1.5	0.067
308	0.1	1.54	0.036	1.5	0.100
309	0.13	1.54	0.036	1.5	0.128
310	0.169	1.54	0.036	1.5	0.166
311	0.04	1.12	0.036	1.5	0.044
312	0.05	1.12	0.036	1.5	0.055
313	0.07	1.12	0.036	1.5	0.083
314	0.109	1.12	0.036	1.5	0.111
315	0.085	1.12	0.036	1.5	0.094
316	0.114	1.12	0.036	1.5	0.128
317	0.047	1.12	0.036	1.5	0.055
318	0.053	1.12	0.036	1.5	0.067
319	0.073	1.12	0.036	1.5	0.083
320	0.088	1.12	0.036	1.5	0.116
321	0.101	1.12	0.036	1.5	0.128
322	0.115	1.12	0.036	1.5	0.139
350	0.044	1.54	0.036	3	0.022
351	0.06	1.54	0.036	3	0.041
352	0.071	1.54	0.036	3	0.047
353	0.087	1.54	0.036	3	0.063
354	0.102	1.54	0.036	3	0.076
355	0.112	1.54	0.036	3	0.092
356	0.045	1.54	0.036	3	0.022
357	0.059	1.54	0.036	3	0.038
358	0.071	1.54	0.036	3	0.054
359	0.088	1.54	0.036	3	0.063
360	0.104	1.54	0.036	3	0.079
361	0.113	1.54	0.036	3	0.089
362	0.051	1.12	0.036	3	0.041
363	0.034	1.12	0.036	3	0.019
364	0.076	1.12	0.036	3	0.066
365	0.097	1.12	0.036	3	0.092
366	0.121	1.12	0.036	3	0.123

Experiment #	H (m)	T (s)	D_n (m)	$cot\alpha$	Run-up (m)
367	0.03	1.12	0.036	3	0.013
368	0.051	1.12	0.036	3	0.041
369	0.078	1.12	0.036	3	0.073
370	0.098	1.12	0.036	3	0.101
371	0.122	1.12	0.036	3	0.130

Experiments performed with rock units, 400-series through 600-series

400-series

Experiment #	H (m)	T (s)	D_{n50} (m)	$cot\alpha$	Run-up (m)
400	0.057	1.54	0.065	1.5	0.044
401	0.033	1.54	0.065	1.5	0.033
402	0.084	1.54	0.065	1.5	0.089
403	0.105	1.54	0.065	1.5	0.116
404	0.126	1.54	0.065	1.5	0.139
405	0.033	1.54	0.065	1.5	0.033
406	0.059	1.54	0.065	1.5	0.061
407	0.083	1.54	0.065	1.5	0.094
408	0.108	1.54	0.065	1.5	0.128
409	0.128	1.54	0.065	1.5	0.150
410	0.047	1.12	0.065	1.5	0.039
411	0.066	1.12	0.065	1.5	0.044
412	0.088	1.12	0.065	1.5	0.078
413	0.103	1.12	0.065	1.5	0.100
414	0.121	1.12	0.065	1.5	0.116
415	0.134	1.12	0.065	1.5	0.128
416	0.072	1.12	0.065	1.5	0.050
417	0.047	1.12	0.065	1.5	0.039
418	0.086	1.12	0.065	1.5	0.072
419	0.104	1.12	0.065	1.5	0.100
420	0.119	1.12	0.065	1.5	0.111
421	0.135	1.12	0.065	1.5	0.122
450	0.036	1.54	0.065	3	0.028
451	0.054	1.54	0.065	3	0.044
452	0.078	1.54	0.065	3	0.063
453	0.102	1.54	0.065	3	0.076
454	0.123	1.54	0.065	3	0.098
455	0.034	1.54	0.065	3	0.009
456	0.055	1.54	0.065	3	0.038
457	0.079	1.54	0.065	3	0.066
458	0.104	1.54	0.065	3	0.079
459	0.126	1.54	0.065	3	0.104
460	0.041	1.12	0.065	3	0.038
461	0.055	1.12	0.065	3	0.044
462	0.086	1.12	0.065	3	0.057
463	0.07	1.12	0.065	3	0.032
464	0.11	1.12	0.065	3	0.076
465	0.099	1.12	0.065	3	0.063

Experiment #	H (m)	T (s)	D_{n50} (m)	$cot\alpha$	Run-up (m)
466	0.039	1.12	0.065	3	0.022
467	0.053	1.12	0.065	3	0.035
468	0.068	1.12	0.065	3	0.047
469	0.087	1.12	0.065	3	0.066
470	0.097	1.12	0.065	3	0.076
471	0.111	1.12	0.065	3	0.082
480	0.085	1.12	0.065	4	0.046
481	0.087	1.12	0.065	4	0.051
482	0.1	1.12	0.065	4	0.058
483	0.099	1.12	0.065	4	0.056
484	0.113	1.12	0.065	4	0.065
485	0.115	1.12	0.065	4	0.061

500-series

Experiment #	H (m)	T (s)	D_{n50} (m)	$cot\alpha$	Run-up (m)
500	0.045	1.54	0.045	1.5	0.033
501	0.073	1.54	0.045	1.5	0.055
502	0.101	1.54	0.045	1.5	0.094
503	0.131	1.54	0.045	1.5	0.122
504	0.166	1.54	0.045	1.5	0.155
505	0.047	1.54	0.045	1.5	0.033
506	0.073	1.54	0.045	1.5	0.067
507	0.102	1.54	0.045	1.5	0.100
508	0.133	1.54	0.045	1.5	0.128
509	0.163	1.54	0.045	1.5	0.161
510	0.035	1.12	0.045	1.5	0.028
511	0.078	1.12	0.045	1.5	0.039
512	0.05	1.12	0.045	1.5	0.055
513	0.065	1.12	0.045	1.5	0.078
514	0.09	1.12	0.045	1.5	0.111
515	0.101	1.12	0.045	1.5	0.128
516	0.053	1.12	0.045	1.5	0.055
517	0.029	1.12	0.045	1.5	0.033
518	0.064	1.12	0.045	1.5	0.078
519	0.078	1.12	0.045	1.5	0.089
520	0.089	1.12	0.045	1.5	0.116
521	0.1	1.12	0.045	1.5	0.128
550	0.029	1.54	0.045	3	0.032
551	0.05	1.54	0.045	3	0.051
552	0.071	1.54	0.045	3	0.073
553	0.096	1.54	0.045	3	0.095
554	0.122	1.54	0.045	3	0.130
555	0.03	1.54	0.045	3	0.028
556	0.047	1.54	0.045	3	0.047
557	0.074	1.54	0.045	3	0.085
558	0.094	1.54	0.045	3	0.104
559	0.119	1.54	0.045	3	0.136
560	0.04	1.12	0.045	3	0.032

Experiment #	H (m)	T (s)	D_{n50} (m)	$cot\alpha$	Run-up (m)
561	0.057	1.12	0.045	3	0.047
562	0.07	1.12	0.045	3	0.057
563	0.085	1.12	0.045	3	0.076
564	0.101	1.12	0.045	3	0.092
565	0.111	1.12	0.045	3	0.101
566	0.042	1.12	0.045	3	0.035
567	0.054	1.12	0.045	3	0.044
568	0.07	1.12	0.045	3	0.054
569	0.088	1.12	0.045	3	0.070
570	0.099	1.12	0.045	3	0.082
571	0.112	1.12	0.045	3	0.101
580	0.081	1.12	0.045	4	0.056
581	0.082	1.12	0.045	4	0.061
582	0.093	1.12	0.045	4	0.073
583	0.095	1.12	0.045	4	0.073
584	0.105	1.12	0.045	4	0.082
585	0.104	1.12	0.045	4	0.082

600-series

Experiment #	H (m)	T (m)	D_{n50} (m)	$cot\alpha$	Run-up (m)
600	0.03	1.54	0.027	1.5	0.028
601	0.046	1.54	0.027	1.5	0.050
602	0.064	1.54	0.027	1.5	0.061
603	0.077	1.54	0.027	1.5	0.072
604	0.037	1.54	0.027	1.5	0.044
605	0.047	1.54	0.027	1.5	0.055
606	0.062	1.54	0.027	1.5	0.067
607	0.08	1.54	0.027	1.5	0.083
608	0.028	1.12	0.027	1.5	0.044
609	0.041	1.12	0.027	1.5	0.061
610	0.056	1.12	0.027	1.5	0.083
611	0.028	1.12	0.027	1.5	0.039
612	0.042	1.12	0.027	1.5	0.067
613	0.056	1.12	0.027	1.5	0.089
614	0.069	1.12	0.027	1.5	0.100
615	0.068	1.12	0.027	1.5	0.111
650	0.015	1.54	0.027	3	0.028
651	0.025	1.54	0.027	3	0.038
652	0.034	1.54	0.027	3	0.054
653	0.047	1.54	0.027	3	0.073
654	0.057	1.54	0.027	3	0.085
655	0.016	1.54	0.027	3	0.032
656	0.026	1.54	0.027	3	0.044
657	0.034	1.54	0.027	3	0.057
658	0.044	1.54	0.027	3	0.070
659	0.055	1.54	0.027	3	0.085
660	0.039	1.12	0.027	3	0.038
661	0.055	1.12	0.027	3	0.054

Experiment #	H (m)	T (s)	D_{n50} (m)	$cot\alpha$	Run-up (m)
662	0.07	1.12	0.027	3	0.073
663	0.084	1.12	0.027	3	0.085
664	0.037	1.12	0.027	3	0.038
665	0.057	1.12	0.027	3	0.060
666	0.069	1.12	0.027	3	0.073
667	0.083	1.12	0.027	3	0.085
680	0.062	1.12	0.027	4	0.056
681	0.074	1.12	0.027	4	0.068
682	0.06	1.12	0.027	4	0.056
683	0.08	1.12	0.027	4	0.068
684	0.09	1.12	0.027	4	0.078
685	0.087	1.12	0.027	4	0.078

Appendix V Cross-section of model used in Iran

The cross-sections given in this appendix are the drawings used for the experiments performed in Iran. All dimensions are model dimensions given either in grams or in centimetres.

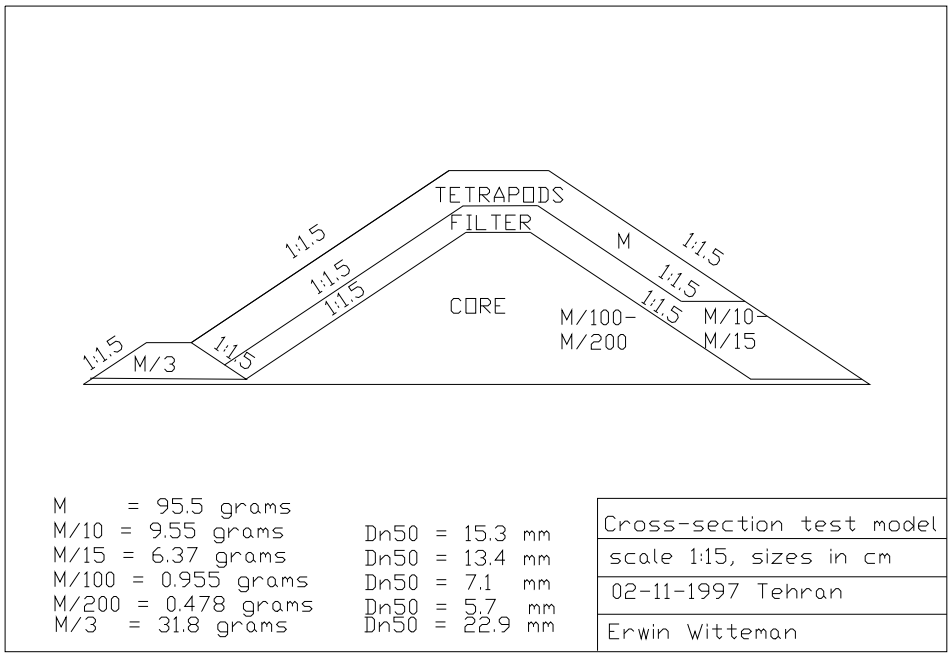

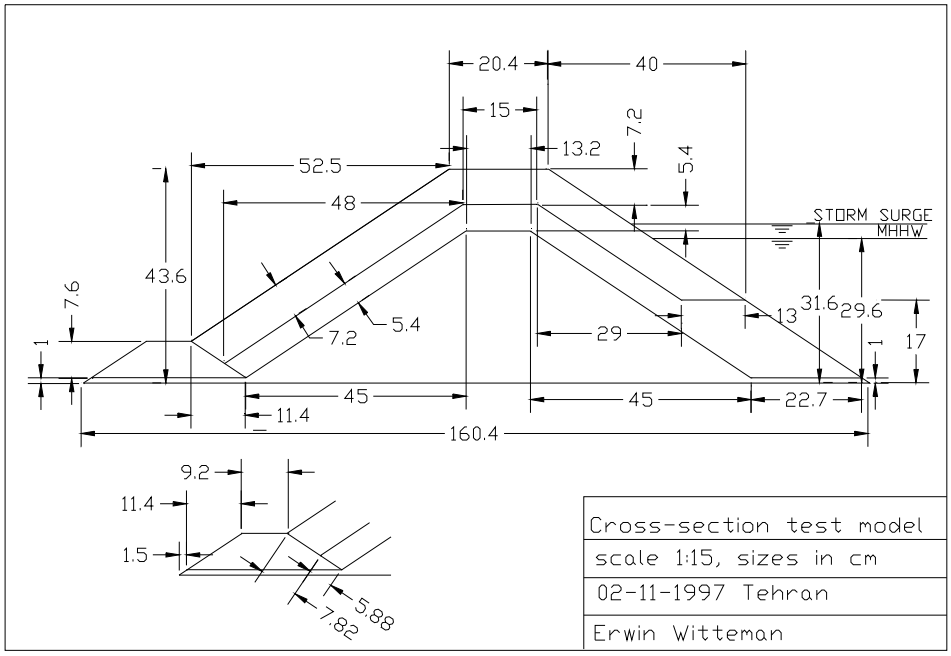

figure V-1, Cross-section of model used in Iran

Appendix VI Plan view flume Iran

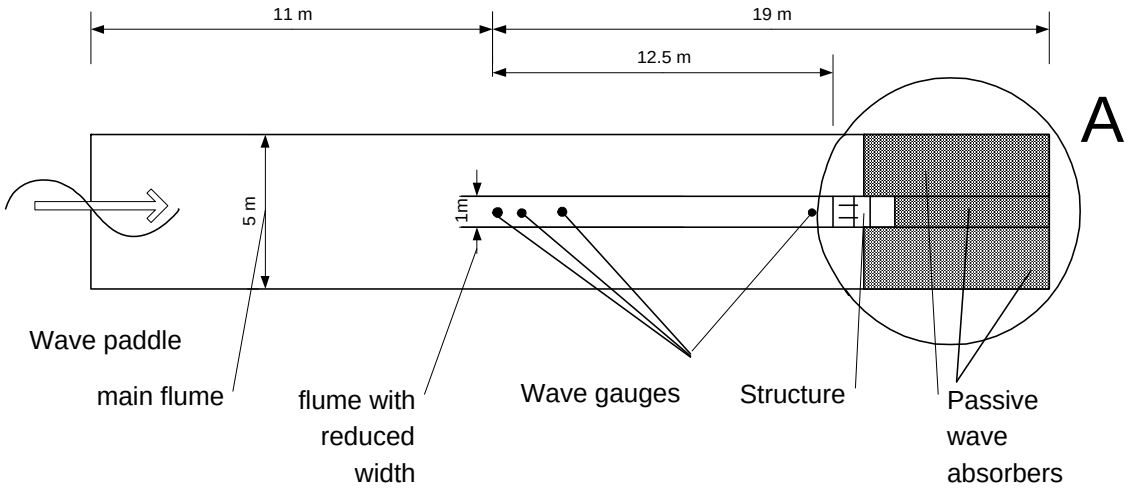

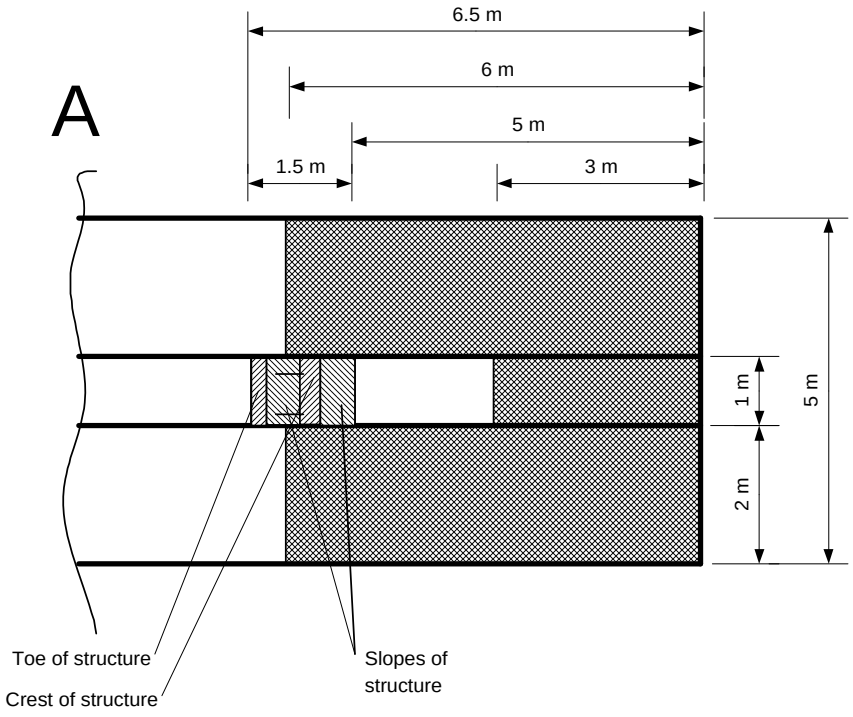

figure VI-1, Plan view flume Iran

Appendix VII, Data of experiments performed in Iran

test #	H_s (m)	T_p (s)	T_m (s)	$R_{u2\%}$ (m)	ξ_p	ξ_m
1101	2.69	6.24	5.64	3.91	3.17	2.86
1102	3.73	8.23	6.94	3.5	3.55	2.99
1103	3.41	8.23	6.99	3.24	3.71	3.15
1104	2.73	8.23	7	2.62	4.15	3.53
1105	2.45	9.05	8.52	2.63	4.82	4.53
1106	2.08	12.41	9.98	3.33	7.17	5.76
1107	2.36	12.41	9.95	3.78	6.73	5.4
1109	2.82	6.24	5.65	2.73	3.1	2.8
1110	3.38	6.24	5.77	3.16	2.83	2.61
1116	4.09	6.73	5.95	3.76	2.77	2.45
1118	3.69	6.24	5.85	3.44	2.71	2.54
1124	4.77	8.23	6.4	5.11	3.14	2.44
1131	5.62	8.23	5.84	5.4	2.89	2.05
1132	5.3	8.23	5.72	5.27	2.98	2.07
1137	4.06	9.05	8.09	4.82	3.74	3.34

table VII-1 Data of experiments performed with $\lambda = 50$, prototype values

test #	H_s (m)	T_p (s)	T_m (s)	$R_{u2\%}$ (m)	ξ_p	ξ_m
1101	0.0538	0.8825	0.7976	0.0782	3.17	2.86
1102	0.0746	1.1639	0.9815	0.0700	3.55	2.99
1103	0.0682	1.1639	0.9885	0.0648	3.71	3.15
1104	0.0546	1.1639	0.9899	0.0524	4.15	3.53
1105	0.0490	1.2799	1.2049	0.0526	4.82	4.53
1106	0.0416	1.7550	1.4114	0.0666	7.17	5.76
1107	0.0472	1.7550	1.4071	0.0756	6.73	5.4
1109	0.0564	0.8825	0.7990	0.0546	3.1	2.8
1110	0.0676	0.8825	0.8160	0.0632	2.83	2.61
1116	0.0818	0.9518	0.8415	0.0752	2.77	2.45
1118	0.0738	0.8825	0.8273	0.0688	2.71	2.54
1124	0.0954	1.1639	0.9051	0.1022	3.14	2.44
1131	0.1124	1.1639	0.8259	0.1080	2.89	2.05
1132	0.1060	1.1639	0.8089	0.1054	2.98	2.07
1137	0.0812	1.2799	1.1441	0.0964	3.74	3.34

table VII-2 Data of experiments performed with $\lambda = 50$, model values

test #	H_s (m)	T_p (s)	T_m (s)	$R_{u2\%}$ (m)	ξ_p	ξ_m
1201	3.31	7.43	6.26	2.02	3.39	2.86
1202	2.79	7.27	6.19	1.78	3.61	3.08
1203	2.91	8.32	6.83	1.92	4.05	3.32
1204	3.14	10.77	8.14	1.94	5.04	3.81
1205	2.57	10.77	8.18	1.79	5.57	4.23
1206	2.51	12	9.46	2.25	6.29	4.96
1207	2.37	13.87	10.8	2.55	7.48	5.84
1208	3.68	7.43	6.35	2.33	3.21	2.75
1209	3.6	8.32	6.83	2.31	3.64	2.99
1210	3.51	10.61	8.1	2.44	4.7	3.59
1211	3.3	12	9.31	3.05	5.48	4.25
1212	3.29	13.87	10.8	3.79	6.35	4.94
1213	3.45	13.87	10.8	3.52	6.2	4.82
1215	4.56	10.61	8.07	2.87	4.12	3.14
1216	4.36	12.67	9.36	3.47	5.04	3.72
1217	4.28	13.87	10.7	4.91	5.56	4.28
1218	4.55	13.87	10.7	5.25	5.4	4.17
1220	5.09	8.32	7.02	3.15	3.06	2.58
1221	5.1	10.35	8.05	3.15	3.8	2.96
1222	5.08	12.84	9.01	4.04	4.73	3.32
1223	5.14	13.87	10.7	6.06	5.08	3.92
1225	5.42	10.35	8.09	3.28	3.69	2.88
1226	5.35	12.84	8.93	4.39	4.61	3.2
1227	5.55	12.84	8.97	4.49	4.52	3.16
1228	5.69	13.87	9.54	6.74	4.83	3.32
1229	4.55	7.43	6.54	2.85	2.89	2.54
1230	4.82	7.43	6.6	2.95	2.81	2.49
1231	5.26	7.43	6.66	3.19	2.69	2.41

table VII-3 Data of experiments performed with $\lambda = 66$, prototype values

test #	H_s (m)	T_p (s)	T_m (s)	$R_{u2\%}$ (m)	ξ_p	ξ_m
1201	0.0502	0.9146	0.7706	0.0306	3.39	2.86
1202	0.0423	0.8949	0.7619	0.0270	3.61	3.08
1203	0.0441	1.0241	0.8407	0.0291	4.05	3.32
1204	0.0476	1.3257	1.0020	0.0294	5.04	3.81
1205	0.0389	1.3257	1.0069	0.0271	5.57	4.23
1206	0.0380	1.4771	1.1644	0.0341	6.29	4.96
1207	0.0359	1.7073	1.3294	0.0386	7.48	5.84
1208	0.0558	0.9146	0.7816	0.0353	3.21	2.75
1209	0.0545	1.0241	0.8407	0.0350	3.64	2.99
1210	0.0532	1.3060	0.9970	0.0370	4.70	3.59
1211	0.0500	1.4771	1.1460	0.0462	5.48	4.25
1212	0.0498	1.7073	1.3294	0.0574	6.35	4.94
1213	0.0523	1.7073	1.3294	0.0533	6.20	4.82
1215	0.0691	1.3060	0.9933	0.0435	4.12	3.14
1216	0.0661	1.5596	1.1521	0.0526	5.04	3.72
1217	0.0648	1.7073	1.3171	0.0744	5.56	4.28
1218	0.0689	1.7073	1.3171	0.0795	5.40	4.17

test #	H_s (m)	T_p (s)	T_m (s)	$R_{u2\%}$ (m)	ξ_p	ξ_m
1220	0.0771	1.0241	0.8641	0.0477	3.06	2.58
1221	0.0773	1.2740	0.9909	0.0477	3.80	2.96
1222	0.0770	1.5805	1.1091	0.0612	4.73	3.32
1223	0.0779	1.7073	1.3171	0.0918	5.08	3.92
1225	0.0821	1.2740	0.9958	0.0497	3.69	2.88
1226	0.0811	1.5805	1.0992	0.0665	4.61	3.20
1227	0.0841	1.5805	1.1041	0.0680	4.52	3.16
1228	0.0862	1.7073	1.1743	0.1021	4.83	3.32
1229	0.0689	0.9146	0.8050	0.0432	2.89	2.54
1230	0.0730	0.9146	0.8124	0.0447	2.81	2.49
1231	0.0797	0.9146	0.8198	0.0483	2.69	2.41

table VII-3 Data of experiments performed with λ = 66, prototype values

Appendix VIII Influences of H, cotα, $D_{n(50)}$, n and T on run-up

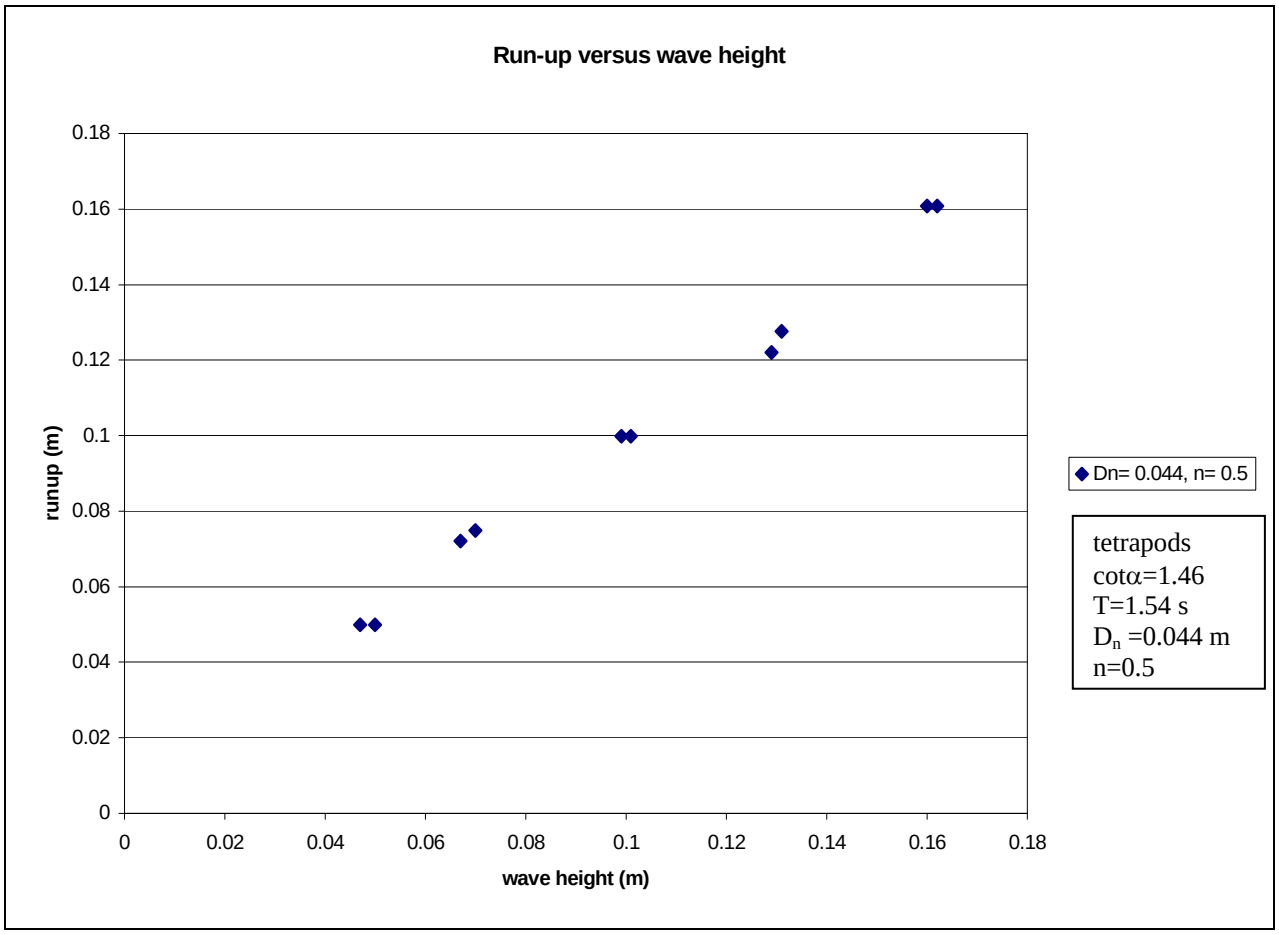

figure VIII-1, Influence of wave height on run-up

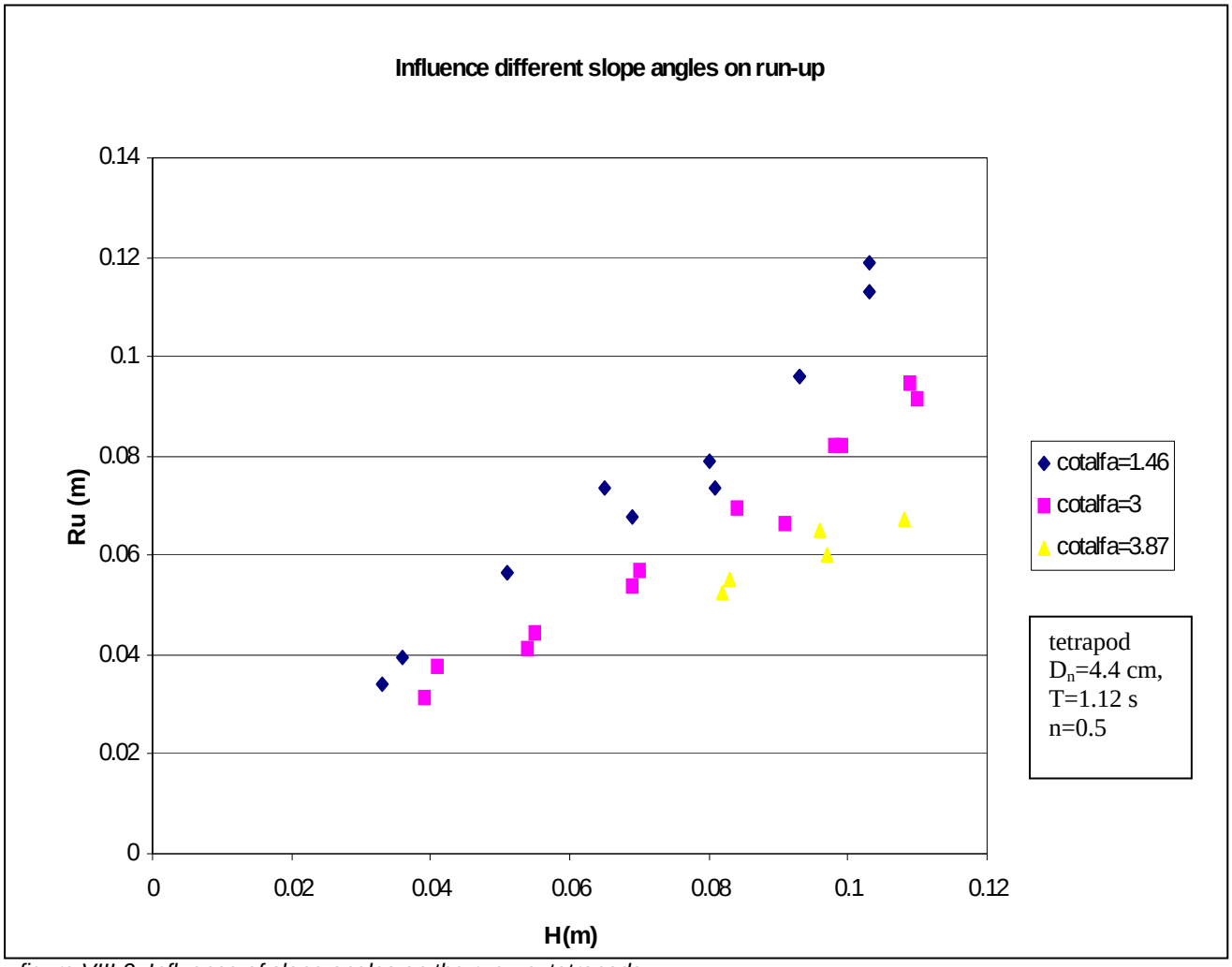

figure VIII-2, Influence of slope angles on the run-up, tetrapods

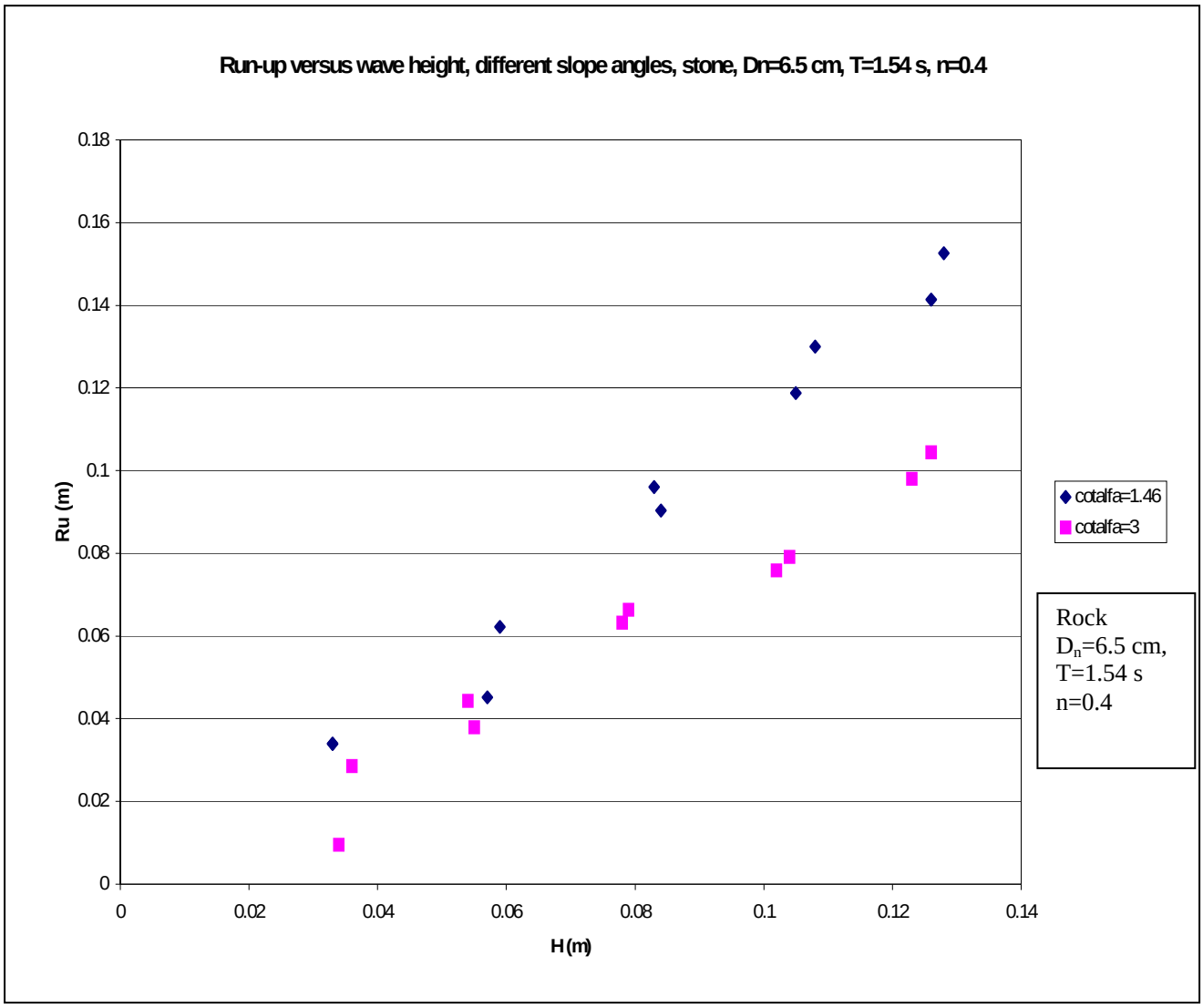

figure VIII-3, Influence of slope angles on run-up, rock

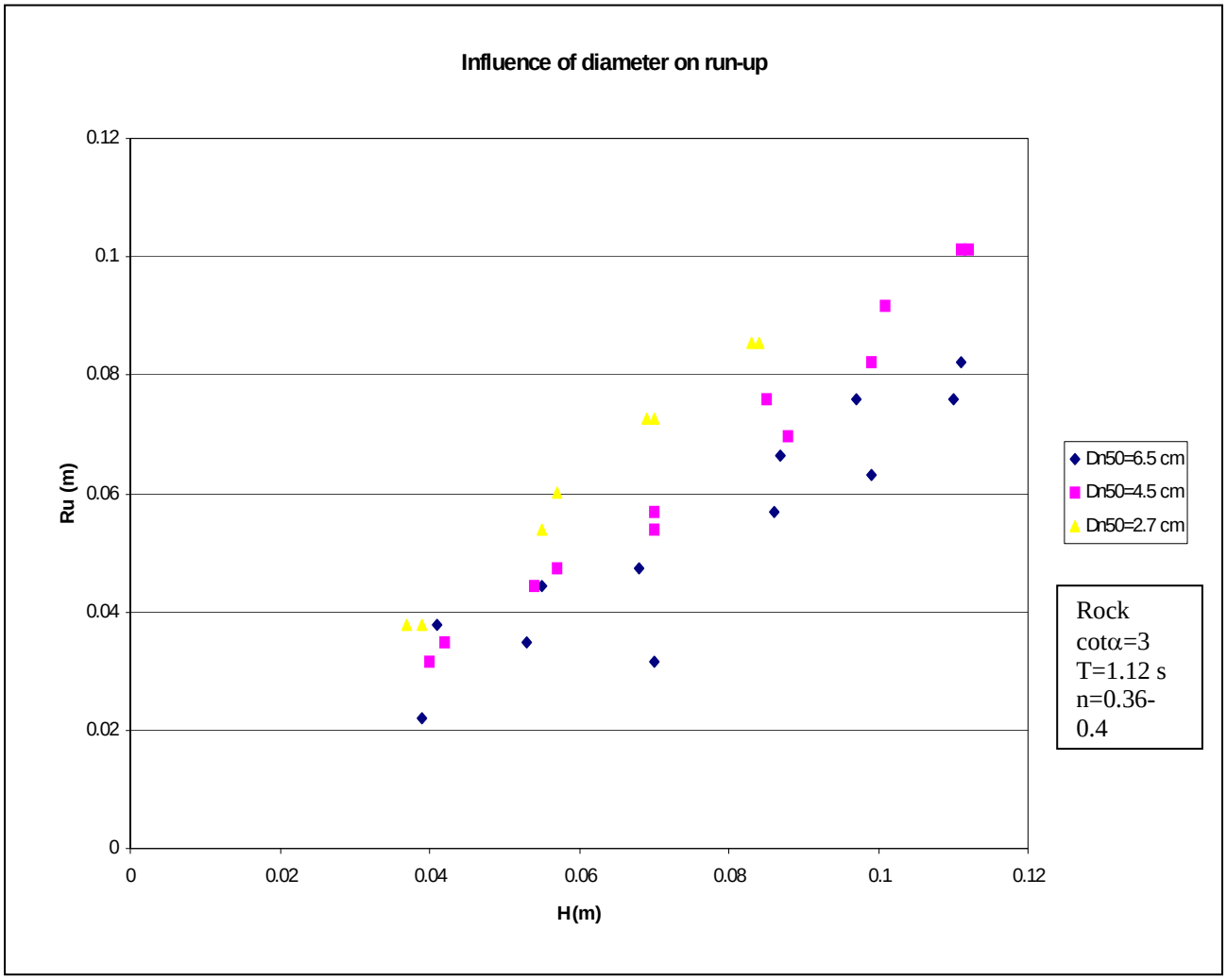

figure VIII-4, Influence of diameter on run-up, rock

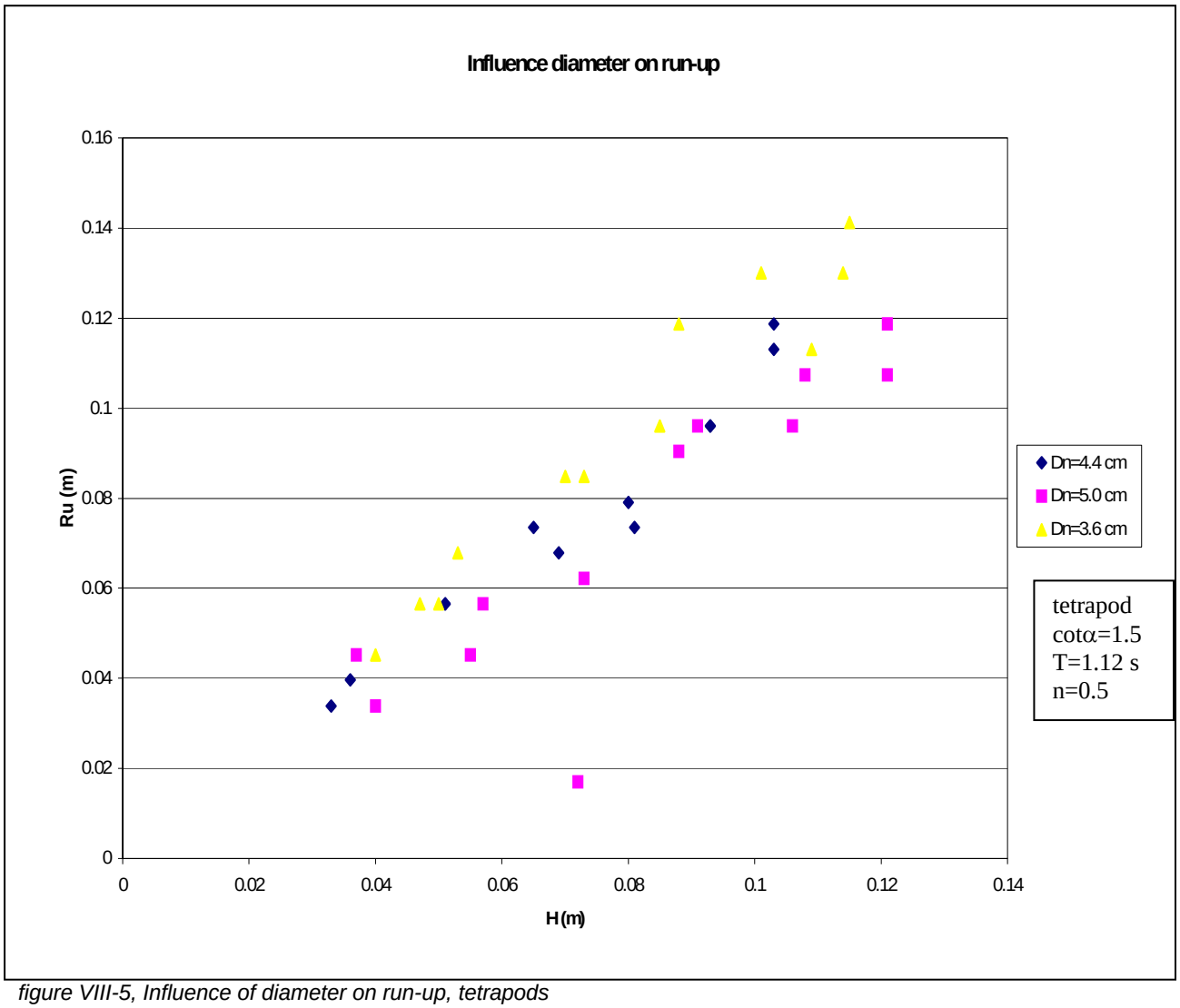

figure VIII-5, Influence of diameter on run-up, tetrapods

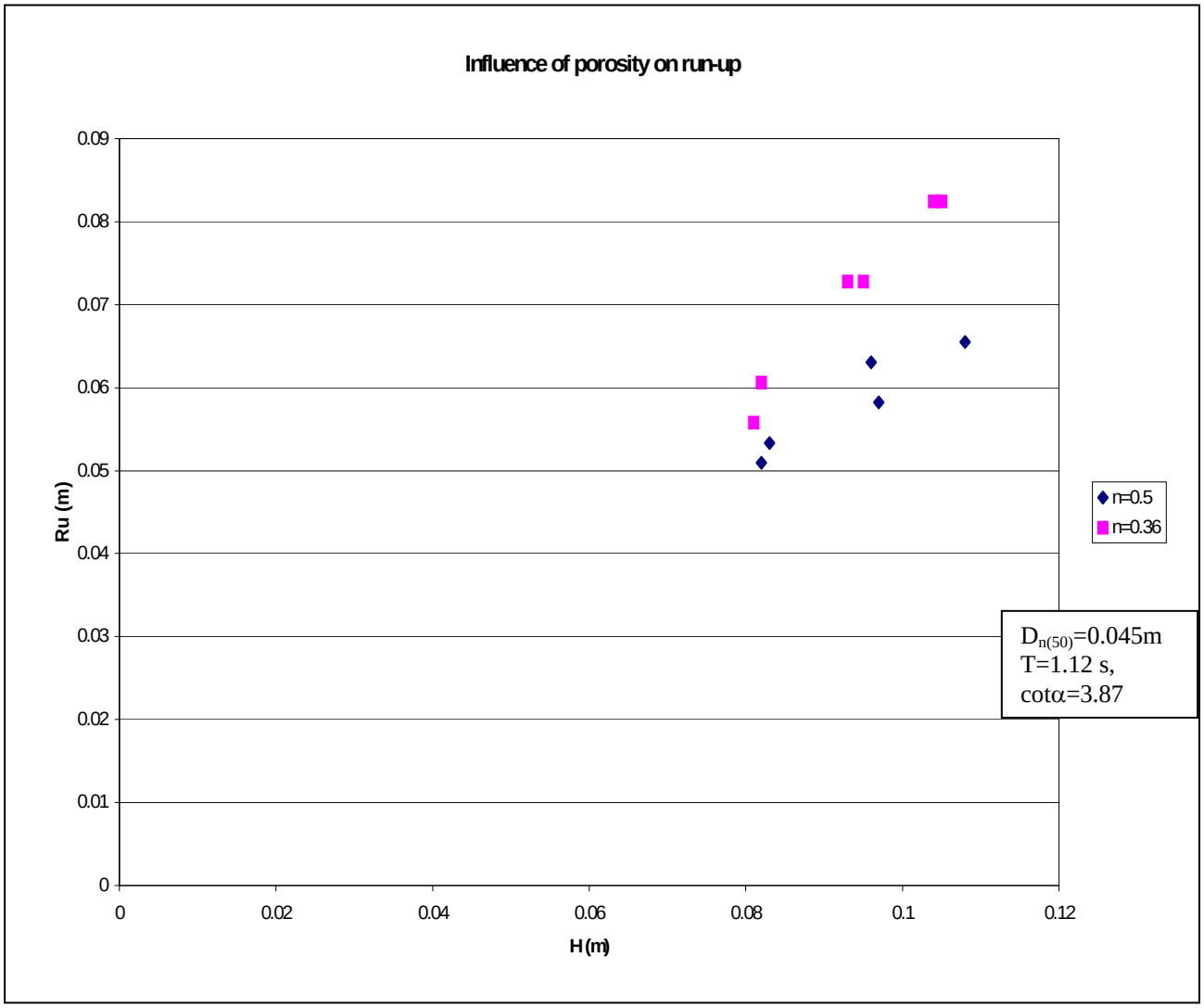

figure VIII-6, Influence of porosity on the run-up

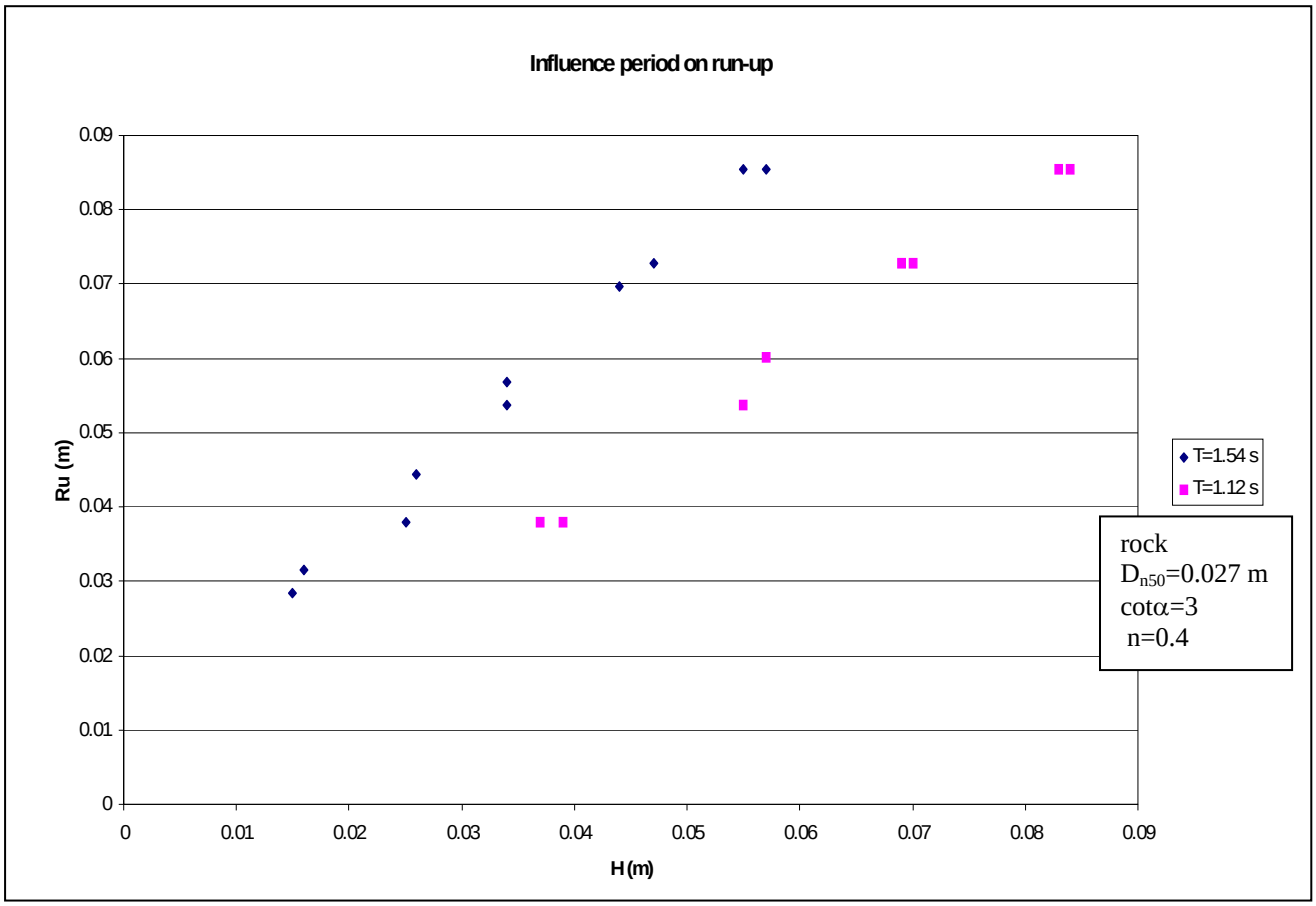

figure VIII-7, Influence of period on the run-up, rock

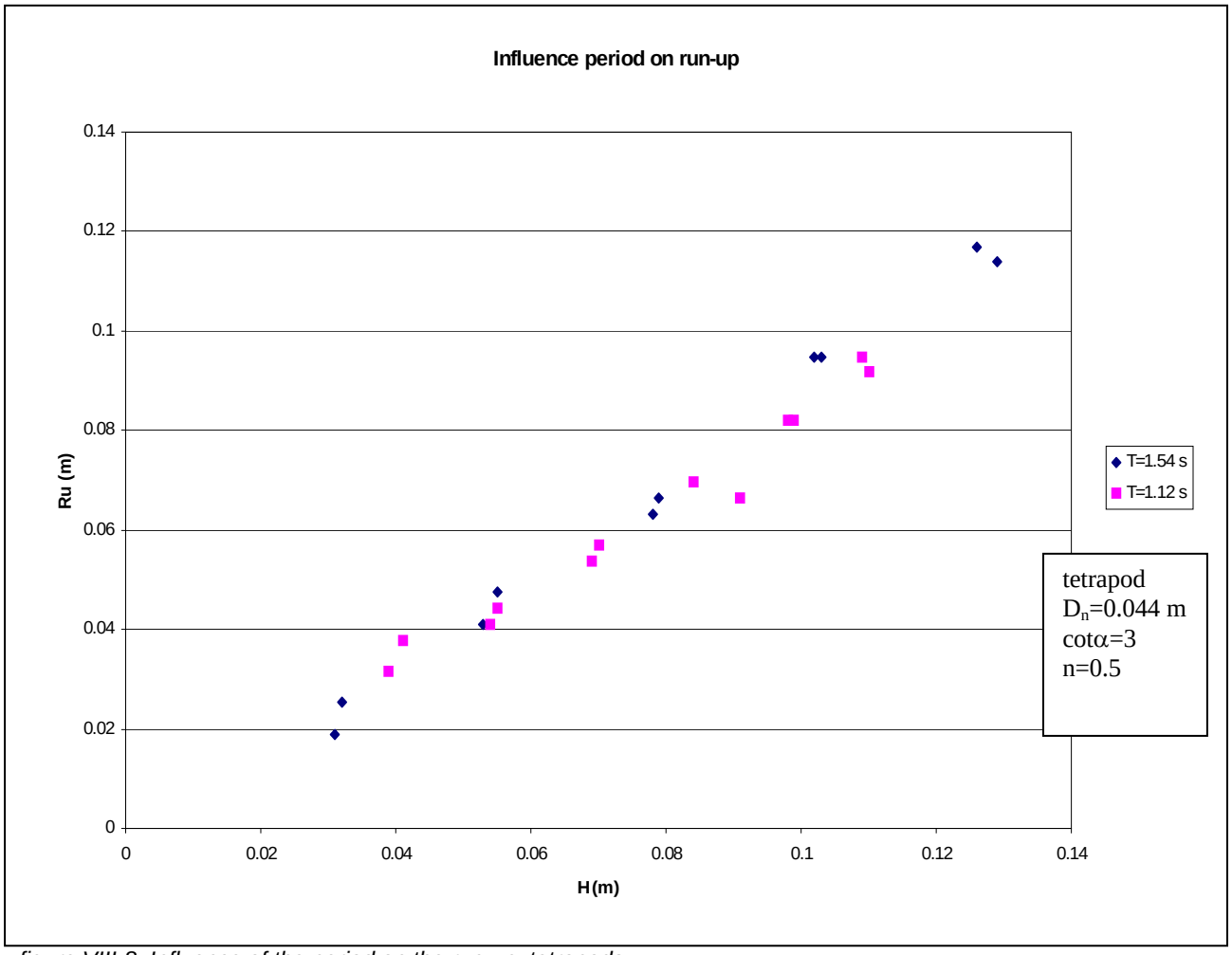

figure VIII-8, Influence of the period on the run-up, tetrapods

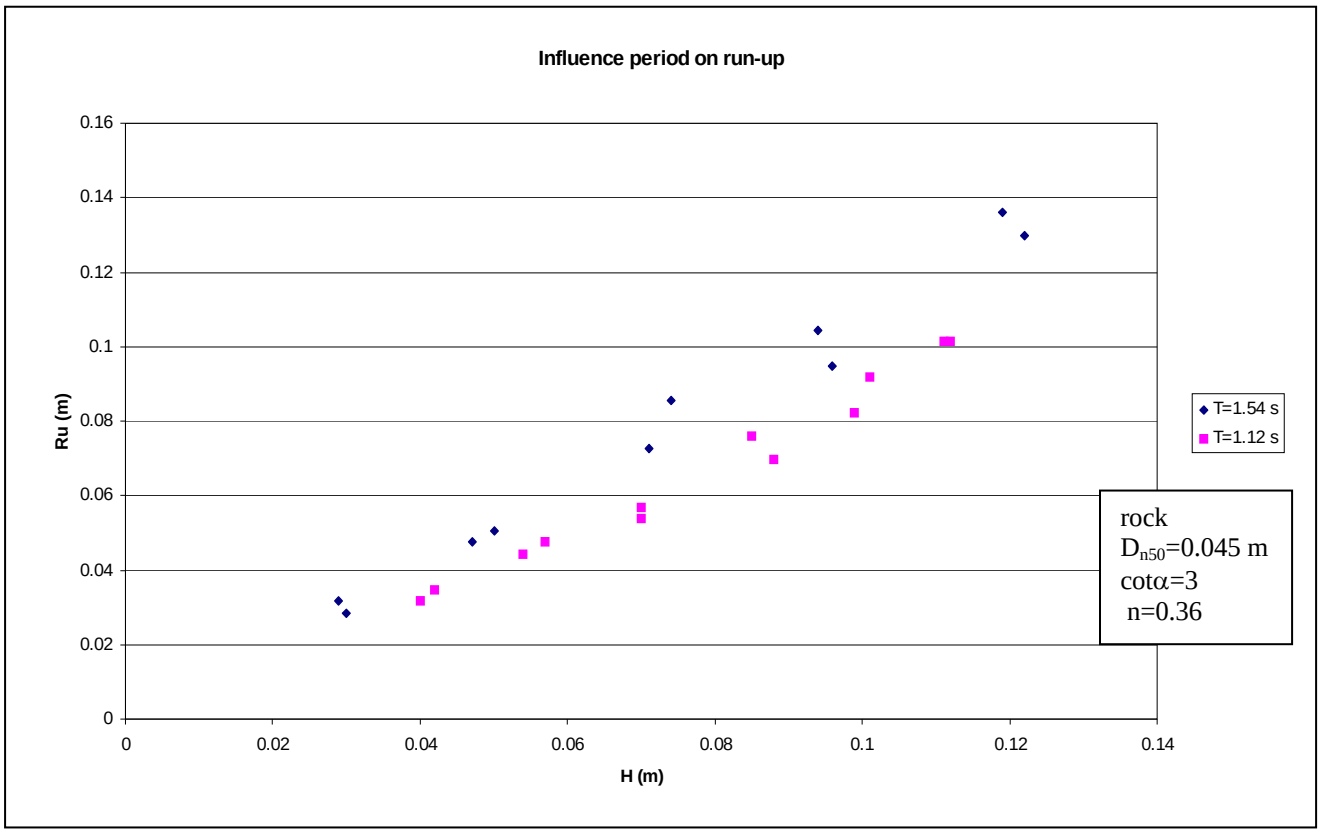

figure VIII-9, Influence of the period on run-up, rock

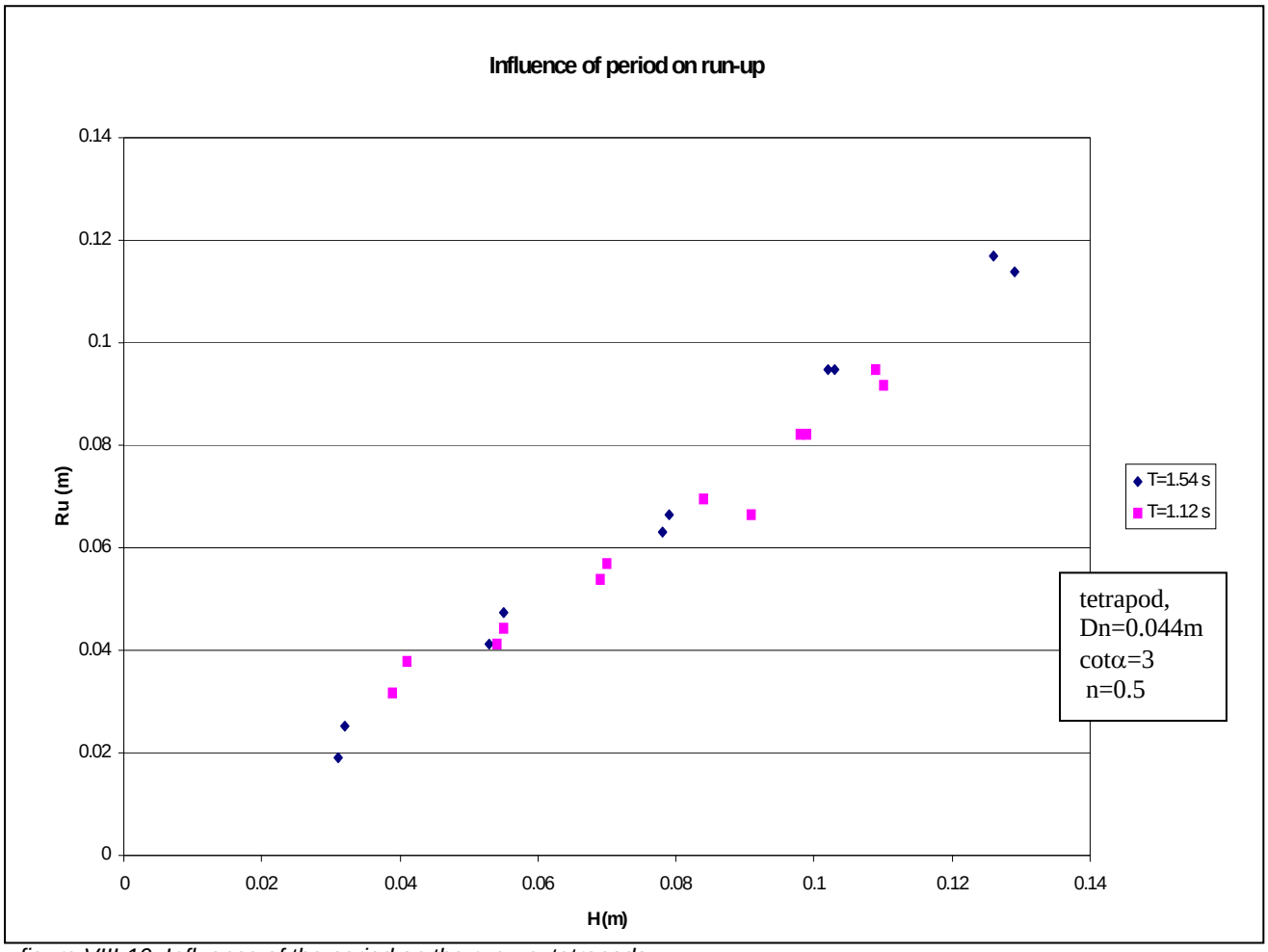

figure VIII-10, Influence of the period on the run-up, tetrapods

Appendix IX Relative run-up (R_u/ H) versus ξ, Delft experiments

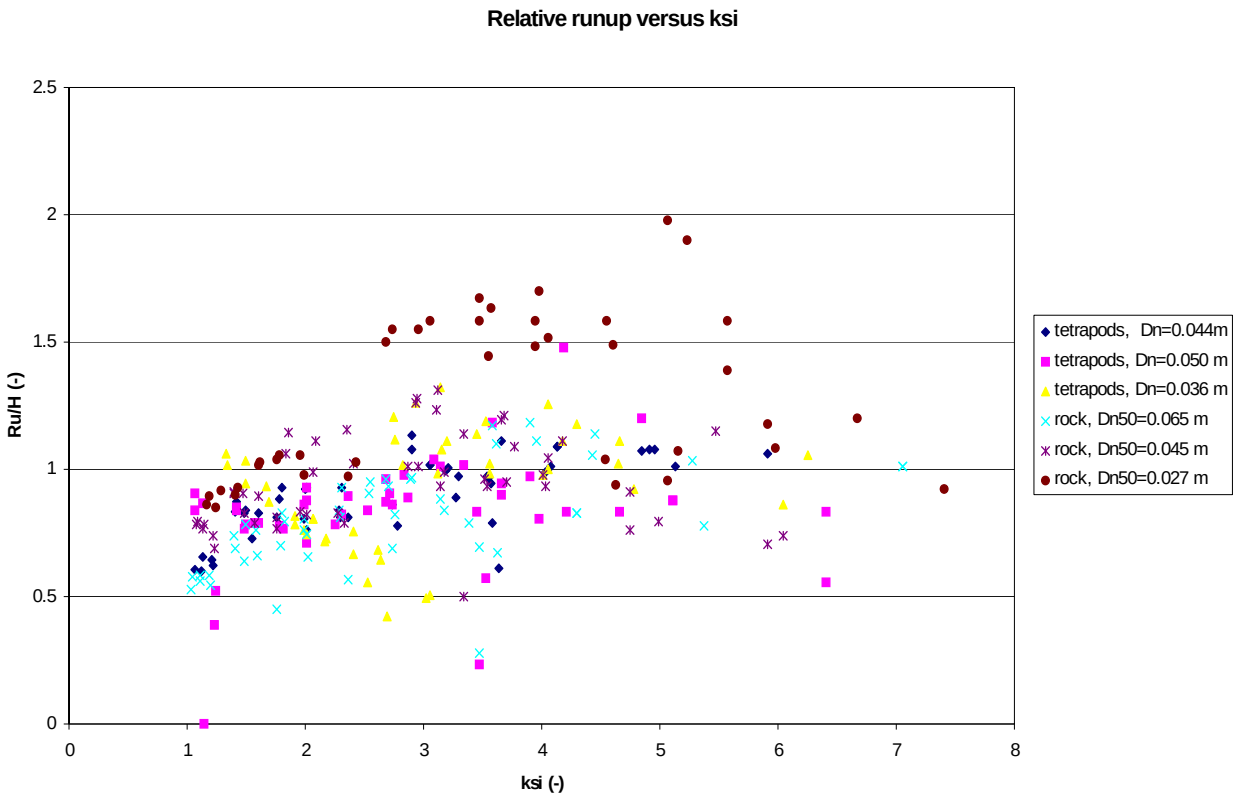

figure IX-1, Relative run-up (R_u/H) versus ξ

Appendix X Non-dimensional parameter describing roughness

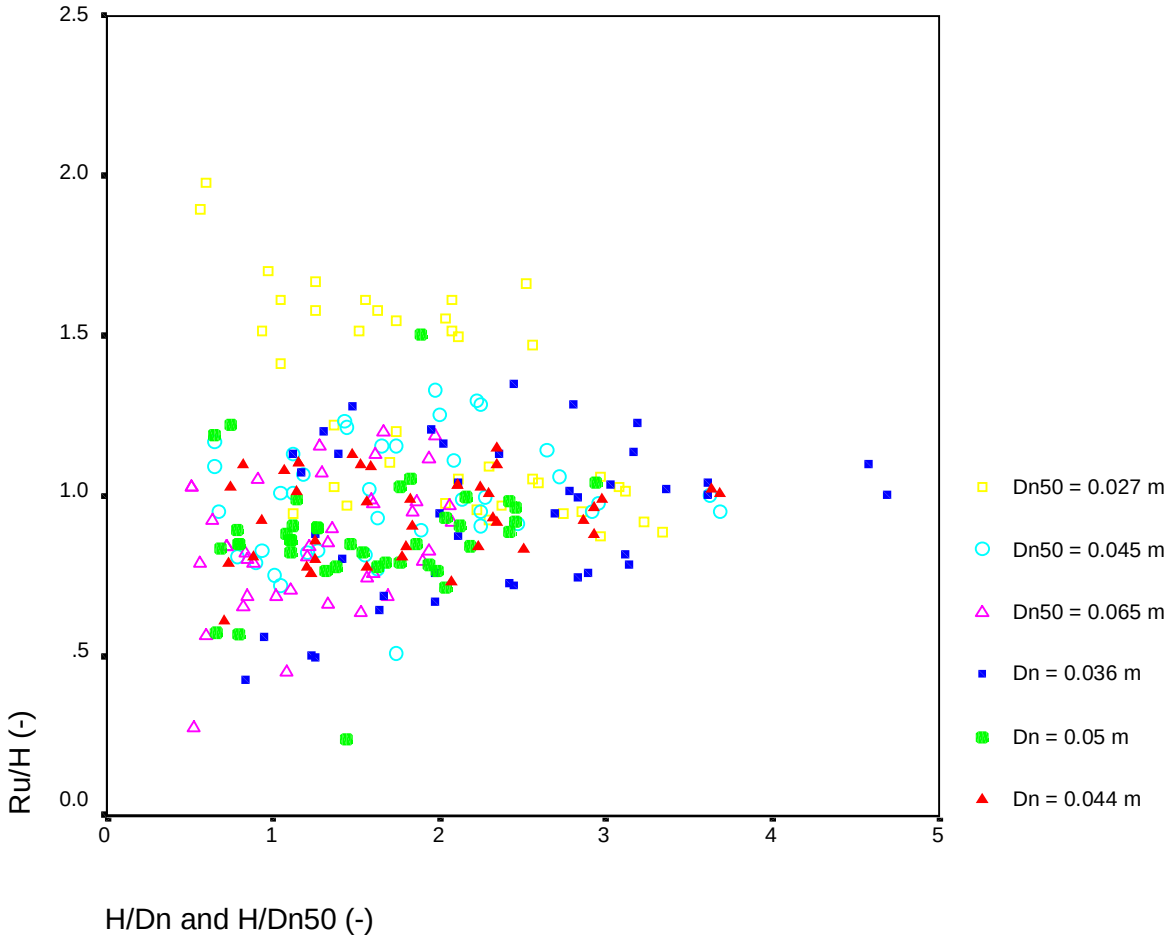

figure X-1, Relative run-up (R_u/H) versus $H/D_{n(50)}$

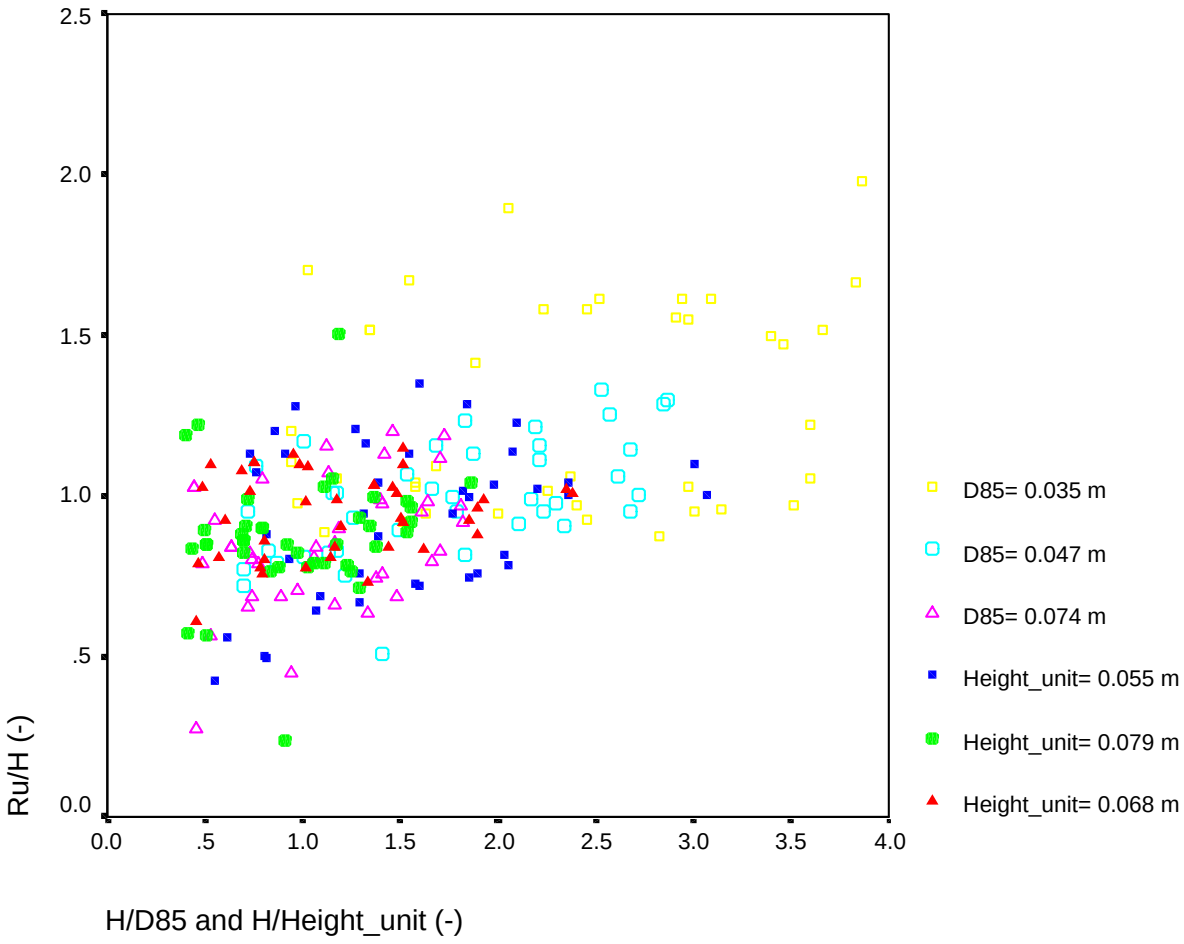

figure X-2, Relative run-up (R_u/H) versus roughness (H/D_{85}) and (H/Htet)

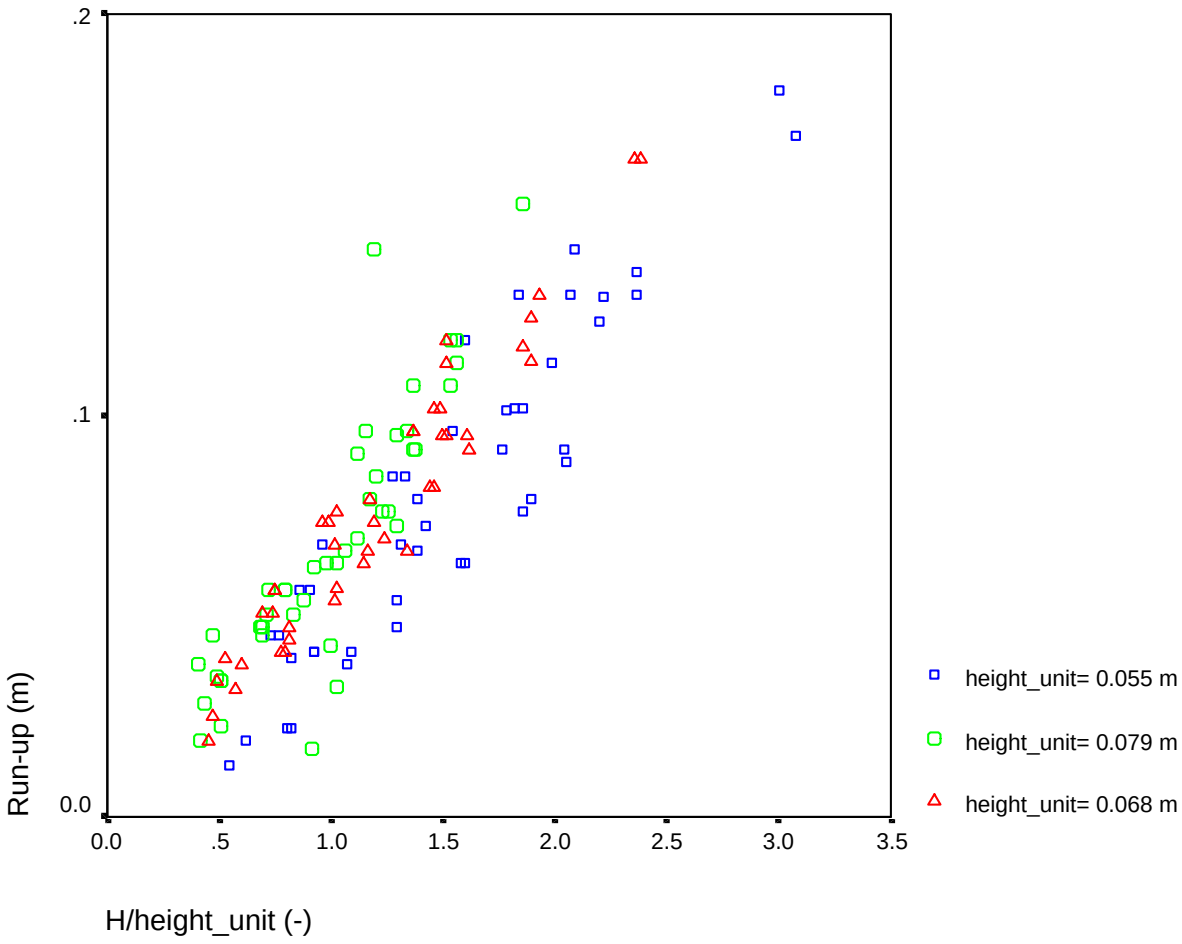

figure X-3, Run-up versus roughness (H/Htet), tetrapods

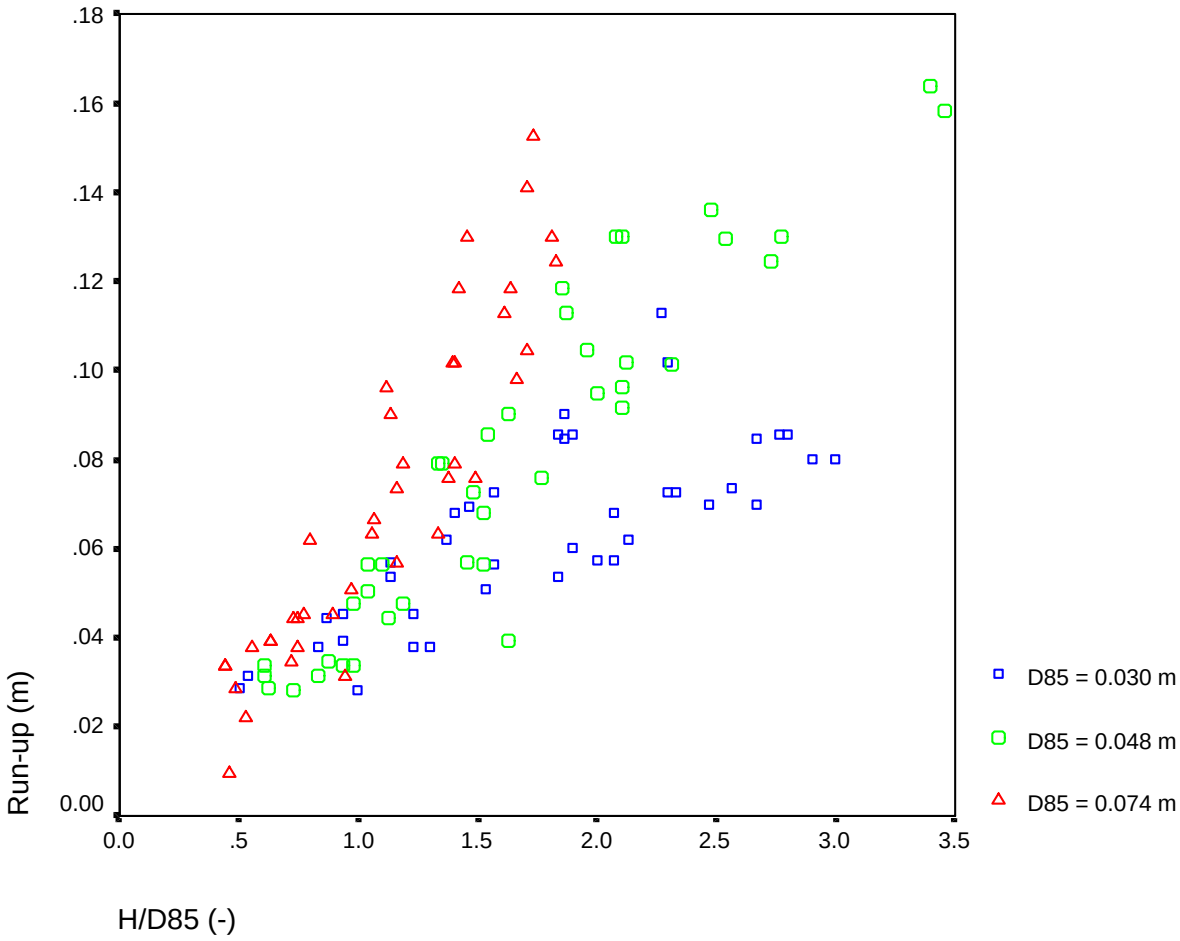

figure X-4, Run-up versus roughness (H/D_{85}), rock

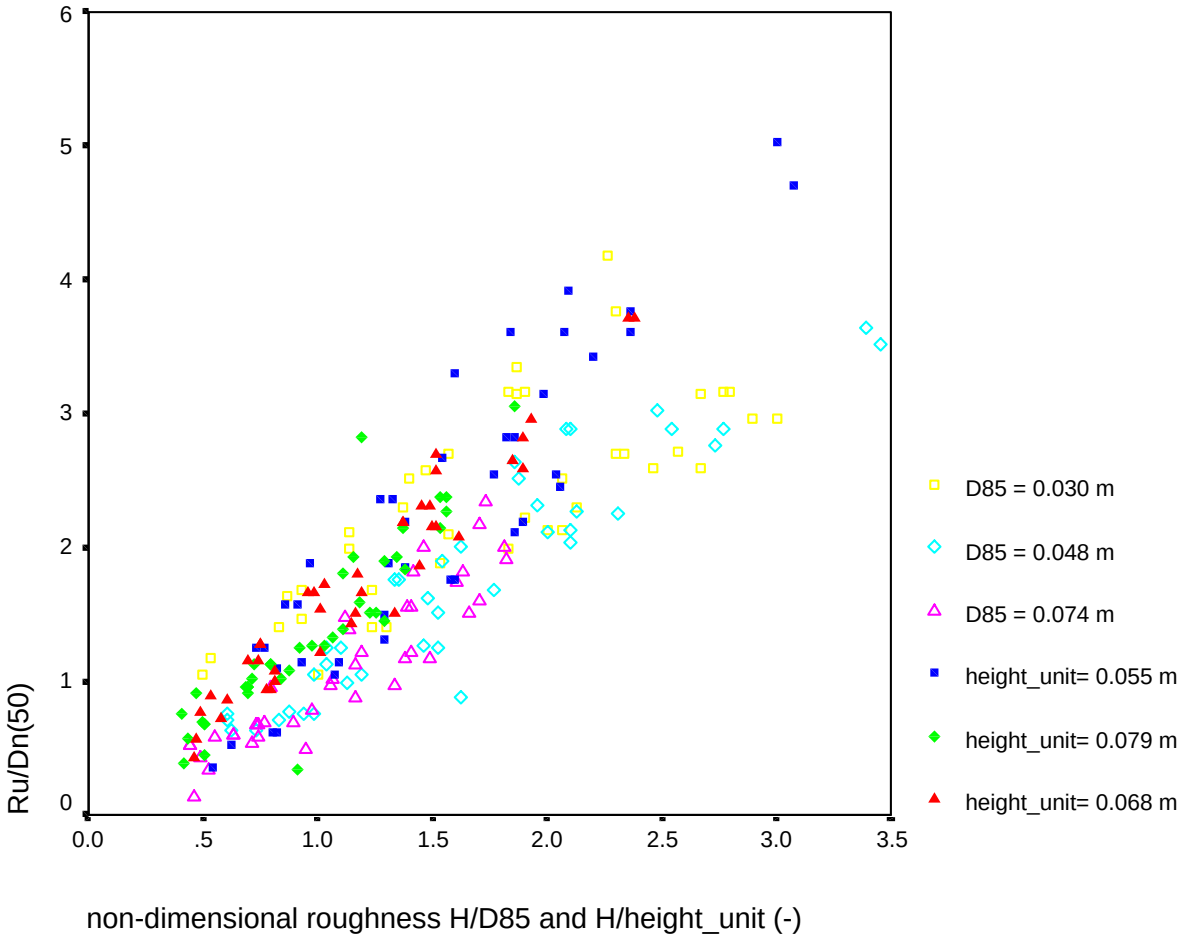

figure X-5, Non-dimensional run-up ($R_u/D_{n(50)}$) versus non-dimensional roughness (H/D_{85}) and (H/Htet)

Appendix XI Non-dimensional permeability parameter

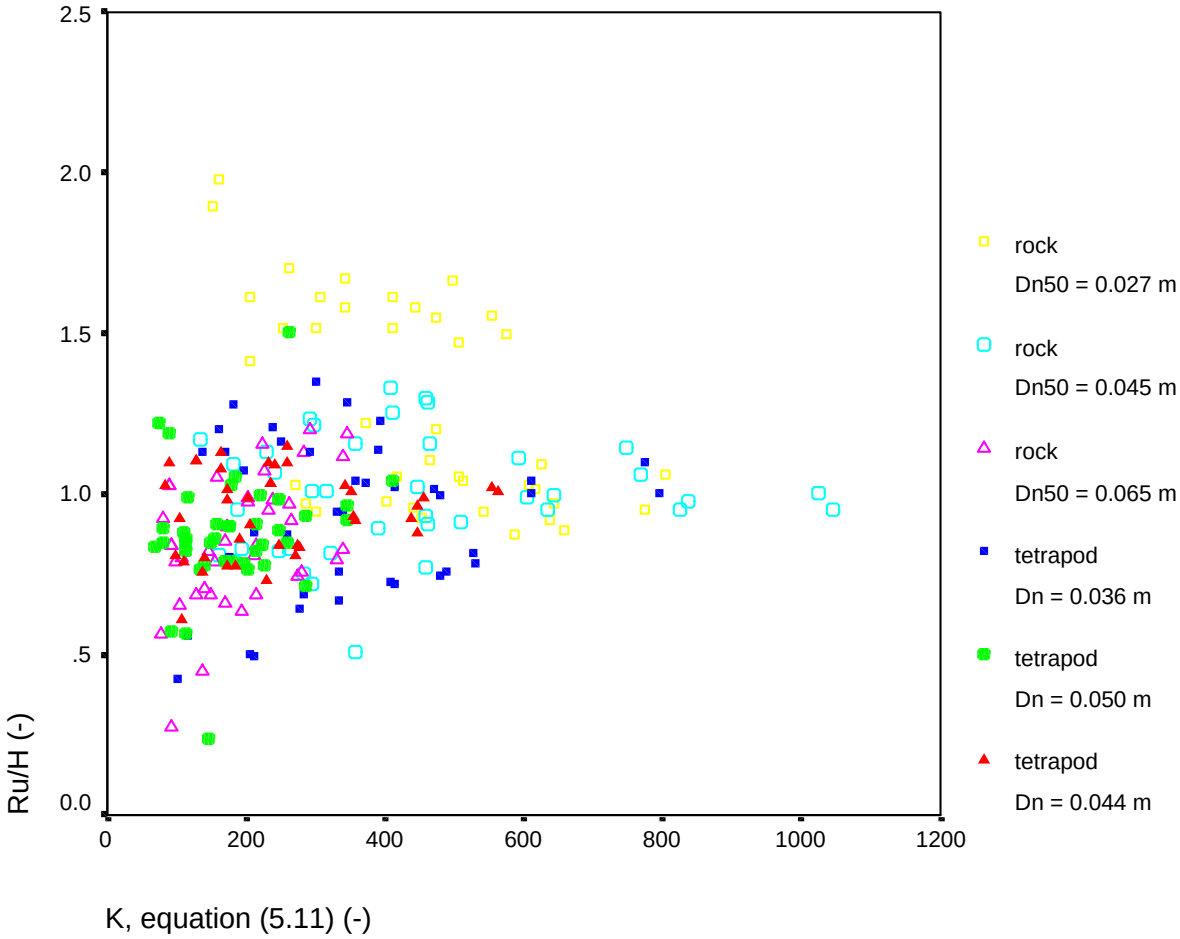

figure XI-1, Relative run-up (R_u/H) versus K, equation (5.11)

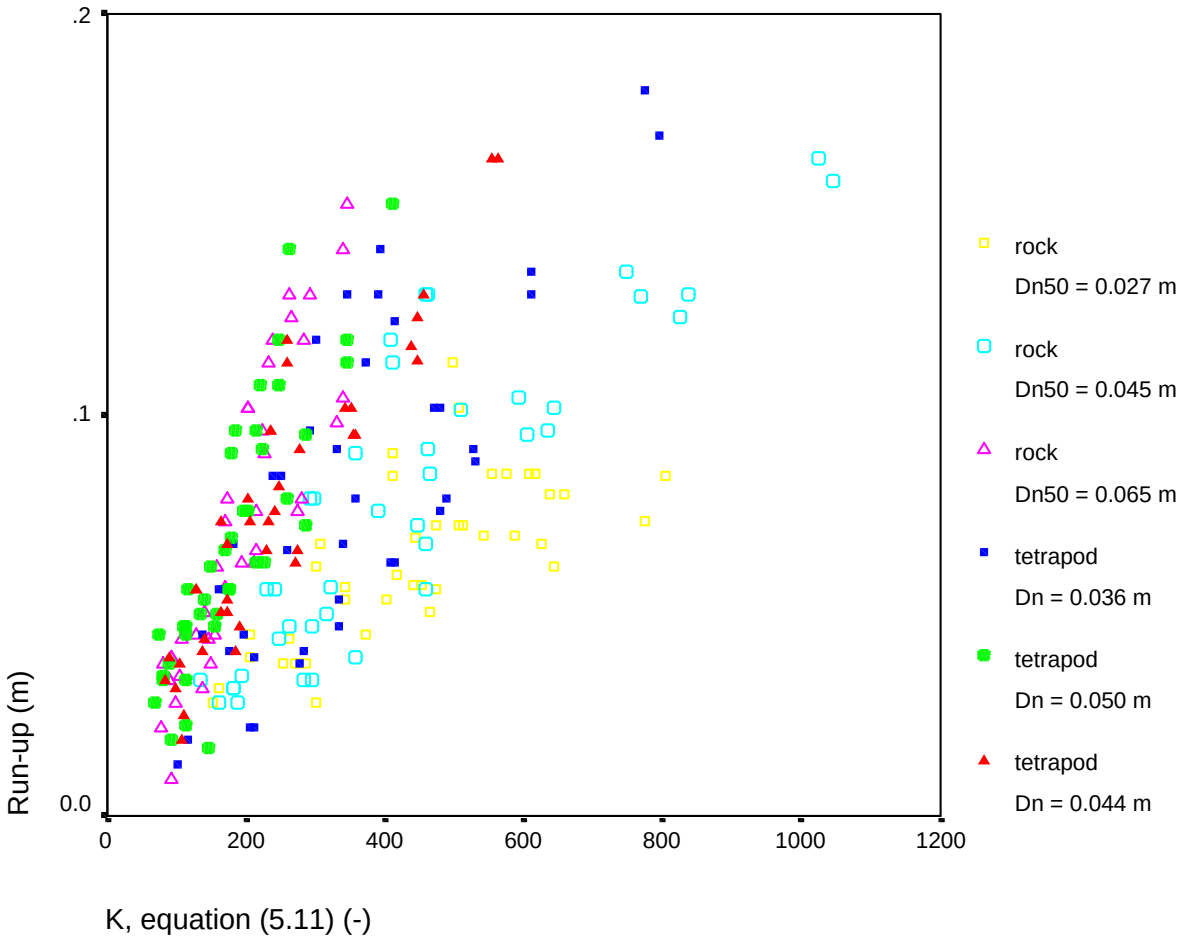

figure XI-2, Run-up versus K, equation (5.11)

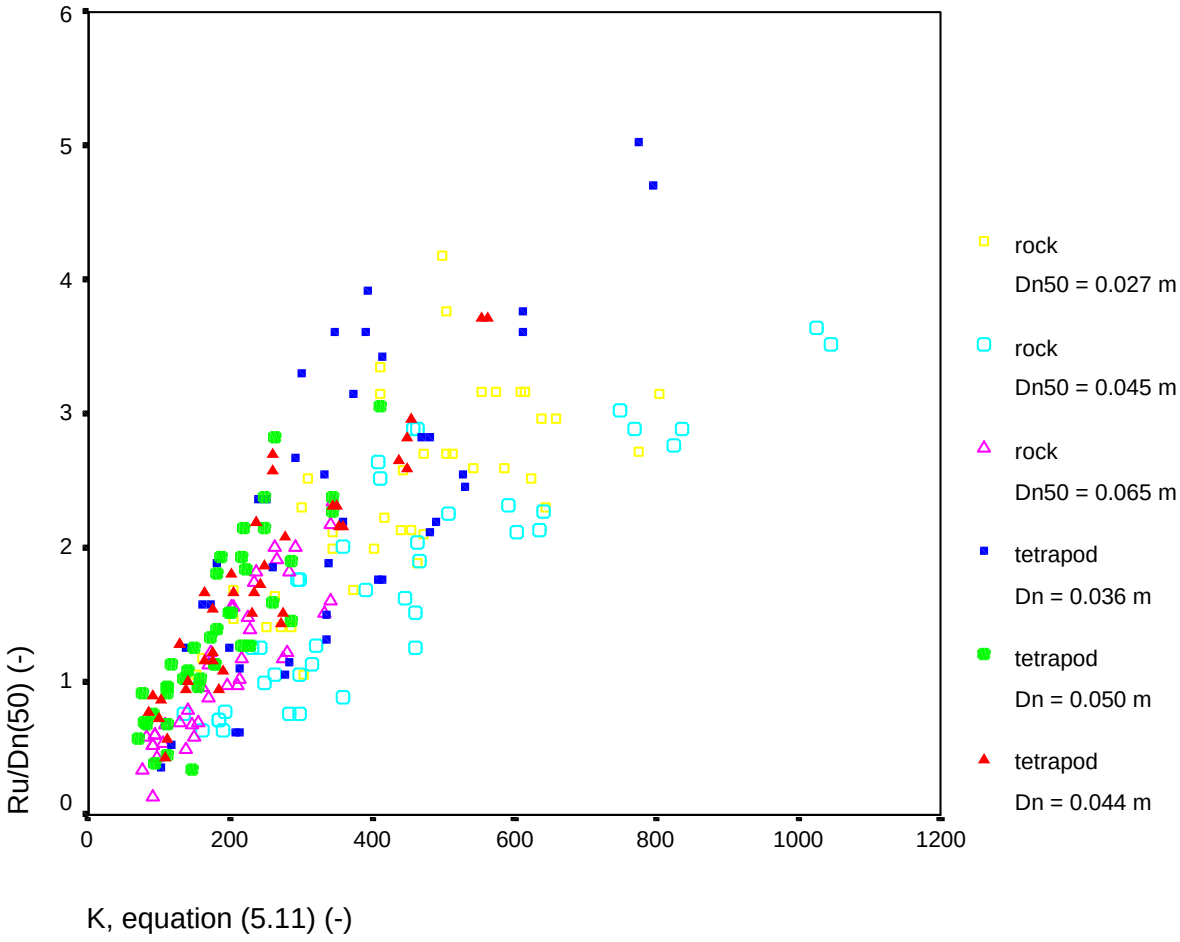

figure XI-3, Non-dimensional run-up ($R_u/D_{n(50)}$) versus K, equation (5.11)

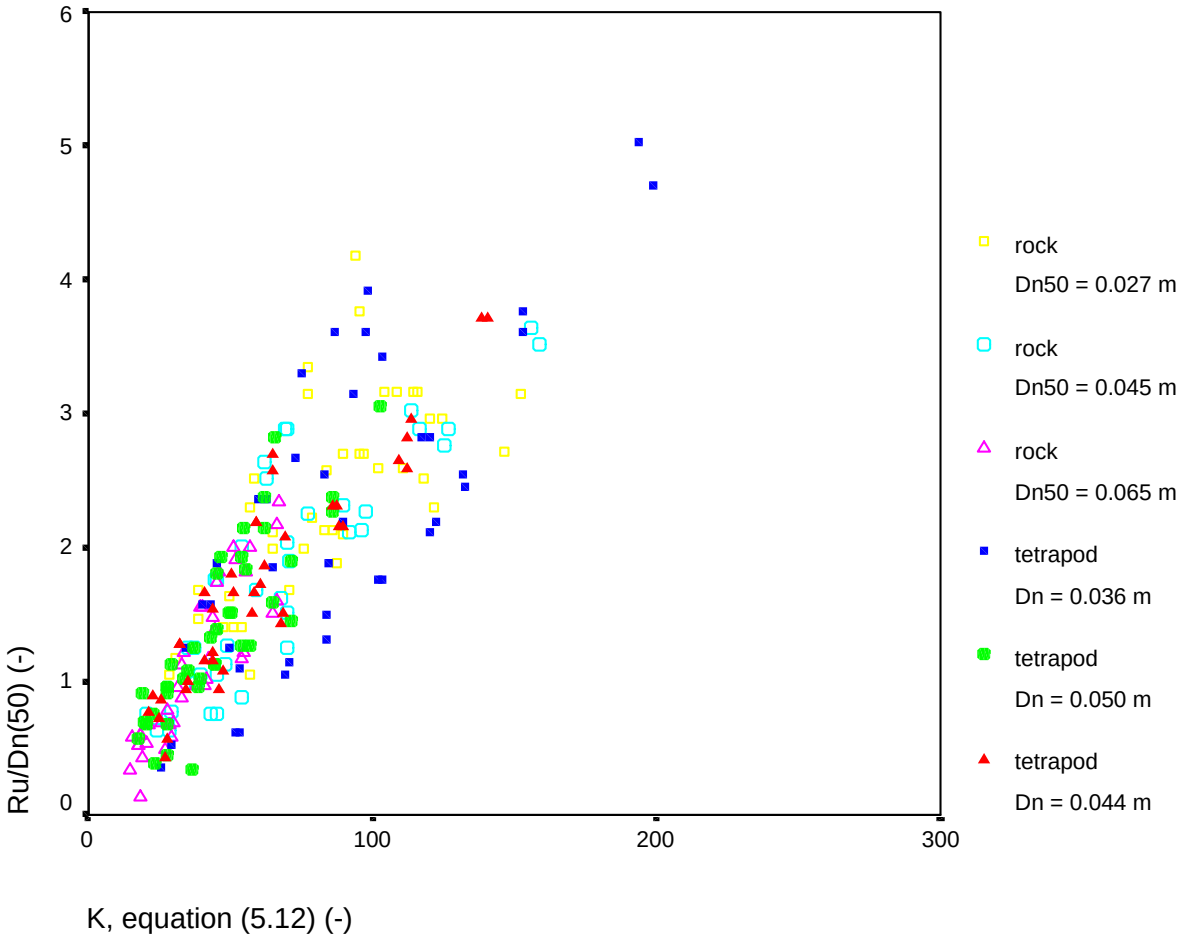

figure XI-4, Non-dimensional run-up ($R_u/D_{n(50)}$) versus K, equation (5.12)

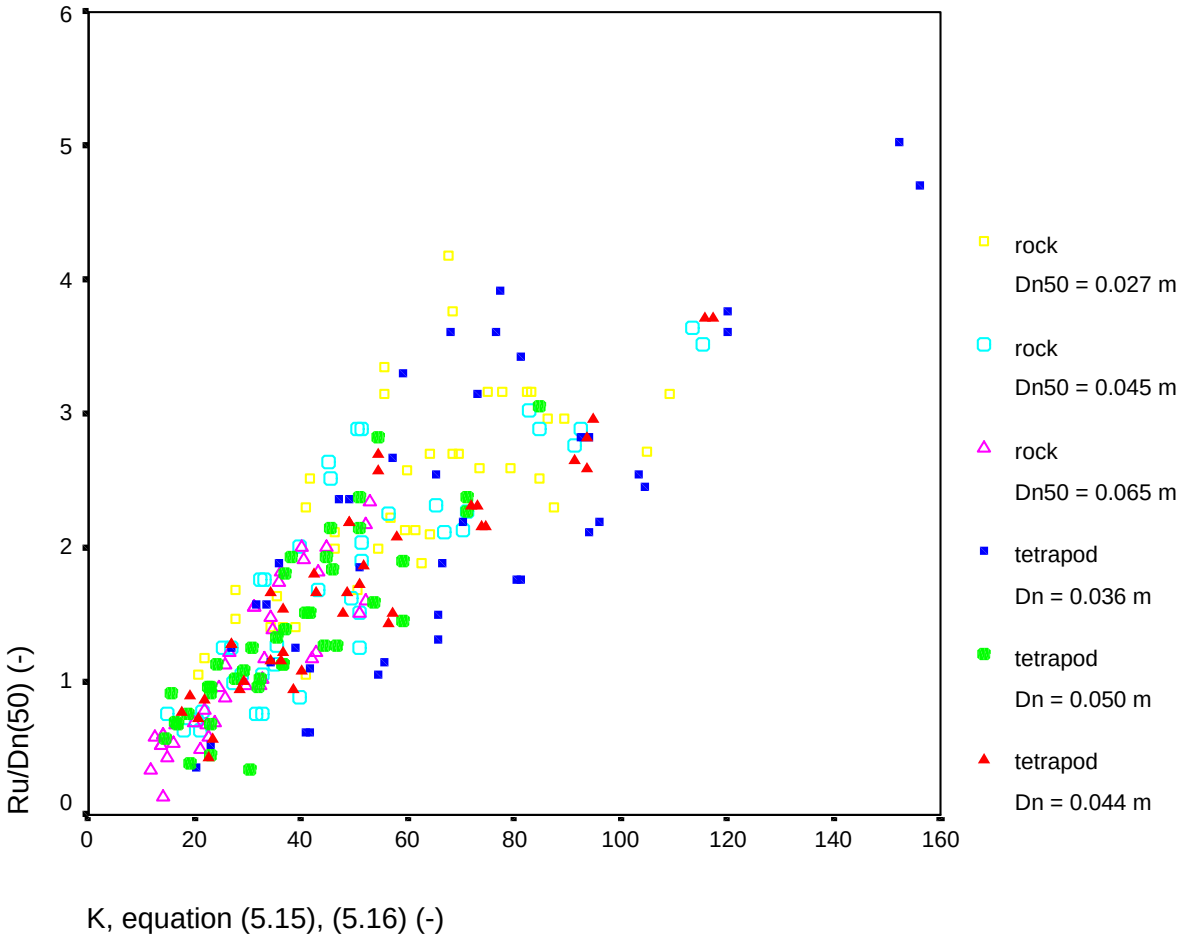

figure XI-5, Non-dimensional run-up ($R_U/D_{n(50)}$) versus K, equation (5.15), and (5.16)

Appendix XII Relative run-up ($R_{u2\%}/H_s$) versus ξ_m, Iran experiments

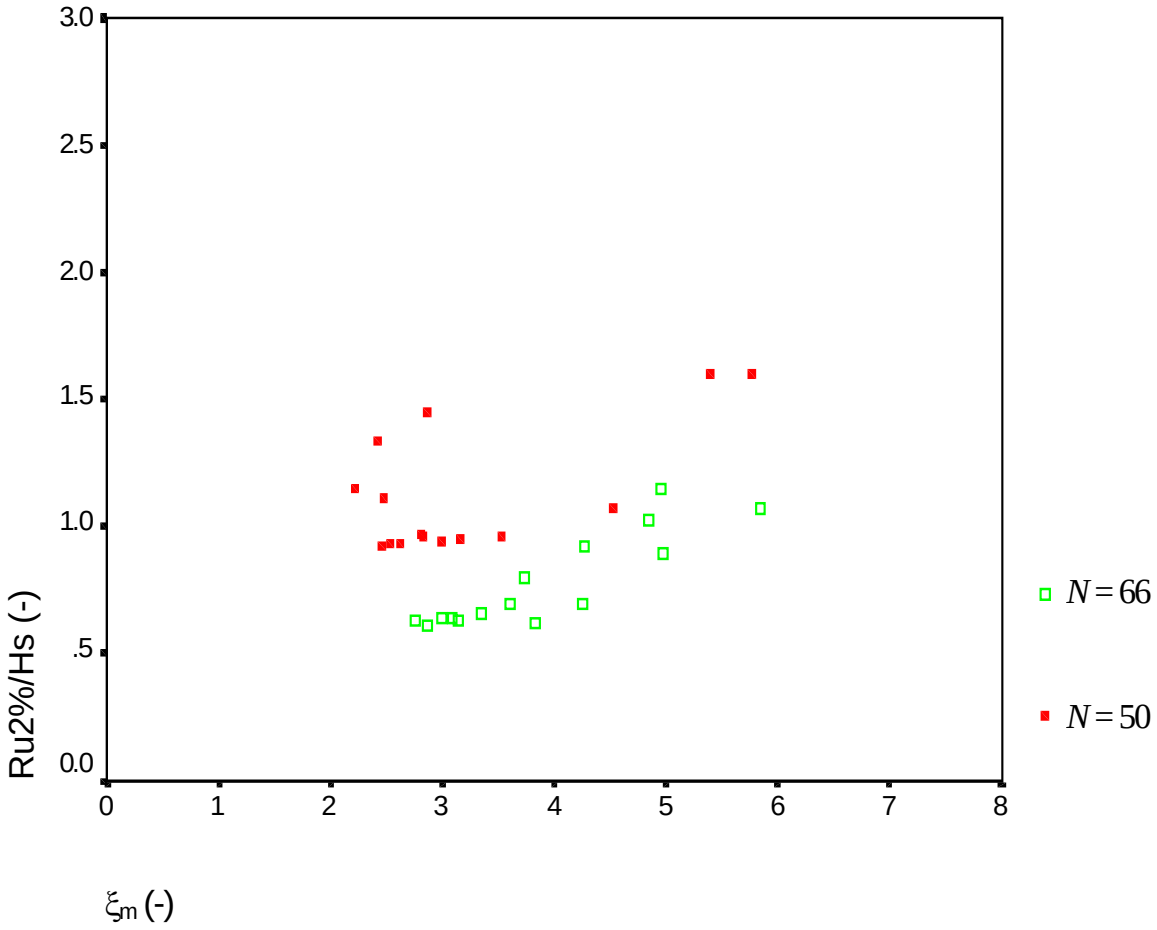

figure XII-1, Relative run-up ($R_{u2\%}/H_s$) versus ξ_m

Appendix XIII Scaling of core material, Le Méhauté

In the underlayers and core of model breakwaters, geometric scaling of the material sizes may lead to viscous scale effects because these layers can become less permeable and lead to relatively higher down rush pressures from inside the structure or different values of transmission, run-up and reflection than what occurs at prototype scale. This scale effect is encountered by increasing the size of the model stones over that dictated by geometric scaling so that:

$$\frac{L_p}{L_m} = K\frac{D_p}{D_m} \quad \text{or } \lambda_L = K\lambda_D \qquad \text{(XIII.1)}$$

where L is the geometrically undistorted characteristic length, D is the characteristic diameter, K is a factor greater than unity and p and m represent prototype and model respectively.

Le Méhauté (1965) developed a nomogram method for selecting of an appropriate value for K. He assumed that the scale effects are negligible in the outer armour layers and that the prototype and model have the same gradation in core material sizes. His method, therefore corrects for scale effects arising from flow through the core of the structure. Le Méhauté's nomogram is given in figure XIII-1.

The factor on the abscissa is:

$$\frac{H_i}{\Delta L} D_p^3 P_p^5 \qquad \text{(XIII.2)}$$

where:
H_I - incoming wave height
ΔL - the average width of the core
D_p - the effective quarrystone diameter, taken 10% smaller than quarrystone from the core material gradation curve
P - the porosity of the core material

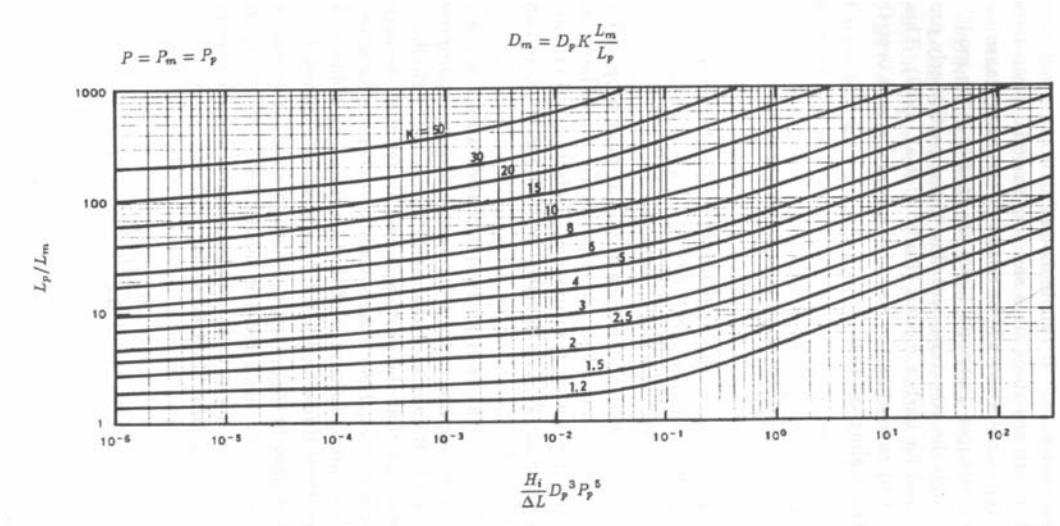

figure XIII-1, Le Méhauté's nomogram

Appendix XIV Data Iran compared to present formulae

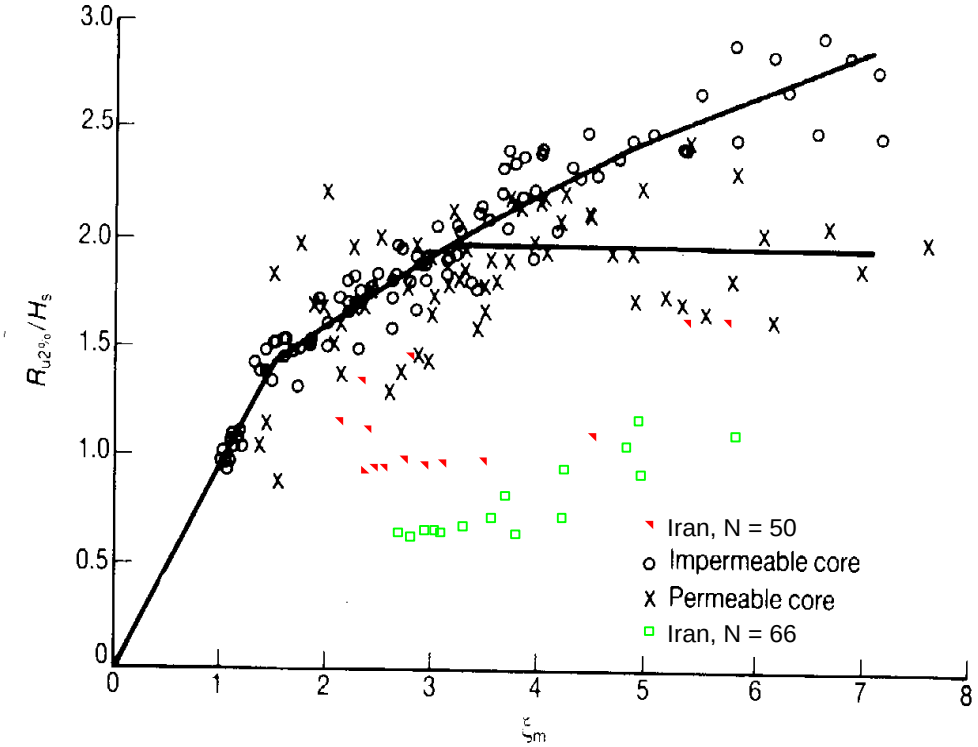

figure XIV-1, Data obtained in Iran versus known run-up data

Appendix XV Measured data versus calculated data, breaking waves

In the figure below, the measured data of the experiments performed in Delft are presented versus the calculated data. These data cover the range of breaking waves. The calculated data points are obtained using:

$$\frac{R_u}{D_{n(50)}} = 0.37R(0.021K + \xi)$$

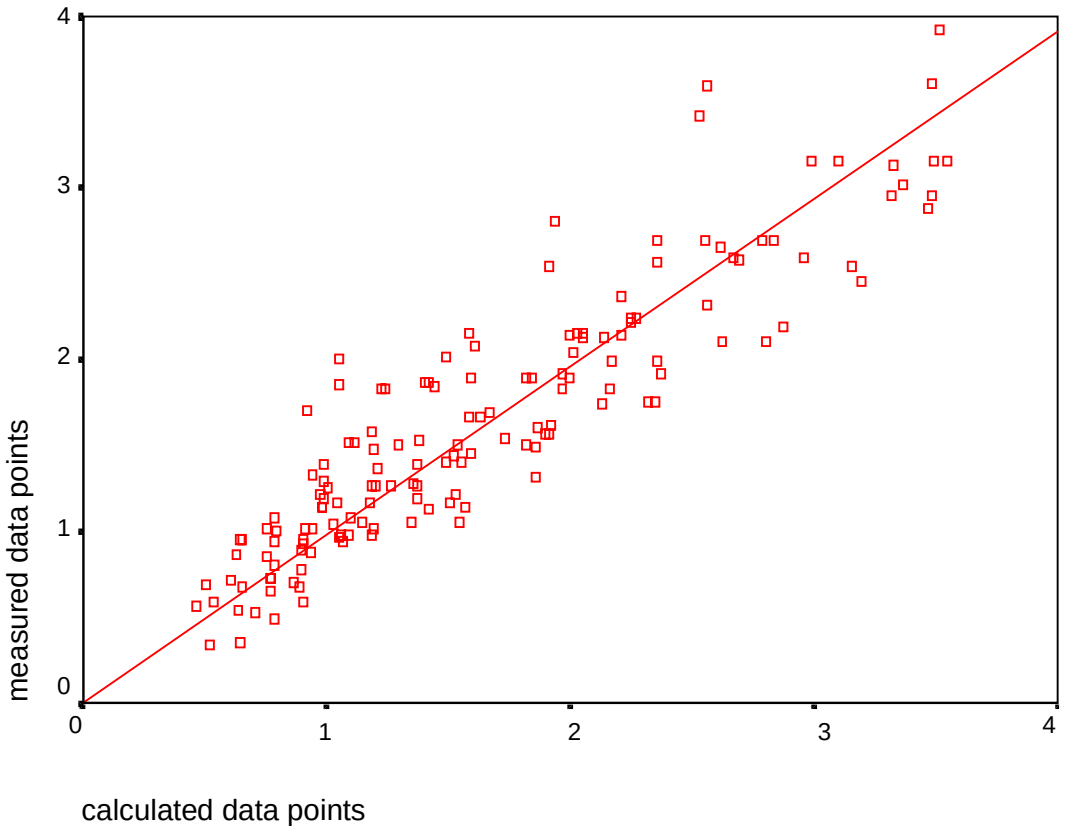

figure XV, Measured data versus calculated data, breaking waves

Appendix XVI Measured data versus calculated data, non-breaking waves

In the figure below, the measured data of the experiments performed in Delft are presented versus the calculated data. These data cover the range of non-breaking waves. The calculated data points are obtained using:

$$\frac{R_u}{D_{n(50)}} = 0.27R(0.017K + \xi)$$

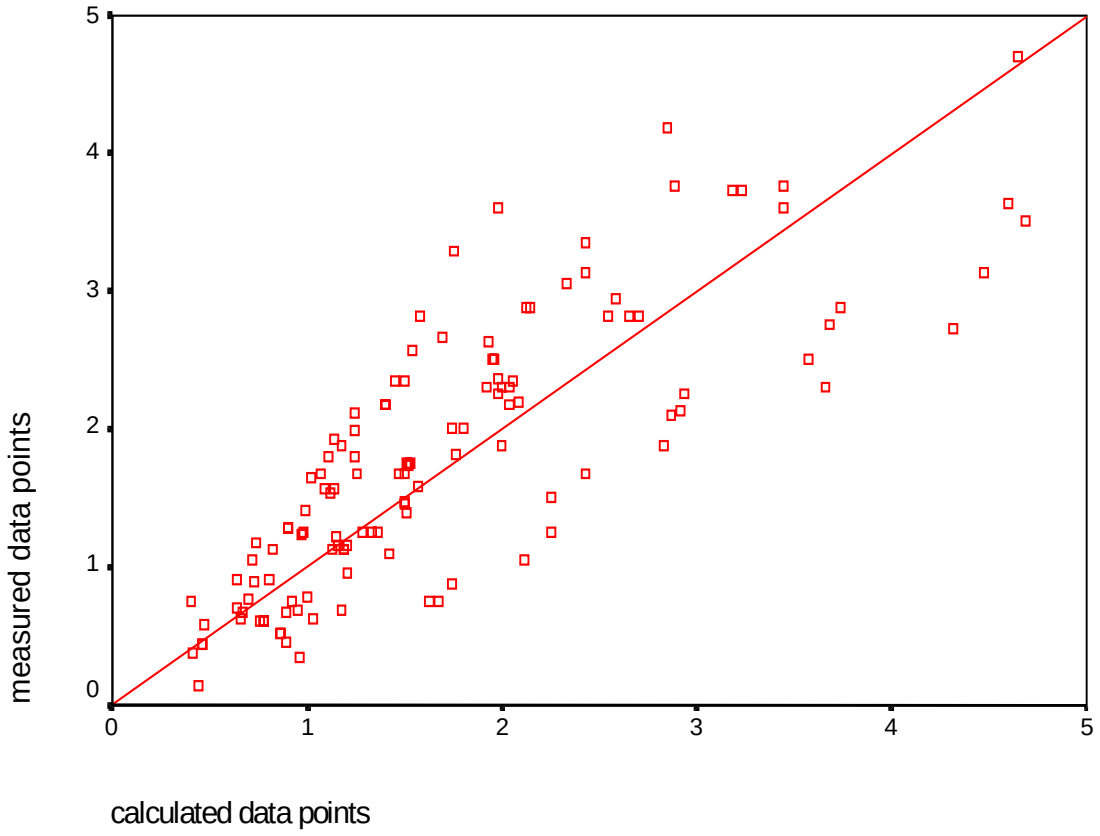

figure XVI-1, Measured data points versus calculated data points, non-breaking waves

Appendix XVII Measured data versus calculated data, Iran experiments

In the two figures below, the relation derived in chapter 6, describing run-up on a rough, permeable slope for non-breaking waves is applied to the data obtained in Iran. The first figure shows the data when ξ_m is used, the second figure shows the data using ξ_p. For both figures the calculated data points are acquired by using the following relation:

$$\frac{R_u}{D_{n(50)}} = 0.27R(0.017K + \xi)$$

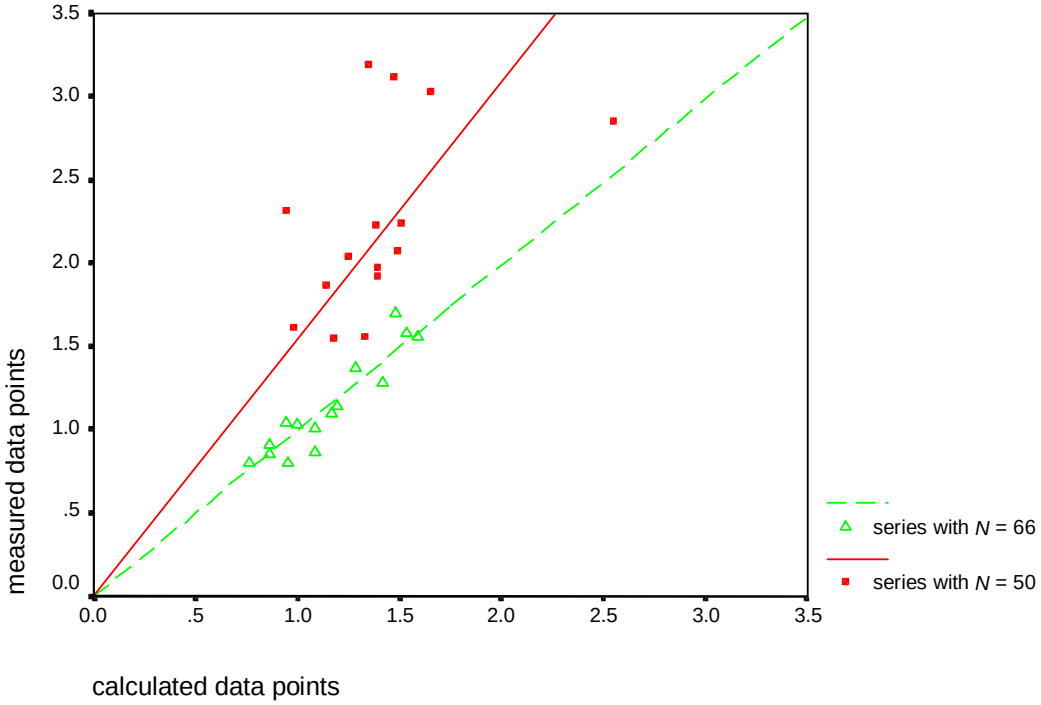

figure XVII-1, Measured data points versus calculated data points, using data obtained in Iran and ξ_m

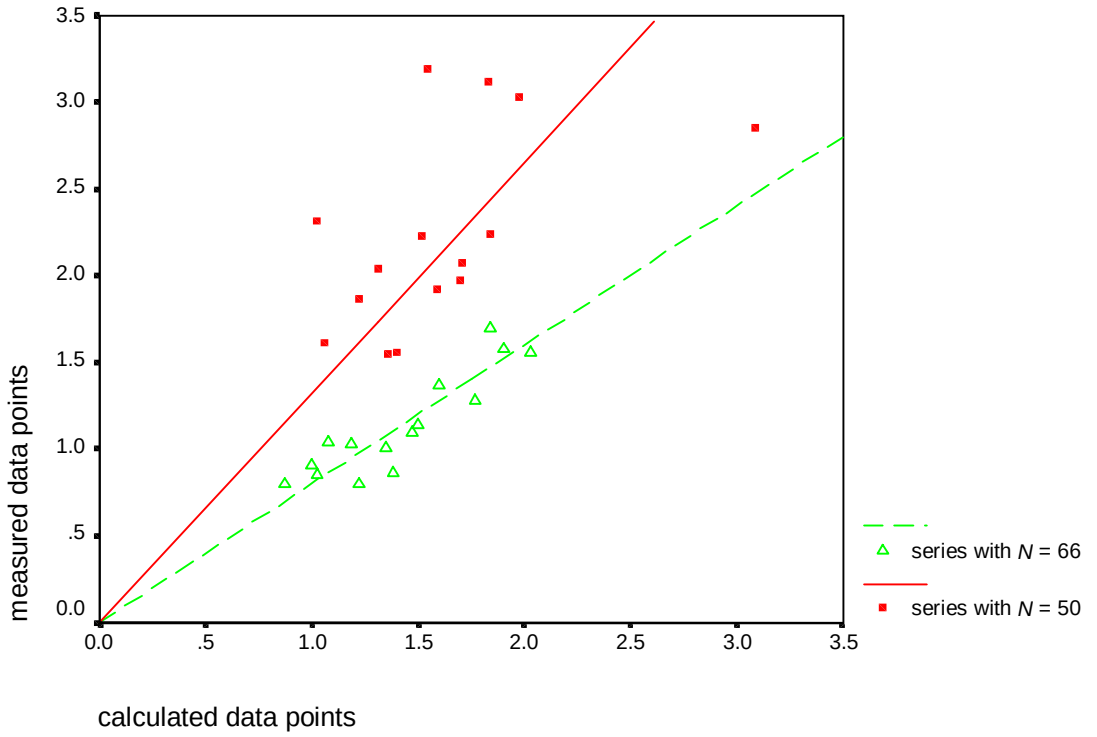

figure XVII-2, Measured data points versus calculated data points, using data obtained in Iran and ξ_p

Appendix XVIII, Influence tanα

In this appendix Q is used. This parameter is defined next:

$$Q = \frac{T\sqrt{g}}{\sqrt{nD}}$$

with D is a characteristic diameter, for rock: D_{20} and in the case of tetrapods, c, the size of one leg of a tetrapod.

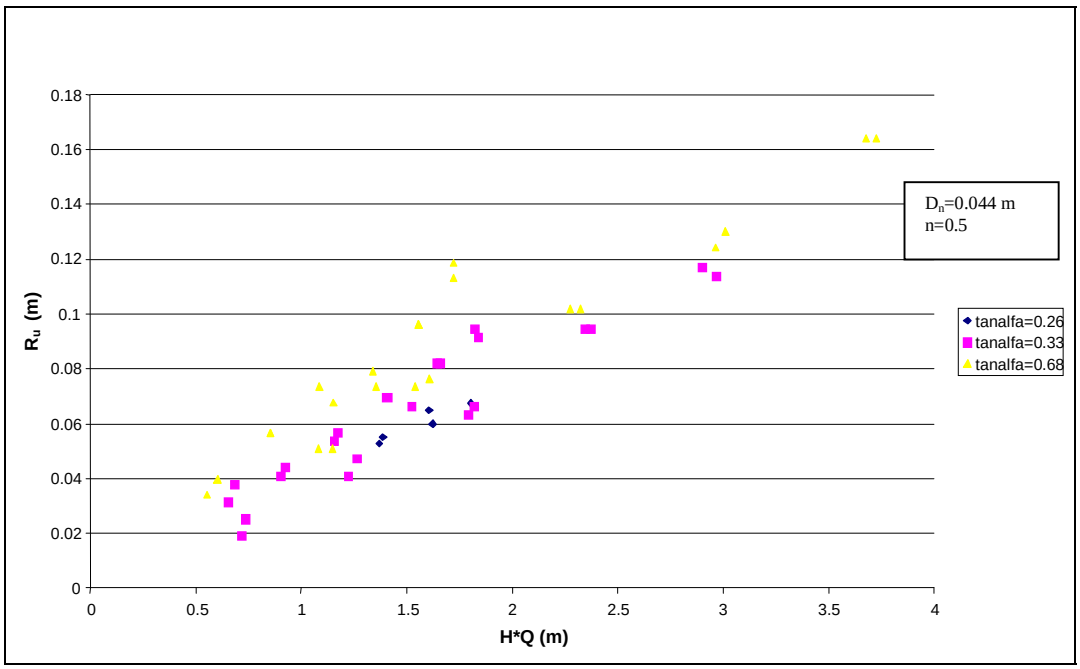

figure XVIII-1, Influence of tanα on run-up, tetrapods, D_n = 0.044 m

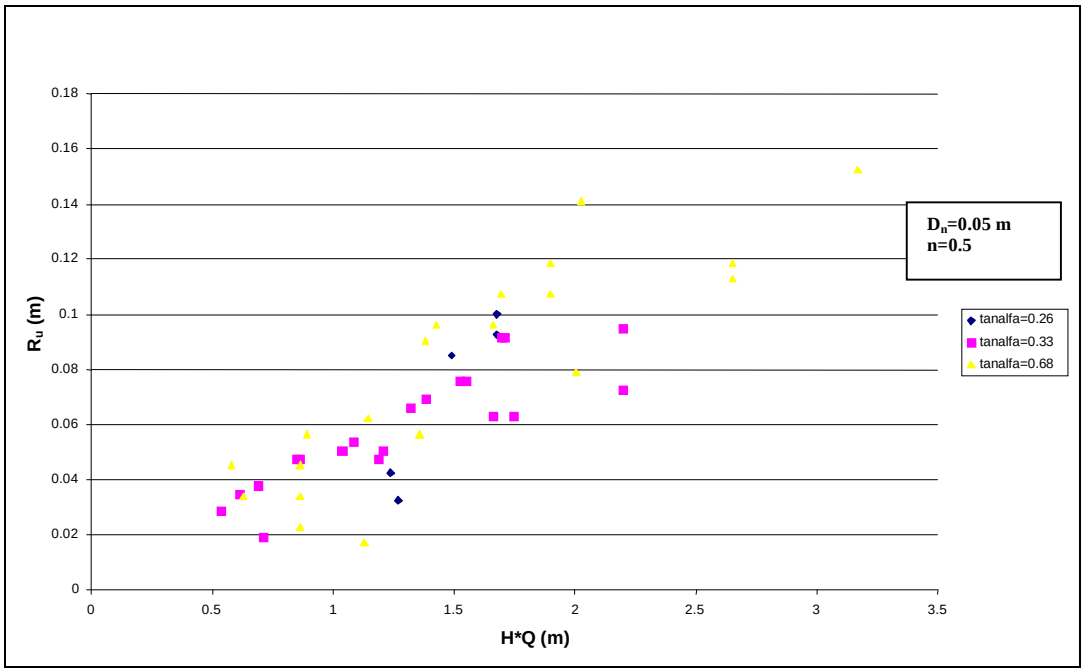

figure XVIII-1, Influence of tanα on run-up, tetrapods, D_n = 0.05 m

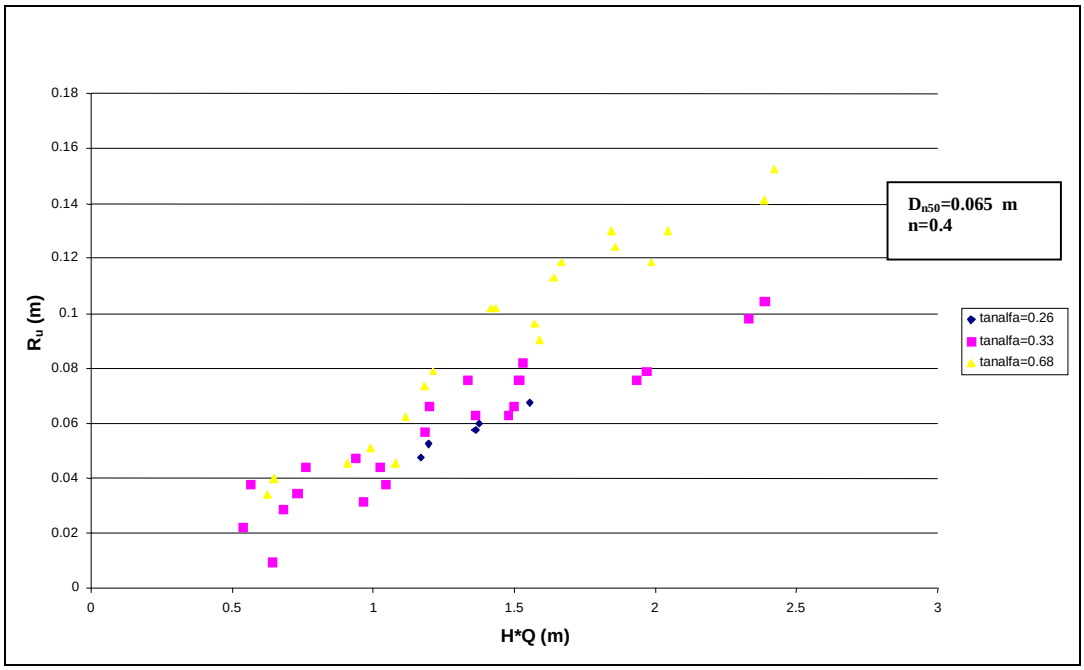

figure XVIII-1, Influence of tanα on run-up, rock, D_{n50} = 0.065 m

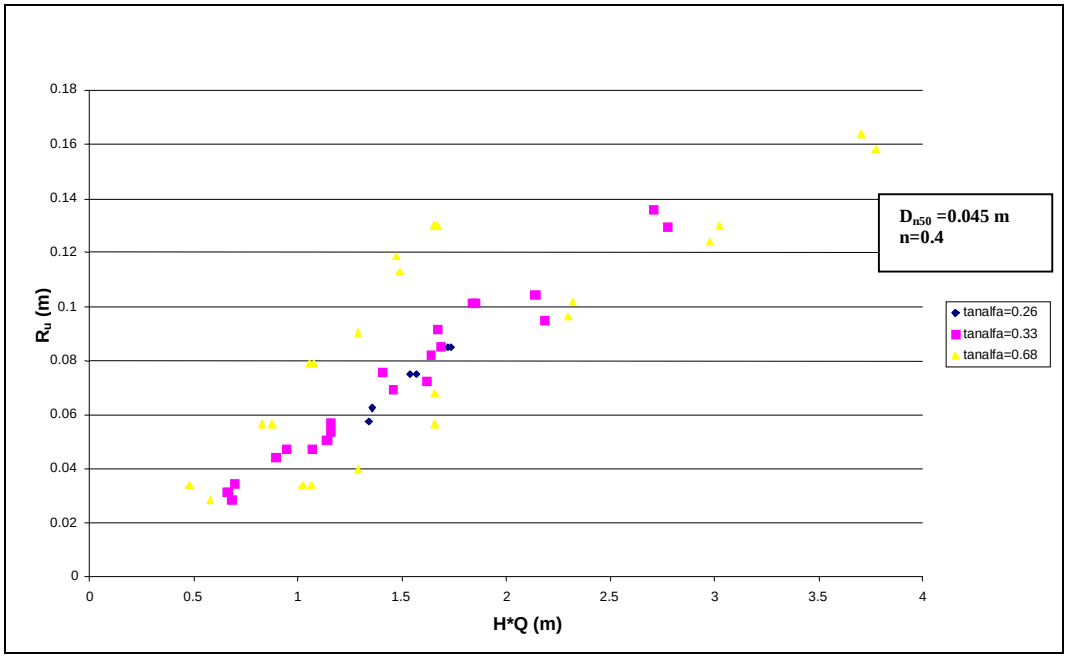

figure XVIII-1, Influence of tanα on run-up, rock, D_{n50} = 0.045 m

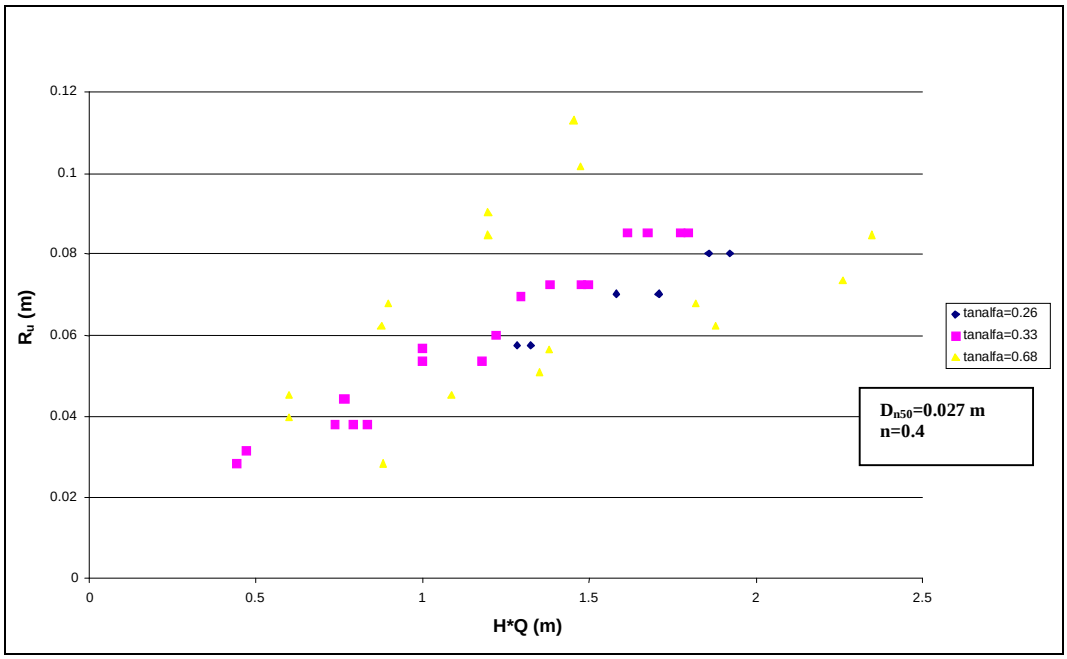

figure XVIII-1, Influence of tanα on run-up, rock, D_n = 0.027 m

Appendix XIX, Comparison of scatter, using n^5 and n

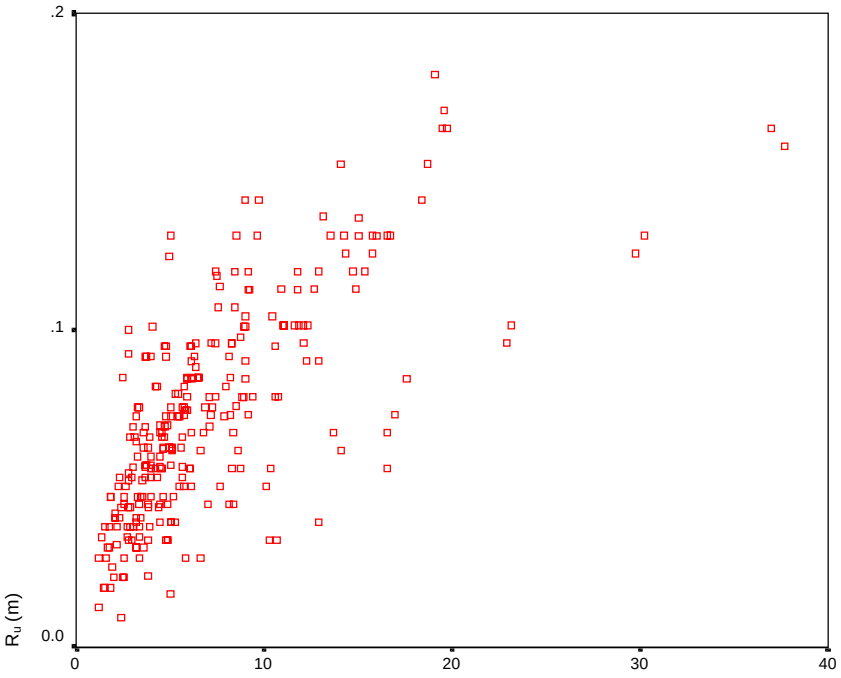

$$H\left(\frac{\tan\alpha T\sqrt{g}}{\sqrt{Dn^5}}\right) \text{ (m)}$$

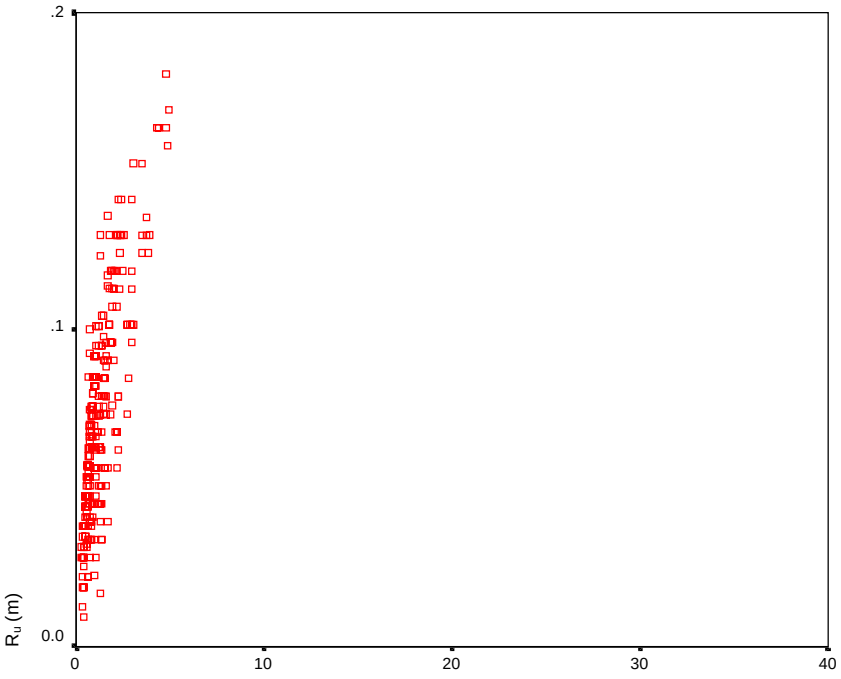

$$H\left(\frac{\tan\alpha T\sqrt{g}}{\sqrt{Dn}}\right) \text{ (m)}$$

Appendix XX, Comparison of run-up scatter, using n and $N_a D^2_{n(50)}$

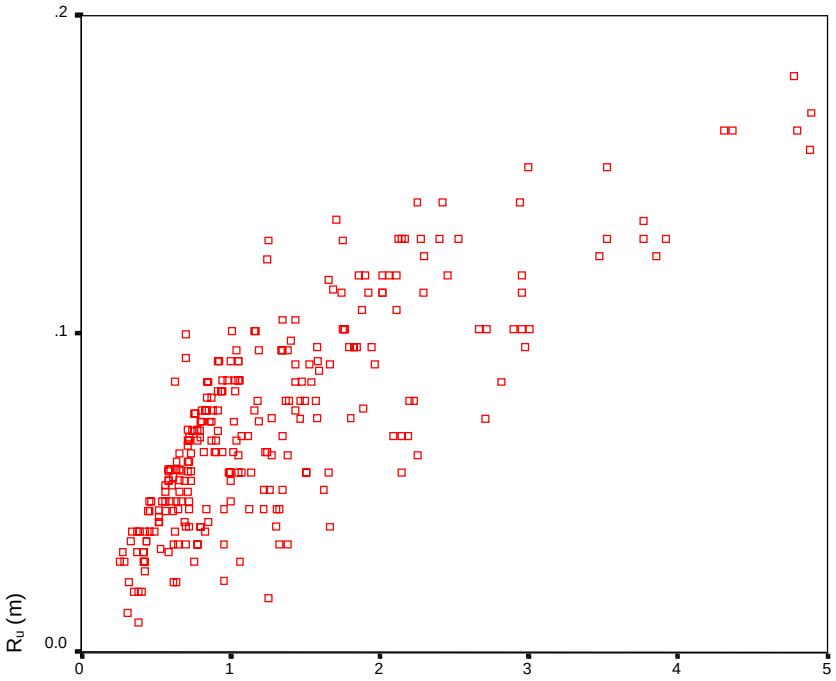

$$H\left(\frac{\tan\alpha T\sqrt{g}}{\sqrt{Dn}}\right)\text{ (m)}$$

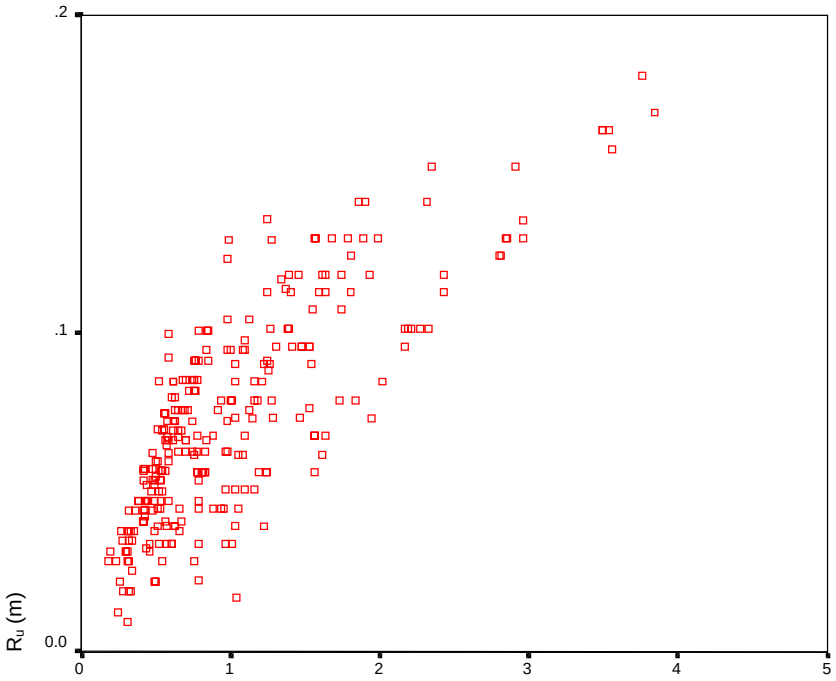

$$H\left(\frac{\tan\alpha T\sqrt{g}}{D_{n(50)}\sqrt{N_a D}}\right)\text{ (m)}$$

Appendix XXI, Comparison between ξ and Ω

R_u versus $H*\xi$, all data points

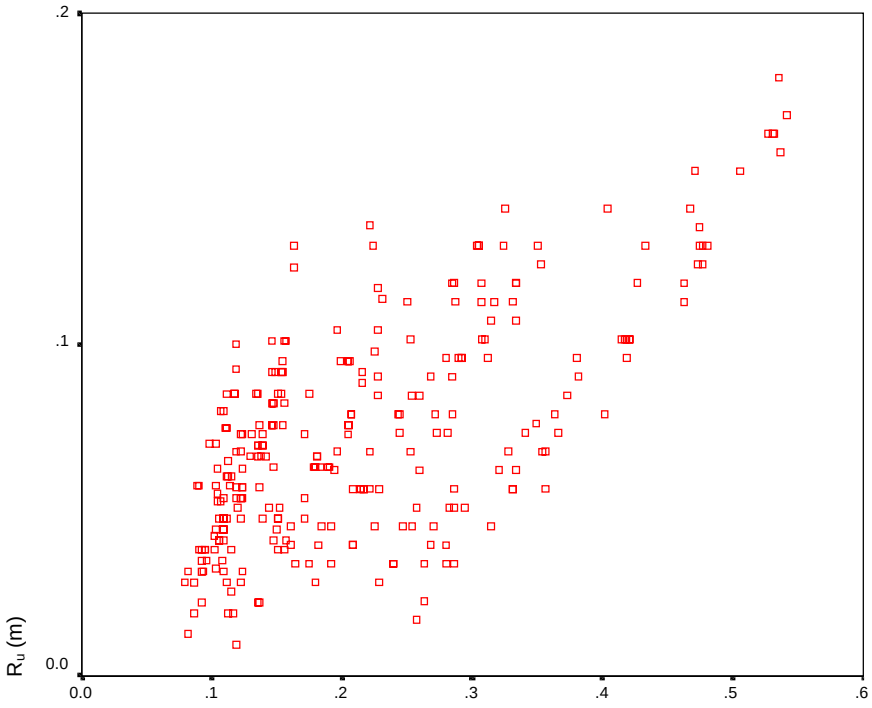

R_u versus $H*\Omega$, all data points

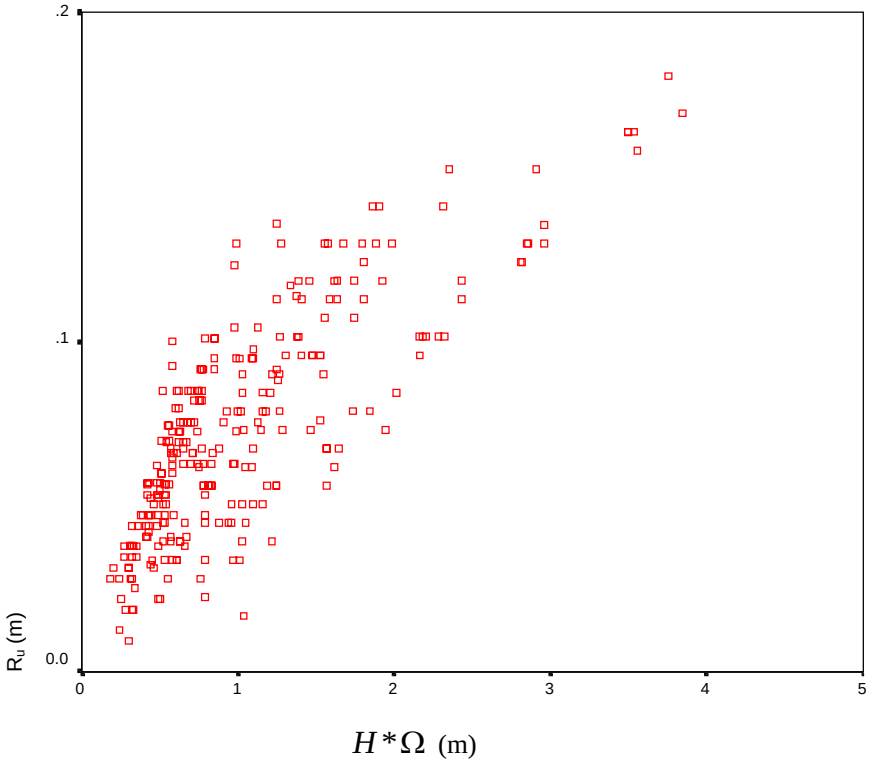

Appendix XXII, Relative run-up versus Ω

Relative run-up versus Ω, breaking waves, $\xi < 3$

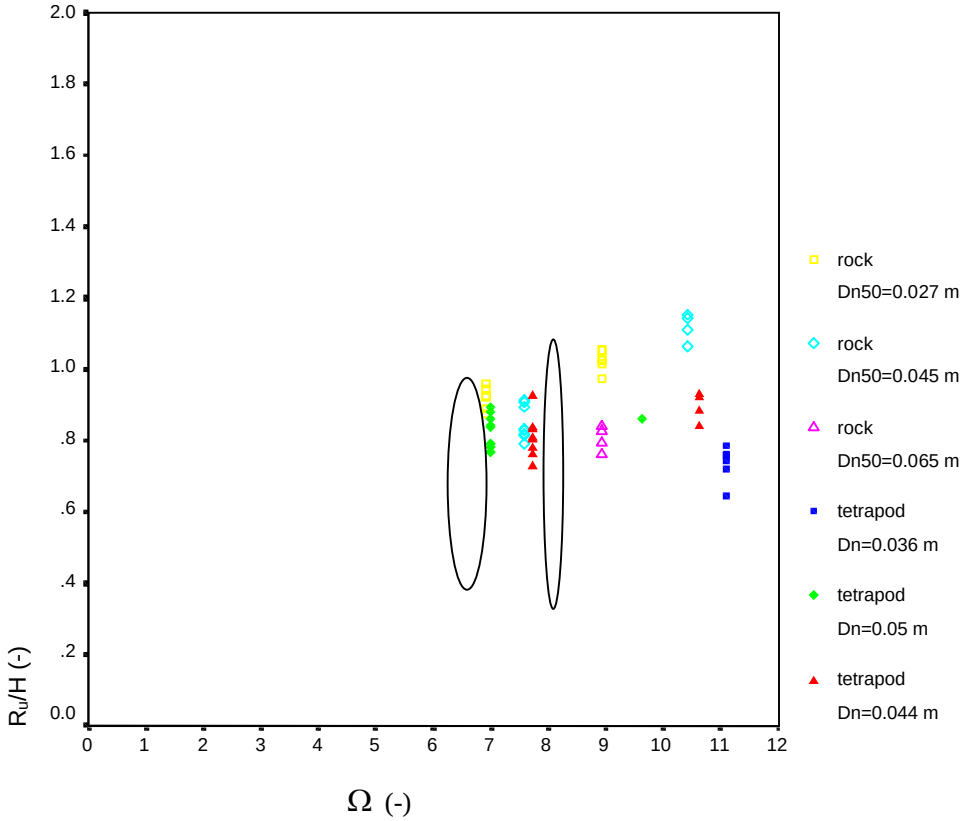

figure XXII-1, Scatter for relative run-up versus Ω, breaking waves

Relative run-up versus Ω, non-breaking waves, ξ >= 3

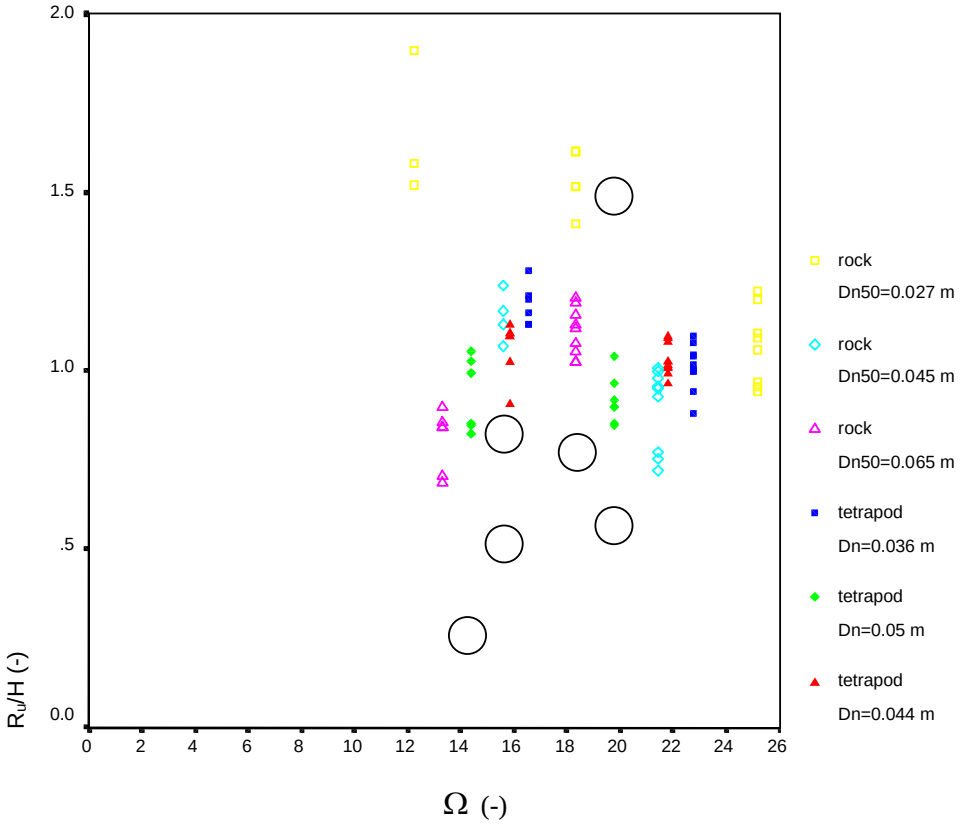

figure XXII-2, Scatter for relative run-up versus Ω, non-breaking waves

Relative run-up versus Ω, non-breaking waves, ξ >= 3

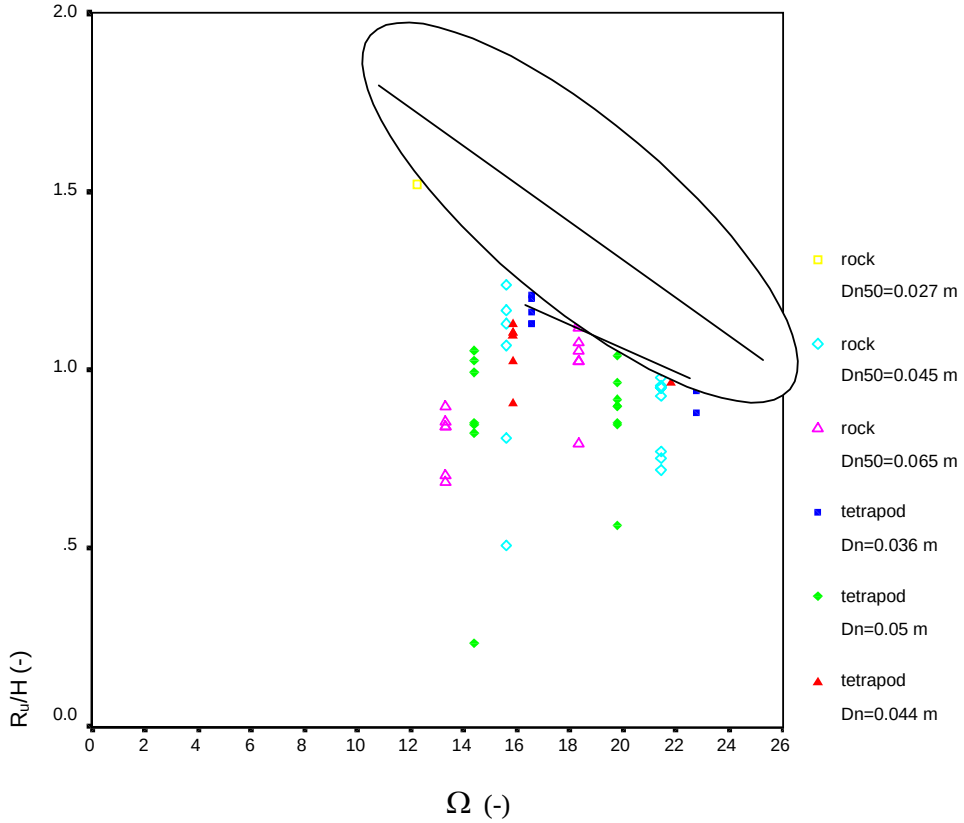

figure XXII-3, Scatter for small units, non-breaking waves

Appendix XXIII, Run-up on a slope with small diameter units

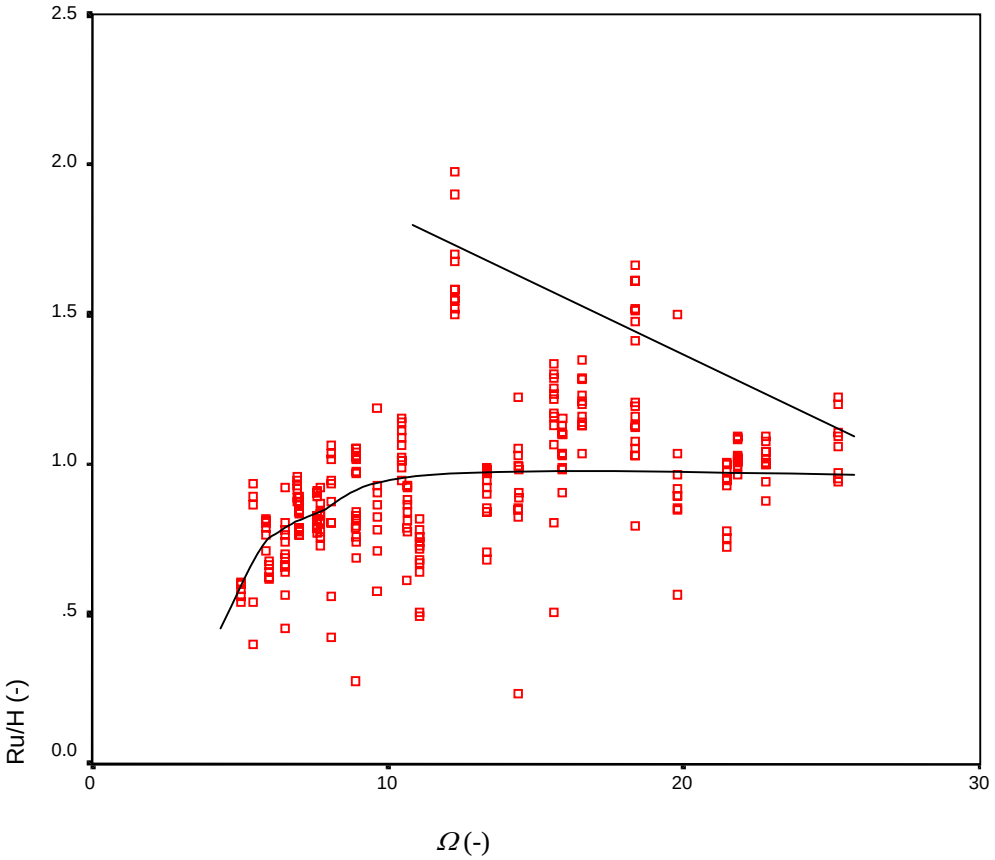

figure XXIII-1, Relative run-up versus Ω, all data points

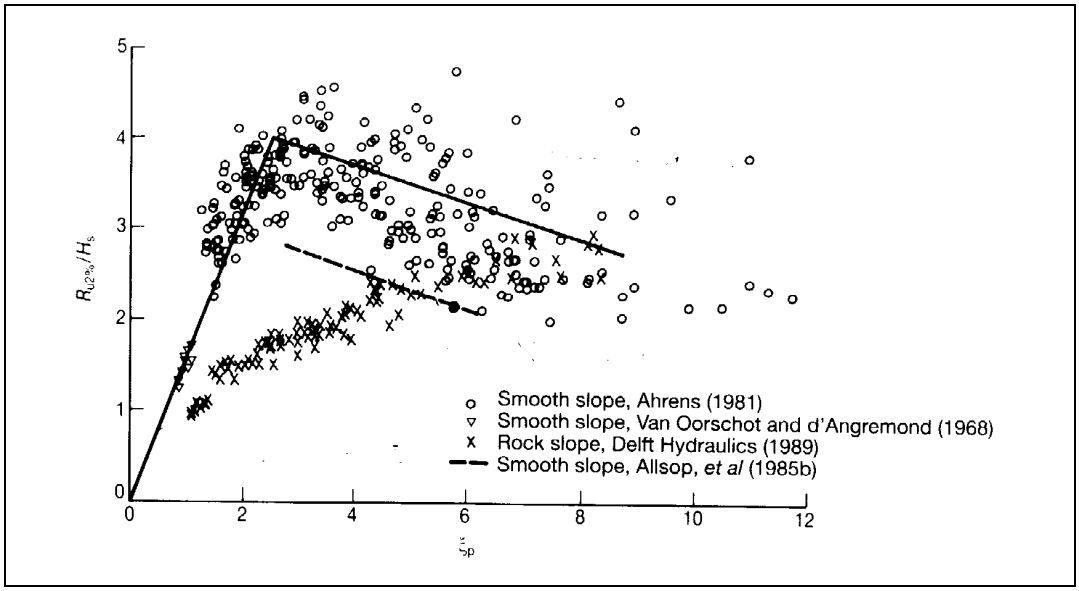

figure XXIII-2, Comparison of relative 2% run-up for smooth and rubble slopes

Appendix XXIV, Relative run-up versus Ω, all data points

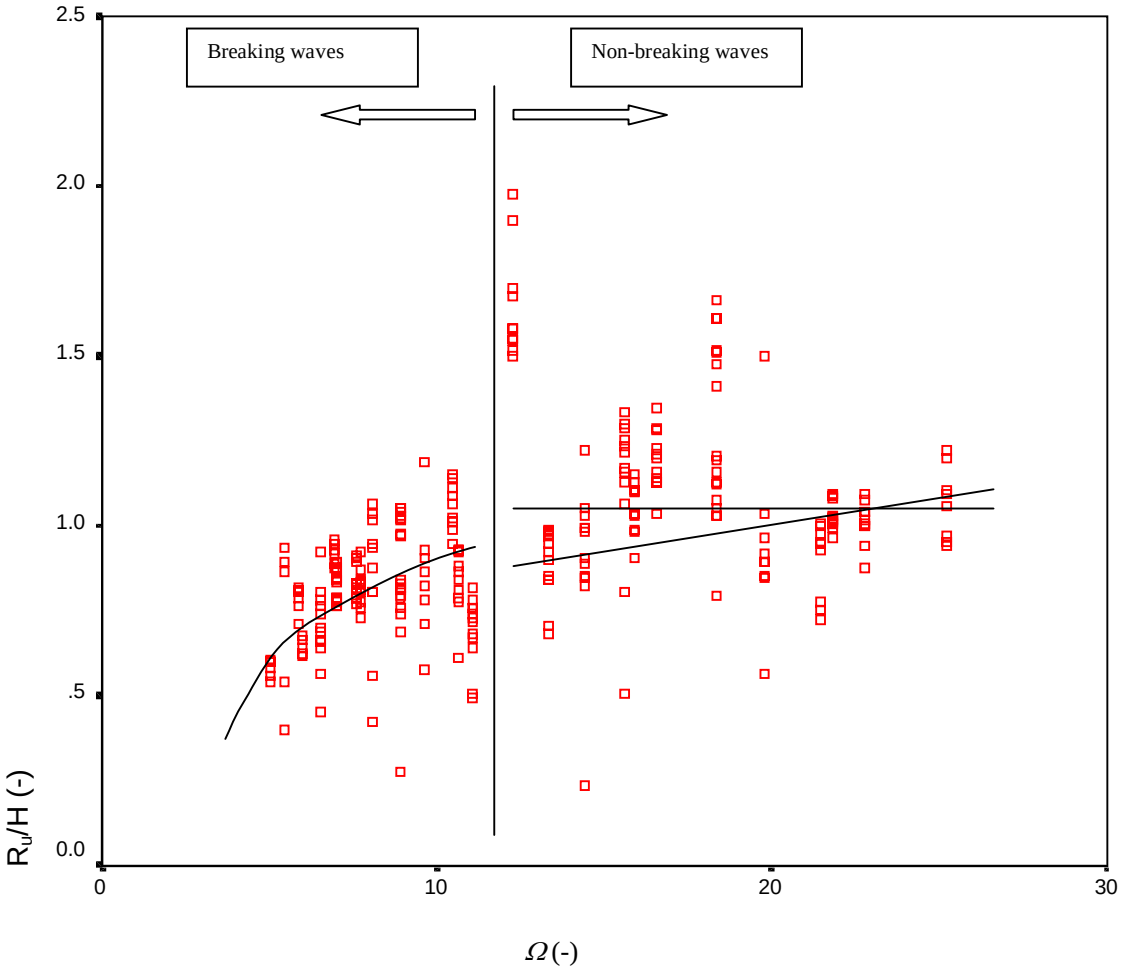

figure XXIV-1, Relative run-up versus Ω, all data points

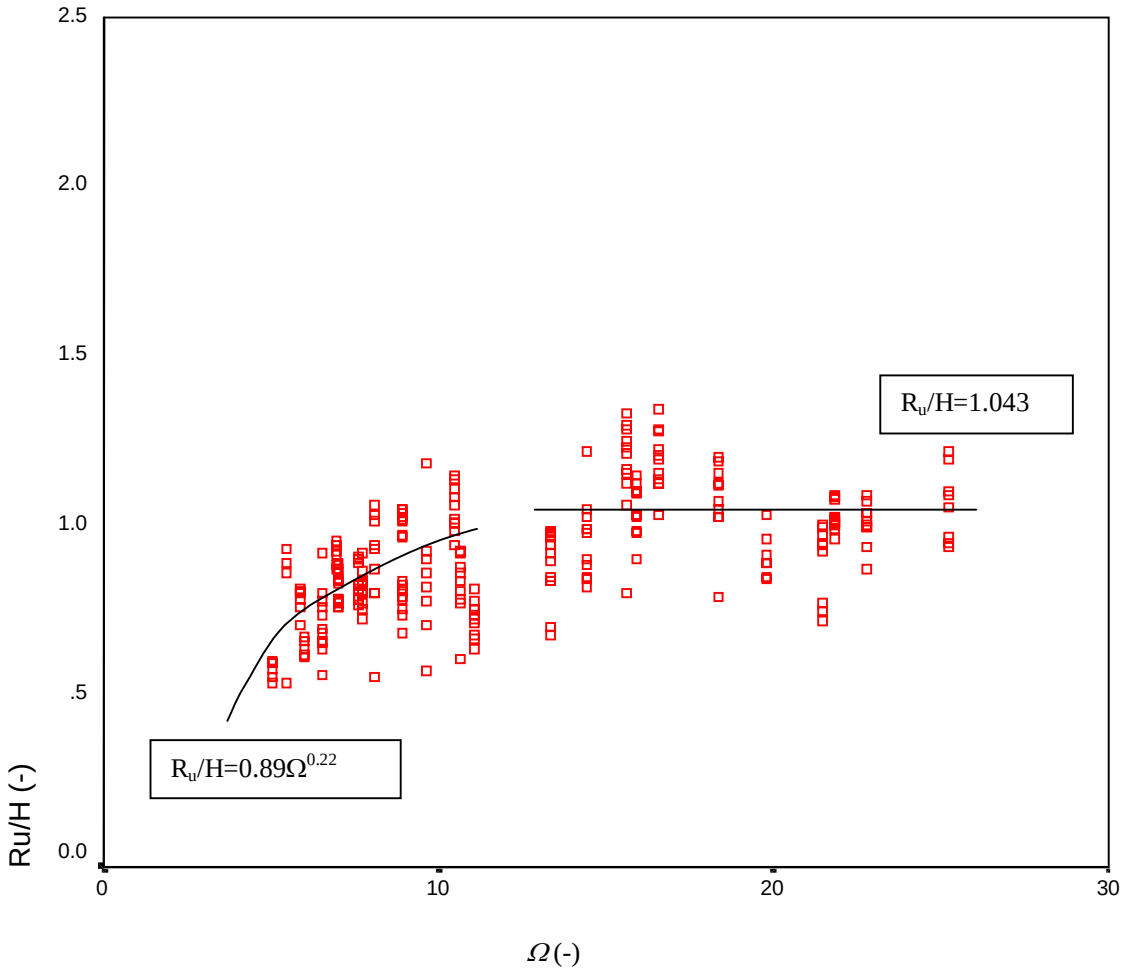

figure XXIV-2, Relative run-up versus Ω, data fitting